



Universiteit  
Leiden  
The Netherlands

## **Ruthenium polypyridyl complexes with anticancer properties**

Corral Simón, E.

### **Citation**

Corral Simón, E. (2007, September 25). *Ruthenium polypyridyl complexes with anticancer properties*. Retrieved from <https://hdl.handle.net/1887/12358>

Version: Corrected Publisher's Version

License: [Licence agreement concerning inclusion of doctoral thesis in the Institutional Repository of the University of Leiden](#)

Downloaded from: <https://hdl.handle.net/1887/12358>

**Note:** To cite this publication please use the final published version (if applicable).

# **Ruthenium polypyridyl complexes with anticancer properties**

*Synthesis, characterization and mechanistic studies in search for  
structure-activity relationships*

PROEFSCHRIFT

ter verkrijging van

de graad van Doctor aan de Universiteit Leiden,

op gezag van Rector Magnificus prof.mr. P.F. van der Heijden,

volgens besluit van het College voor Promoties

te verdedigen op dinsdag 25 september 2007

klokke 16.15 uur

door

**Eva Corral Simón**

geboren te Miranda de Ebro (Spanje) in 1979

## **Promotiecomissie**

**Promotor** Prof. Dr. J. Reedijk

**Referent** Prof. Dr. E. Alessio (Università di Trieste, Italië)

**Overige leden** Prof. Dr. J. Brouwer (Universiteit Leiden, Nederland)

Dr. J.G. Haasnoot (Universiteit Leiden, Nederland)

Dr. A.C.G. Hotze (Octopus Leiden, Nederland)

<< Salimos de Salamanca, y llegando a la puente, está a la entrada della un animal de piedra, que casi tiene forma de toro, y el ciego mandóme que llegáse cerca del animal, y allí puesto, me dijo:

"Lázaro, llega el oído a este toro, y oirás gran ruido dentro del." Yo simplemente llegué, creyendo ser así; y como sintió que tenía la cabeza par de la piedra, afirmó recio la mano y dióme una gran calabazada en el diablo del toro, que más de tres días me duró el dolor de la cornada, y díjome:

"Necio, aprende que el mozo del ciego un punto ha de saber más que el diablo", y rió mucho la burla. >>

*La vida de Lazarillo de Tormes, y de sus fortunas y adversidades. Anónimo, 1554.*

*Para mi familia (con Rosi)  
y para el resto de las 7,  
por estar ahí, siempre.*

# Table of contents

<b>List of abbreviations</b>	<b>8</b>
<b>1. Introduction</b>	<b>11</b>
<i>1.1. Metals in medicine. The discovery of cisplatin as an anticancer agent</i>	12
History of cisplatin, a leading anti-cancer drug	13
<i>1.2. Cisplatin: mechanism of action</i>	14
DNA adducts formed by coordination of cisplatin	14
DNA repair mechanism	17
<i>1.3. Development of new platinum anticancer agents</i>	18
Platinum(IV) complexes	19
Sterically hindered <i>cis</i> -platinum(II) complexes	20
<i>trans</i> - platinum(II) complexes	20
Polynuclear platinum drugs	21
<i>1.4. A possible alternative to platinum therapy: ruthenium chemistry</i>	24
Ruthenium properties that make it suitable for biological applications	25
Anticancer activity	26
<i>1.5. Classification of ruthenium complexes with anticancer properties</i>	27
Ammine-chlorido derivatives	27
Dimethylsulfoxide complexes	27
Complexes with other heterocyclic ligands	29
Ruthenium polyaminocarboxylate complexes	31
Organoruthenium complexes	31
Photoreactive ruthenium compounds that induce DNA cleavage	32
Dinuclear ruthenium complexes	33
<i>1.6. How these drugs work: mechanisms of action</i>	36
<i>1.7. Aim and scope of this thesis</i>	38
<i>1.8. References</i>	39
<b>2. Ruthenium polypyridyl complexes containing the bischelating ligand</b>	
<b>2,2'-azobispyridine. Synthesis, characterization and crystal structures</b>	<b>47</b>
<i>2.1. Introduction</i>	48

2.2. <i>Experimental</i>	48
Materials and reagents	48
Physical measurements	49
X-ray structural determination	49
Synthesis and characterization of the [Ru(apy)(tpy)L](ClO <sub>4</sub> ) <sub>(2-n)</sub> compounds	51
2.3. <i>Results and discussion</i>	53
Synthesis and characterization of the [Ru(apy)(tpy)L](ClO <sub>4</sub> ) <sub>(2-n)</sub> compounds	53
X-ray structural determinations	54
<sup>1</sup> H NMR characterization of the [Ru(apy)(tpy)L](ClO <sub>4</sub> ) <sub>(2-n)</sub> compounds	58
2.4. <i>Concluding remarks</i>	63
2.5. <i>References</i>	63
<b>3. Interaction between the DNA model base 9-ethylguanine and a group of ruthenium polypyridyl complexes: kinetics and conformational temperature dependence</b>	<b>65</b>
3.1. <i>Introduction</i>	66
3.2. <i>Experimental</i>	67
Materials and reagents	67
Physical measurements	67
[Ru(apy)(tpy)(9-EtGua)] <sup>2+</sup> titration	68
Synthesis and characterization of [Ru(apy)(tpy)(9-EtGua)](ClO <sub>4</sub> ) <sub>2</sub>	68
Computational details	68
3.3. <i>Results and discussion</i>	69
<sup>1</sup> H NMR studies of the interaction between three ruthenium polypyridyl complexes and 9-ethylguanine	69
DFT calculations	72
Synthesis and characterization of [Ru(apy)(tpy)(9-EtGua)](ClO <sub>4</sub> ) <sub>2</sub> . pH titration. Variable temperature and 2D NMR studies	75
3.4. <i>Conclusions</i>	81
3.5. <i>References</i>	81
<b>4. Ruthenium polypyridyl complexes and their modes of interaction with DNA: is there a correlation between these interactions and the antitumour activity of the compounds?</b>	<b>83</b>
4.1. <i>Introduction</i>	84

4.2. <i>Experimental</i>	86
Materials and reagents	86
Physical measurements	86
Synthesis and characterization of	
$[\{\text{Ru}(\text{apy})(\text{tpy})\}_2\{\mu\text{-H}_2\text{N}(\text{CH}_2)_6\text{NH}_2\}](\text{ClO}_4)_4$	87
Interaction between ruthenium polypyridyl complexes and 9-ethylguanine	87
Interaction between ruthenium polypyridyl complexes and <i>ct</i> -DNA	88
<i>In vitro</i> cytotoxicity assays	88
4.3. <i>Results and discussion</i>	90
Synthesis and characterization of	
$[\{\text{Ru}(\text{apy})(\text{tpy})\}_2\{\mu\text{-H}_2\text{N}(\text{CH}_2)_6\text{NH}_2\}](\text{ClO}_4)_4$	90
Interaction between ruthenium polypyridyl complexes and 9-ethylguanine	91
Interaction between ruthenium polypyridyl complexes and <i>ct</i> -DNA	93
<i>In vitro</i> cytotoxicity assays	99
4.4. <i>Concluding remarks</i>	101
4.5. <i>References</i>	102
<b>5. Explorations towards novel ruthenium anticancer drugs</b>	<b>105</b>
5.1. <i>Alternative ways of interaction between metallodrugs and DNA</i>	106
5.1.1. <i>Introduction</i>	106
Groove binding	106
Intercalation	107
5.1.2. <i>Experimental</i>	109
Materials and reagents	109
Physical measurements	109
Synthesis and characterization of $[\{\text{Ru}(\text{tpy})\text{Cl}_2\}(\mu\text{-paa})](\text{BF}_4)_2$ ( <b>1h</b> )	109
Synthesis and characterization of $[\text{Ru}(\text{abpt})(\text{bpy})_2](\text{PF}_6)_2$ ( <b>1i</b> )	110
<i>In vitro</i> cytotoxicity assays	110
5.1.3. <i>Results, discussion and concluding remarks</i>	110
5.2. <i>Interactions between metallodrugs and other biological molecules</i>	112
5.2.1. <i>Introduction on serum proteins</i>	112
Albumin	112
Transferrin	112
Cytochrome <i>c</i>	113

Other proteins	113
5.2.2. <i>Interactions between metallodrugs and serum proteins</i>	113
Albumin	113
Transferrin	114
Cytochrome <i>c</i>	115
Other proteins	115
5.2.3. <i>Interactions between Ru(II) polypyridyl complexes and serum transport proteins</i>	115
5.3. <i>Ruthenium complexes and metastasis</i>	116
5.4. <i>References</i>	117
<b>6. Summary, general evaluation and future developments</b>	<b>119</b>
6.1. <i>Introduction</i>	120
6.2. <i>Summary</i>	120
6.3. <i>Conclusions and future perspectives</i>	121
6.4. <i>References</i>	122
<b>Appendix. Nucleic acids in two dimensions: layers of base pairs linked by carboxylate</b>	<b>123</b>
A.1. <i>Introduction</i>	124
A.2. <i>Results and discussion</i>	124
A.3. <i>Experimental</i>	128
Materials and reagents	128
Physical measurements	128
Experimental procedure	128
X-ray structural determination	129
A.4. <i>References</i>	129
<b>Samenvatting</b>	<b>133</b>
<b>Resumen</b>	<b>136</b>
<b>Curriculum Vitae (English)</b>	<b>142</b>
<b>Curriculum Vitae (Español)</b>	<b>143</b>
<b>List of publications</b>	<b>144</b>
<b>Nawoord (Agradecimientos)</b>	<b>145</b>

# List of abbreviations

<i>A</i>	adenine
<i>A2780</i>	human ovarian carcinoma cell line
<i>A2780R</i>	cisplatin-resistant human ovarian carcinoma cell line
<i>A498</i>	human renal cancer cell line
<i>abpt</i>	4-amino-3,5-bis(pyridin-2-yl)-1,2,4-triazole
<i>abs</i>	absolute
<i>AFM</i>	atomic force microscopy
<i>Anal. Calc.</i>	calculated elemental analysis
<i>apy</i>	2,2'-azobispyridine
<i>azpy</i>	2-phenylazopyridine
<i>BI</i>	bond ionicity
<i>bpy</i>	2,2'-bipyridine
<i>c</i>	<i>cis</i>
<i>C</i>	cytosine
<i>CD</i>	circular dichroism
<i>CoLo 320 DM</i>	human colon cancer cell line
<i>COSY</i>	correlation spectroscopy
<i>ct</i>	calf thymus
<i>d</i>	doublet
<i>dd</i>	double doublet
<i>DFT</i>	density functional theory
<i>DMEM</i>	Dulbecco's modified Eagle's Medium
<i>dmsO</i>	dimethylsulfoxide
<i>DNA</i>	deoxyribonucleic acid
<i>eg</i>	9-ethylguanine (also abbreviated as 9-EtGua)
<i>eq.</i>	equation
<i>en</i>	ethylenediamine
<i>ESIMS</i>	electrospray ionization mass spectrometry
<i>9-EtGua</i>	9-ethylguanine (also abbreviated as <i>eg</i> )
<i>EtOH</i>	ethanol
<i>EVSA-T</i>	estrogen receptor -/ progesterone receptor - human breast cancer cell line
<i>Fig.</i>	figure
<i>FTIR</i>	Fourier transform infrared spectroscopy
<i>G</i>	guanine
<i>GSH</i>	glutathione
<i>H226</i>	non-small human cell lung cancer cell line

<i>H7eg</i>	9-ethylguanin-7-ium
<i>Hepes</i>	4-(2-hydroxyethyl)-1-piperazineethanesulfonate
<i>Him</i>	imidazole
<i>HMG</i>	high mobility group
<i>IC<sub>50</sub></i>	concentration of a compound that induces 50% growth inhibition of cells compared to untreated cells
<i>ICP</i>	inductively coupled plasma
<i>IGROV</i>	human ovarian cancer cell line
<i>impy</i>	2-phenylpyridinylmethylene amine
<i>L1210/0</i>	cisplatin-sensitive mouse leukemia
<i>L1210/2</i>	cisplatin-resistant mouse leukemia
<i>LD</i>	linear dichroism
<i>m</i>	multiplet
<i>M19 MEL</i>	human melanoma cell line
<i>m/z</i>	mass to charge ratio
<i>MCF7</i>	estrogen receptor +/- progesterone receptor + human breast cancer cell line
<i>MeOH</i>	methanol
<i>MRI</i>	magnetic resonance imaging
<i>MTT</i>	3-(4,5-dimethylthiazol-2-yl)-2,5-diphenyl-2H-tetrazolium bromide
<i>NER</i>	nucleotide excision repair
<i>NMR</i>	nuclear magnetic resonance
<i>NOESY</i>	nuclear Overhauser effect spectroscopy
<i>phen</i>	phenantroline
<i>PBS</i>	phosphate buffered saline
<i>paa</i>	2-pyridinealdazine
<i>rf</i>	resistance factor: IC <sub>50</sub> cisplatin-resistant cell line / IC <sub>50</sub> cisplatin-sensitive cell line
<i>RNA</i>	ribonucleic acid
<i>RPMI</i>	Roswell Park Memorial Institute
<i>RT</i>	room temperature
<i>s</i>	singlet
<i>SAR's</i>	structure-activity relationships
<i>SRB</i>	sulforhodamine B
<i>T</i>	thymine
<i>t</i>	triplet, <i>trans</i>
<i>TMS</i>	tetramethylsilane
<i>tpy</i>	2,2':6',2''-terpyridine
<i>WiDR</i>	human colon cancer cell line



# 1. Introduction

An overview about Medicinal Inorganic Chemistry is given, with special attention to the role that platinum and ruthenium play in it.

### 1.1. Metals in medicine. The discovery of cisplatin as an anticancer agent

Precious metals have been used for medicinal purposes for at least 3500 years, when records show that gold was included in a variety of medicines in Arabia and China.<sup>1</sup> However, the motivation for the use of these metals often had a superstitious or a religious origin, and was derived from the reasoning: if a metal is rare, it must mean it has special properties. Life was thought to be built exclusively from organic “bricks”. In the late 1800’s, experiments carried out with blood samples revealed the existence of iron-containing compounds in this fluid.<sup>2</sup> The presence of metals in different enzymes was proven<sup>3</sup> and bioinorganic chemistry was granted the status of a separate discipline in the 1970’s.<sup>4</sup> Nowadays, it is known that inorganic elements play diverse biological roles, such as stabilization of structures (e.g.  $\text{CaCO}_3$  stabilizes the structure of the bones; the  $\text{PO}_4^{3-}$  groups stabilize the DNA structure), transport of molecules (e.g. haemoglobin, an iron-containing protein, which transports oxygen in the bloodstream), transfer of electrons (e.g. cytochrome *c*), redox and other enzymatic reactions (copper, iron, zinc and manganese form part of several metalloenzymes), etc. The fact that some metal ions are essential for life also suggested the possibility of incorporating metal atoms into drugs.

In modern history, the first compound containing an inorganic element that was described to be used in the cure of a disease was salvarsan, an arsenic compound used in the treatment of syphilis, which was synthesized and tested in the beginning of the 20th century by Ehrlich (see Fig.1.1).<sup>5, 6</sup> Ehrlich, who was awarded the Nobel Prize in 1908 for his discovery of immunochemistry, is considered the founder of chemotherapy, which he defined as “the use of drugs to injure an invading organism without injury to the host”. Ehrlich introduced the “magic bullet” concept, also known as “drug targeting”, nowadays the object of extensive research worldwide.

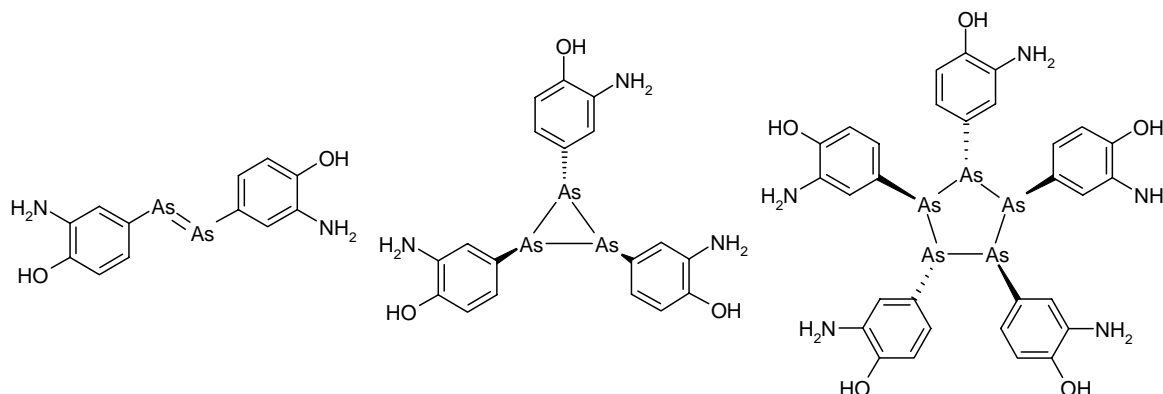


Fig.1.1. Molecular structure of the arsenic drug salvarsan as proposed by Ehrlich (left). In 2005, salvarsan was proven to consist of a mixture of cyclic species (centre and right).<sup>7</sup>

Medicinal inorganic chemistry as a discipline is considered to have boosted with the discovery of the anticancer properties of cisplatin.<sup>1</sup> Cisplatin was the first chemical compound to become the subject of a mechanistic study: its mechanism of action was investigated, as well as the way to optimize its activity. Medicinal inorganic chemistry comprises not only the intentional introduction of a metal ion into a biological system, but also the rescue of a metal ion that has been introduced in a biological system by accident. Examples of the first case are the administration of essential elements and mineral supplements (e.g. iron, copper, zinc, selenium), the use of diagnostic agents (e.g. gadolinium and manganese for MRI, barium and iodine for X-ray), and therapeutic agents (e.g. lithium for bipolar disorder, platinum compounds in anticancer chemistry, gold compounds for arthritis and bismuth for ulcers), as well as the use of radiopharmaceuticals for diagnosis (<sup>99m</sup>Tc) and therapy (<sup>186</sup>Re), and the use of enzyme inhibitors.<sup>8</sup> Chelation therapy is most widely used in the treatment of poisoning by an inorganic (not necessarily metallic) element (e.g. 2,3-dimercapto-1-propanol, known as BAL, used for mercury, arsenic, antimony or nickel poisoning; Na<sub>2</sub>H<sub>2</sub>edta, used for lead removal).

### **History of cisplatin, a leading anti-cancer drug**

*cis*-diamminedichloridoplatinum(II) was first described by Peyrone in 1845.<sup>9</sup> Together with its *trans* analogue, this complex was used by Werner in 1893 as the first example of isomers in Coordination Chemistry.

Its activity against cancer remained, however, unknown until 1964, when Rosenberg realized that the platinum electrodes used in one of his experiments affected bacterial growth.<sup>10, 11</sup> The main species responsible for that was found to be *cis*-Pt(NH<sub>3</sub>)<sub>2</sub>Cl<sub>2</sub>, which was formed slowly by reaction of the electrodes with the electrolyte NH<sub>4</sub>Cl solution. The drug entered clinical trials in 1971 and by the end of 1987 it was already the most widely used anticancer medicine.<sup>12</sup>

Unfortunately, the use of this compound did not bring a definitive end to cancer, since it only showed anticancer activity against certain types of tumours. Some tumours avoid the action of cisplatin, being this resistance in some cases intrinsic, but also in some others acquired. Finally, cisplatin therapy produces severe side-effects, namely neurotoxicity, ototoxicity, nausea, vomiting, bone marrow dysfunction and nephrotoxicity, the latter being dose-limiting. Research has been focused on several fronts. Understanding the transport of the drug in the body and its cellular uptake, as well as its mechanism of action inside the

cell, is crucial for the design of improved pharmaceuticals. The development of synthetic methods that rapidly yield compound libraries to be screened afterwards for anticancer activity allows for a very efficient trial-and-error strategy. Since cisplatin is indeed effective against certain tumours, studies are also being done about how to avoid its undesired side effects, while still retaining the therapeutic value of the drug.

### ***1.2. Cisplatin: mechanism of action***

Cisplatin administration protocols currently include an intravenous infusion. Since this method is far from ideal, requiring patient hospitalization, research has been carried out to find an alternative administration route. A release-controlled formulation of cisplatin with reduced toxicity has recently been developed.<sup>13</sup> The complex is encapsulated inside nano-scale liposomal carriers and administered to the patient via nebulization. This new approach is currently undergoing phase I clinical trials.<sup>13</sup>

In the blood, the high physiological chloride concentration (ca. 100 mM) ensures that the complex remains neutral until it enters the cell. This passage was classically thought to occur mainly by passive diffusion. However, the debate about the importance of the participation of an active transport mechanism in this process was re-opened when cisplatin uptake was discovered to be mediated by the copper transporter Ctr1p both in yeast and in mammals.<sup>14</sup> Once in the cytosol, hydrolysis occurs due to the lower chloride concentration (ca. 4mM).

Cisplatin can bind to nucleic acids, proteins and sulfur-containing biomolecules, such as glutathione (GSH). The ultimate target of cisplatin, which triggers its cytotoxicity, is generally accepted to be DNA.<sup>15</sup>

#### **DNA adducts formed by coordination of cisplatin**

The DNA coordination sites of cisplatin after hydrolysis are, in order of preference, the N7 atom of guanine, the N7 atom of adenine, the N1 of adenine and N3 of cytosine. Two types of platinum-DNA binding have been found: monofunctional and bifunctional. Monofunctional binding is unlikely to be responsible for the cytotoxic action of cisplatin, since transplatin is as capable of forming this kind of adducts as cisplatin, while being inactive. Bifunctional binding results in chelation and subsequent formation of various adducts in DNA. Intrastrand 1,2-d(GpG) cross-links are the most abundant Pt-DNA adducts (60-65% of the platinum bound to DNA is in that form),<sup>16</sup> followed by intrastrand d(ApG)

cross-links (around 20% of the bound platinum). Only about 1.5% of the cisplatin was found to be involved in interstrand adducts; some minor DNA-protein cross-links were also formed (see Fig.1.2).<sup>15, 17</sup>

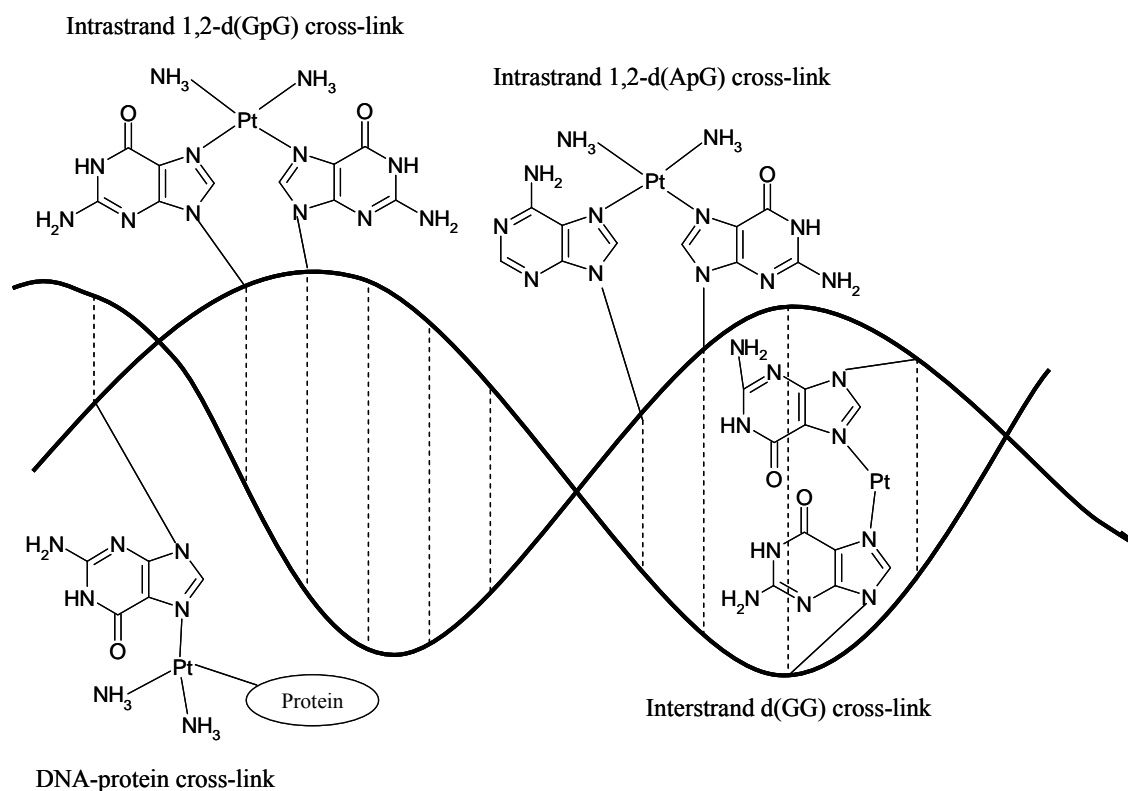


*Fig.1.2. Schematic view of a double-stranded DNA, depicting some of the most commonly occurring Pt-DNA adducts. Geometry considerations (HH, HT orientation) have been ignored.*

Cisplatin-DNA adducts inhibit DNA replication, block transcription by RNA polymerase II and trigger programmed cell death or apoptosis.<sup>15, 18</sup> Experiments carried out to study the kinetics of the Pt-DNA interaction, amongst others, pointed out that the two most abundant adducts, *i.e.* intrastrand 1,2-d(GpG) and d(ApG) cross-links, are responsible for the cytotoxic effects of cisplatin. However, the results obtained in these studies are not unambiguous.<sup>15</sup>

The formation of the above-mentioned cisplatin-DNA cross-links structurally distorts the DNA, resulting in a loss of helix stability and a structural change.<sup>19-22</sup> NMR studies in solution have tried to predict the structural changes provoked by cisplatin in various DNA

fragments (see Fig.1.3); a few crystal structures have also been obtained (see Fig.1.3) that basically agree with the geometries proposed from the NMR spectra.

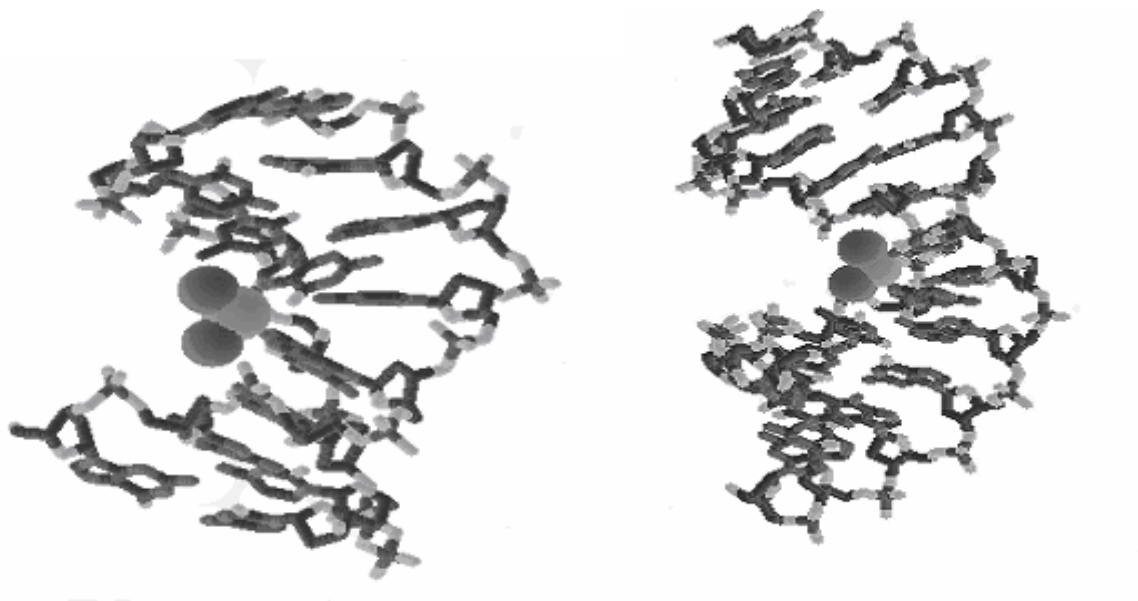


*Fig.1.3. Structure of a DNA double helix fragment containing a 1,2-d(GpG) intrastrand cross-link: NMR-solution structure (left)<sup>23</sup> and schematic crystal structure (right).<sup>24</sup>*

The dihedral angle between the guanine rings in the Pt adduct ranges from  $76^\circ$  to  $87^\circ$ , reflecting distortion of base stacking. All the complementary base-pairing interactions remain, however, intact, even within the G-C base pairs directly involved in the Pt-binding.<sup>15</sup> A bending of the DNA is observed with a kink of  $40\text{--}80^\circ$  towards the major groove. Simultaneously an unwinding of the helix is observed of about  $20^\circ$ , provoking a compression of the major groove and opening up the minor groove.<sup>25-27</sup> The cisplatin–DNA adducts may be stabilized by the formation of a hydrogen bond between one of the platinum ammine ligands and an oxygen atom on the 5'-phosphate group of DNA, which may be crucial for the activity of cisplatin.<sup>28-31</sup>

The resulting wide and shallow minor groove opposite the platinum adduct is recognised by a number of cellular proteins, including DNA repair proteins, histones and high mobility group (HMG) domain proteins such as HMGB1 (see Fig.1.4).<sup>32</sup>

**DNA repair mechanism**

Cisplatin–DNA lesions are repaired in cells primarily through the nucleotide excision repair (NER) pathway, which consists on a group of proteins with enzymatic functions.<sup>33-35</sup> In NER, an enzyme system first recognizes the lesion and then hydrolyzes two phosphodiester bonds, one on either side of the lesion, to generate an oligonucleotide carrying the damage. The gap is then filled in and ligated by a DNA ligase.<sup>35</sup>

The importance of the role of these proteins in the mechanism of action of cisplatin is underlined by the observation that the sensitivity to cisplatin increases in those cells deficient in DNA repair, while the DNA repair is more efficient in some cisplatin-resistant cell lines.<sup>36</sup>

Numerous HMG-domain proteins have been found to specifically recognize and bind to cisplatin-modified DNA. Examples of these proteins are TBP, TATA-binding protein<sup>37-39</sup> and the transcription factor FACT (Facilitates Chromatin Transcription).<sup>40</sup>

HMGB1 and other cellular proteins that recognize platinum-DNA adducts (see Fig.1.4) may play a role in the mechanism of action of cisplatin, according to two main hypotheses.<sup>41</sup> The first of these hypotheses proposes that cisplatin-damaged DNA hijacks proteins away from their natural binding sites, leading to cellular stress and eventually cell death. The second hypothesis suggests that binding by cellular proteins shields cisplatin adducts from nucleotide excision repair (NER), allowing them to persist and drive apoptosis.<sup>42, 43</sup> These two mechanisms are not mutually exclusive. Although many studies have demonstrated that HMG-domain proteins enhance cisplatin antitumour efficiency, others reached the opposite conclusion.<sup>44-46</sup> It seems, therefore, that the effect of these proteins in modulating the activity of cisplatin depends upon the cell type and context.

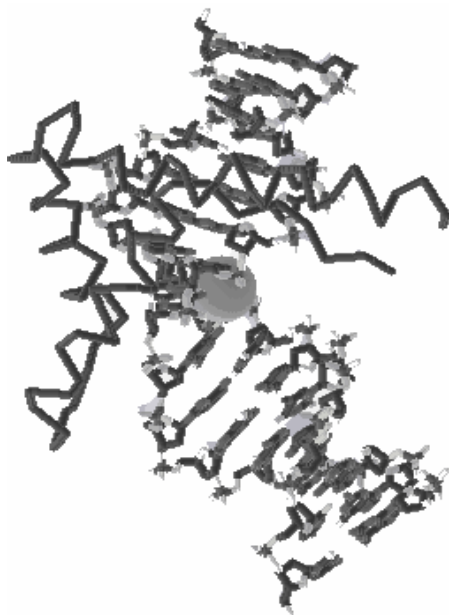


*Fig.1.4. Schematic crystal structure of the HMGB1a protein bound to a cisplatin-modified DNA duplex.*<sup>32</sup>

### **1.3. Development of new platinum anticancer agents**

Thousands of platinum compounds have been synthesized in an attempt to overcome the problems of cisplatin. Surprisingly none of these has been able to substitute cisplatin in routine chemotherapy treatments.

The observation of the first platinum complexes synthesized and their efficacies as antitumour agents led to what was called the “structure-activity relationships” (SAR’s).<sup>12</sup> This was a list of structural characteristics that a platinum complex was thought to require in order to show an antitumour activity. Subsequently every new compound was designed according to these rules.

The most successful of the second-generation platinum compounds is *cis*-diammine-1,1-cyclobutane-dicarboxylatoplatinum(II), also known as carboplatin (See Fig.1.5). Since its introduction in 1986 it has been preferred to cisplatin in the treatment of many platinum-sensitive malignancies. Carboplatin has less severe side effects than cisplatin, but it is cross-resistant with it. Its activity is equivalent to cisplatin in the treatment of ovarian cancers, however in the treatment of testicular, head and neck cancers cisplatin is superior.<sup>47, 48</sup>

Two other second- and third-generation compounds have been approved for clinical use. *cis*-diammine(glycolato)platinum(II) (nedaplatin)<sup>49</sup> (see Fig.1.5) was approved in 1995

by the Health and Welfare Ministry in Japan<sup>50</sup> and various studies of combined therapies of the platinum complex with other drugs are undergoing clinical trials for the treatment of urothelial, uterine, lung, esophageal or testicular cancer, amongst others.<sup>51-56</sup> (1R,2R-diaminocyclohexane)oxalatoplatinum(II) (oxaliplatin)<sup>57</sup> (see Fig.1.5) was approved in France<sup>50</sup> and in a few other European countries mainly for the treatment of metastatic colorectal cancer. Clinical studies pointed out that the myelosuppression and nephrotoxicity caused by oxaliplatin are less intense in comparison with cisplatin treatment, however neuropathy occurs more frequently in case of the patients treated with this third-generation compound.<sup>50</sup>

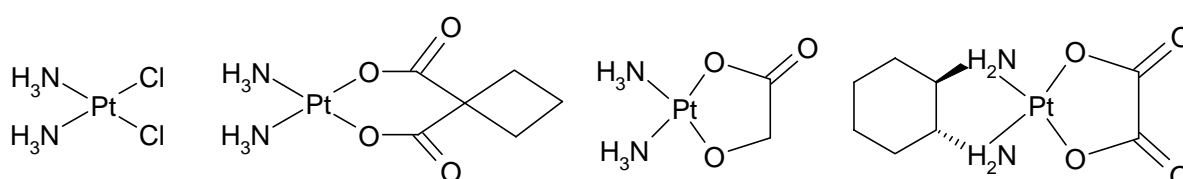


*Fig.1.5. Molecular structure of a few selected platinum drugs. From left to right: cisplatin, carboplatin, nedaplatin and oxaliplatin.*

Since it became evident that mere analogues of cisplatin or carboplatin would probably not offer any substantial clinical advantages over the existing drugs, as complexes of this kind can be expected to have similar biological consequences to cisplatin, some platinum complexes were synthesised which contradicted the SAR's.

### **Platinum(IV) complexes**

The design of platinum(IV) complexes yielded a new concept in platinum anticancer therapy. These compounds with lipophilic groups at axial positions would facilitate intestinal absorption of the drug, making oral administration possible.<sup>58</sup> Moreover they would act as pro-drugs, which get reduced to platinum(II) by intracellular glutathione, ascorbic acid or other reducing agents. The platinum(II) would bind subsequently to DNA and exert the desired action.<sup>59, 60</sup> The most successful Pt(IV) complex is bis(acetato)-amminedichlorido(cyclohexylamine)platinum(IV) (see Fig.1.6), also known as satraplatin or JM216. Phase II trials of this drug have been completed by GPC-Biotech in hormone-refractory prostate cancer (HRPC), ovarian cancer and small cell lung cancer.<sup>61</sup> Phase III evaluation of satraplatin combined with prednisone is ongoing as a second-line

chemotherapy treatment for patients with HRPC. Other trials evaluating the effects of satraplatin in combination with radiation therapy, in combination with other cancer therapies and in various other cancers are underway or planned.<sup>61</sup> Satraplatin also shows *in vivo* oral antitumour activity against a variety of murine and human subcutaneous tumour models, comparable to the activity of cisplatin. In addition, it has a relatively mild toxicity profile, being myelosuppression instead of nephrotoxicity the dose-limiting factor.<sup>62</sup>

### Sterically hindered *cis*-platinum(II) complexes

In the search for platinum drugs that show activity in those cell lines in which cisplatin is inefficient, a strategy was tried which consisted on designing complexes with sterically crowded non-leaving groups. These compounds would react preferentially with nucleic acids over sulfur-containing biomolecules, thus avoiding inactivation by GSH and others. *cis*-amminedichlorido(2-methylpyridine)platinum(II) (ZD0473 or AMD473; see Fig.1.6) exhibited no cross-resistance to cisplatin in *in vitro* tests carried out with human ovarian carcinoma cells,<sup>63</sup> so it was selected for clinical trials. Phase-II clinical trials carried out with lung and metastatic breast cancer patients showed a good tolerability of the drug, but no greater efficacy over existing agents in platinum-resistant patients.<sup>64, 65</sup> Studies are ongoing using the drug in combination with other drugs, including docetaxel.<sup>65, 66</sup> The results obtained in phase II clinical trials with ovarian cancer patients also suggested that ZD0473 may not completely circumvent the platinum-resistance mechanisms.<sup>67</sup> Studies are ongoing of combined therapy with liposomal doxorubicin or paclitaxel.<sup>67</sup>

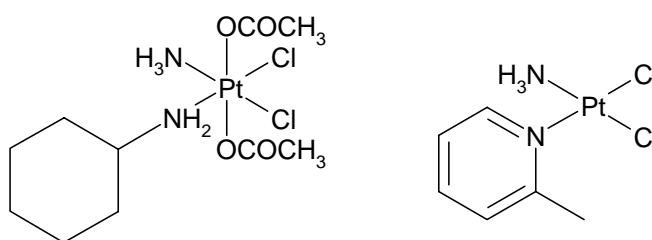


Fig.1.6. Molecular structure of the anticancer platinum complexes satraplatin or JM216 (a Pt(IV) complex, on the left) and ZD0473 (a Pt(II) complex, on the right).

### *trans*- platinum(II) complexes

Since transplatin displays no antitumour activity, one of the early conclusions drawn in the SAR's was that the *cis*- geometry was an essential requisite. On the other hand a

complex that reacts exactly like cisplatin will never overcome resistance to it. In the search for complexes that followed a different mechanism to cisplatin the first SAR-rule was revised. Indeed a series of active *trans*-Pt(II) compounds was found.<sup>68</sup>

The *trans*-Pt(II) complexes that have been synthesised so far can be divided into several groups that respond to the general formula *trans*-[PtCl<sub>2</sub>(L)(L')]. The pioneers were Farrell and his group, with complexes where L = a pyridine-like ligand and L' = an ammine, a sulfoxide or a pyridine-like group.<sup>69-72</sup> Following his example, other groups synthesised more *trans*-Pt(II) complexes, finding in some cases very good anticancer activities. Navarro-Ranninger and her group focused on complexes with L = L' = branched aliphatic amines.<sup>73, 74</sup> Gibson and others reported that the replacement of one of transplatin's ammine ligands by a heterocyclic ligand, such as piperidine, piperazine or 4-picoline, resulted in a radical enhancement of the cytotoxicity.<sup>75, 76</sup> Finally the group of Natile and Coluccia synthesised complexes where L = an iminoether ligand and L' = an amine or one more iminoether ligands.<sup>77, 78</sup>

All these groups have reported that the cytotoxic ability of the above-described *trans*-platinum complexes with bulky non-leaving groups is in some cases superior to that shown by cisplatin, and often better than the cytotoxicity of their respective *cis*- analogues. These *trans*- complexes are characterized by a spectrum of activity different from cisplatin and they often overcome resistance. The background concept for designing these complexes is that sterically crowded carrier ligands slow down the reaction between the platinum centre and the biomolecules.<sup>68</sup> In addition, these complexes will cause different DNA alterations from those generated by *cis*-platinum complexes.<sup>71, 79</sup> Finally, the cellular response towards these *trans* complexes is expected to be different than the response towards the cisplatin analogues.<sup>80</sup> This is a mechanistically crucial point, which requires further investigation from a molecular pharmacology point of view.<sup>80, 81</sup>

### **Polynuclear platinum drugs**

In the search for platinum complexes that interact with DNA in a drastically different way to cisplatin, several dinuclear compounds were studied.<sup>82</sup> This new approach allowed many variations to be introduced, to fine-tune or drastically change the DNA binding modes and the biological activity of these complexes. Symmetric complexes have been synthesised and also complexes with two inequivalent coordination spheres;<sup>82</sup> the compounds can vary from bifunctional to tetrafunctional; flexible amine linkers were used,

as well as rigid bridges. These dinuclear complexes were later amplified, becoming trinuclear, tetranuclear and even pentanuclear complexes. The interaction between each of these complexes, with its characteristic size and charge, and DNA is expected to be unique, as is the cellular processing of each drug. The final aim is the synthesis of a heterogeneous group of compounds some of which could overcome both intrinsic and acquired resistance to cisplatin.<sup>82</sup>

A comparative study involving several dinuclear bifunctional and trifunctional platinum(II) complexes (see Fig.1.7) was carried out to investigate the effects of geometry and polyfunctionality on their biological activity.<sup>83</sup> The results obtained showed that some of the complexes display a good antitumour activity, in various cases improving that of cisplatin. More interestingly, some of these complexes overcome cisplatin resistance. Mechanistically these compounds are expected to interact with DNA in different ways.

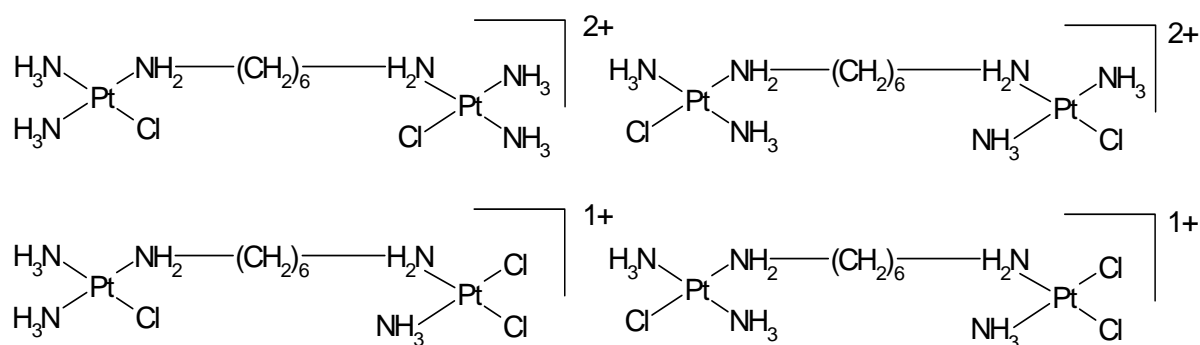


Fig.1.7. The platinum(II) dinuclear complexes 1,1/c,c (above, left), 1,1/t,t (above, right), 1,2/c,c (below, left) and 1,2/t,t (below, right). Counterions are not shown in the picture.

Dinuclear (and trinuclear) complexes incorporating the 4,4'-dipyrazolylmethane (dpzm) ligand have been reported by Collins *et al* (see Fig.1.8).<sup>84</sup> The presence of the heteroaromatic rings in the dpzm group could allow for favourable van der Waals interactions and hydrogen bonding within the DNA minor groove. These compounds display, however, less cytotoxicity than the dinuclear complexes with straight-chain diamine linkers.

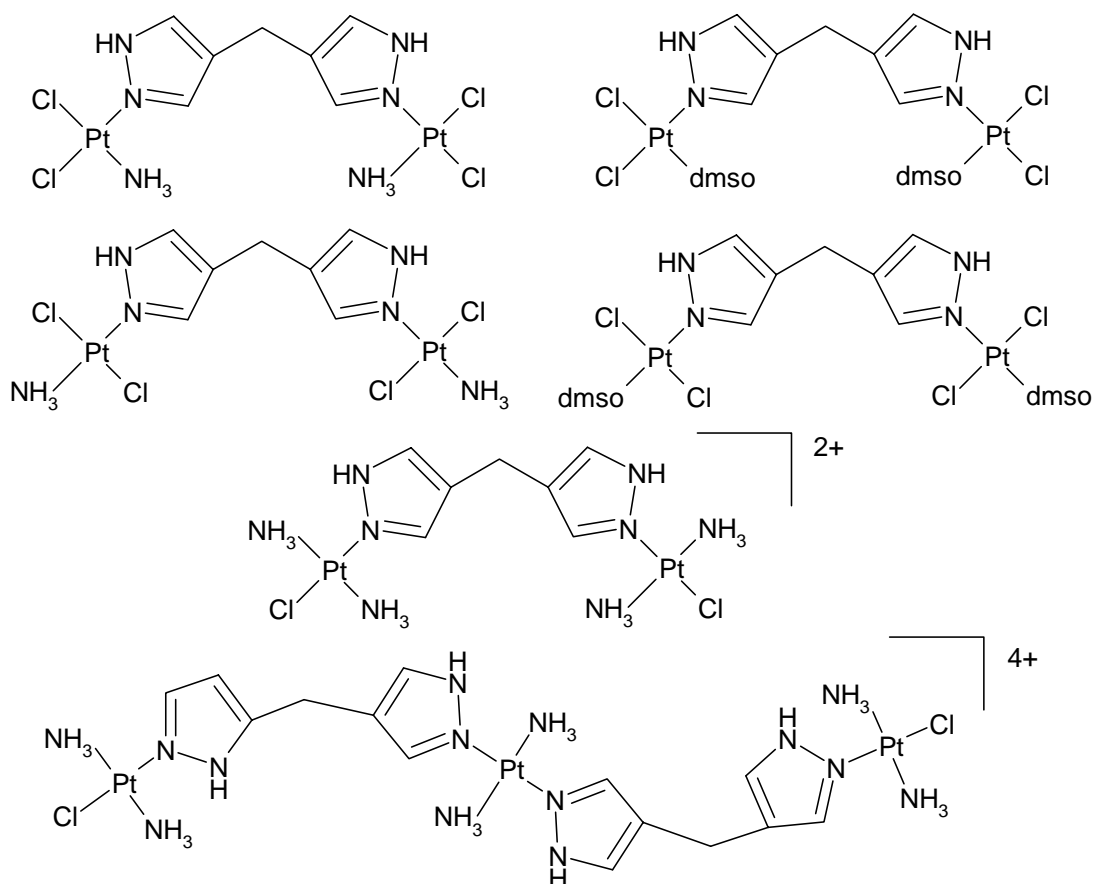


Fig.1.8. Singularly bridged, multi-nuclear platinum complexes linked by the 4,4'-dipyrazolylmethane (dpzm) ligand.

Within the group of dinuclear platinum(II) complexes, a remarkable example consists in the use of pyrazole and triazole as rigid bridging ligands. The groups of Chikuma and Reedijk synthesised dinuclear platinum(II) complexes (see Fig.1.9) that display much higher *in vitro* cytotoxicity than cisplatin on several human tumour cell lines and largely overcome cross-resistance to cisplatin.<sup>85, 86</sup>

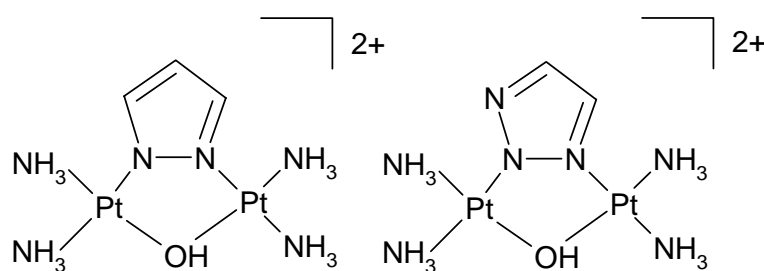


Fig.1.9. Molecular structure of two azole-bridged dinuclear platinum(II) complexes.

The trinuclear platinum(II) complex 1,0,1/*t,t,t* or BBR3464 (see Fig.1.10) was selected for phase II trials once promising pre-clinical data had been obtained.<sup>87</sup> BBR3464, which provides long-range intrastrand crosslink upon DNA, was found to be very potent as a cytotoxic agent, besides being effective against cisplatin-resistant tumour cells. Notable features are the potency, the ten-fold lower maximum tolerated dose (MTD) in comparison to cisplatin and the broad spectrum of tumours sensitive to this agent. Importantly, BBR3464 also displays high antitumour activity in human tumour xenografts characterized as mutant p53, tumours that are known to be insensitive to drug intervention.

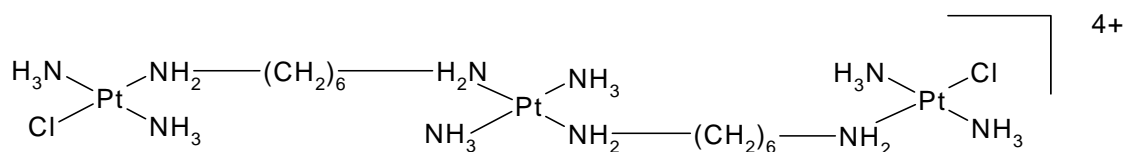


Fig.1.10. The platinum(II) trinuclear complex 1,0,1/*t,t,t*.

#### 1.4. A possible alternative to platinum therapy: ruthenium chemistry

In the search for drugs with improved clinical effectiveness, reduced toxicity and a broader spectrum of activity, other metals than platinum have been considered, such as rhodium and ruthenium. Non-platinum active compounds are likely to have different mechanisms of action, biodistribution and toxicities than platinum-based drugs and might therefore be active against human malignancies that have either an intrinsic or an acquired resistance to them. Ruthenium complexes are very promising, especially from the viewpoint of overcoming cisplatin resistance with a low general toxicity.

Ruthenium has found its way into the clinic, where its properties are exploited for very miscellaneous uses. The radiophysical properties of <sup>97</sup>Ru can be applied to radiodiagnostic imaging.<sup>88, 89</sup> Other ruthenium compounds have potential as immunosuppressants (*cis*-[Ru(III)(NH<sub>3</sub>)<sub>4</sub>(HIm)<sub>2</sub>]<sup>3+</sup>), antimicrobials (e.g. organic drugs coordinated to ruthenium centres, such as [Ru(II)Cl<sub>2</sub>(chloroquine)<sub>2</sub>] against malaria and others for the treatment of Chaga's disease), antibiotics (ruthenium complexes of organic antibiotic compounds, e.g. the Ru(III) derivative of thiosemicarbazone against *Salmonella typhi* and *Enterobacteria faecalis*), nitrosyl delivery/scavenger tools (e.g. the Ru(III) polyaminocarboxylates known as AMD6245 and AMD1226 to treat stroke, septic shock,

arthritis, epilepsy and diabetes), vasodilator/vasoconstrictor agents and, as above mentioned, as drugs for cancer chemotherapy.<sup>90</sup>

### **Ruthenium properties that make it suitable for biological applications**

Ruthenium(II) and ruthenium(III) complexes have similar ligand-exchange kinetics to those of platinum(II) complexes. This property makes them the first choice in the search for compounds that display similar biological effects to platinum(II) drugs.<sup>90, 91</sup> Very few metal drugs reach the biological target without being modified, which makes ligand exchange an important determinant of biological activity. Most metallodrugs undergo interactions with macromolecules such as proteins, or with small S-donor compounds, or even with water. Some interactions are essential for inducing the desired therapeutic properties of the complexes. As the rate of ligand exchange is dependent on the concentration of the exchanging ligands in the surrounding solution, diseases that alter these concentrations in cells or in the surrounding tissues may have an effect on the activity of the drug.

The range of accessible oxidation states of ruthenium under physiological conditions makes this metal unique amongst the platinum group. The ruthenium centre, predominantly octahedral, can be Ru(II), Ru(III) or Ru(IV). Ru(III) complexes tend to be more biologically inert than related Ru(II) and Ru(IV) complexes. The redox potential of a metal complex can be modified by varying the ligands. In biological systems glutathione, ascorbate and single-electron-transfer proteins, like those involved in the mitochondrial electron-transfer chain, are able to reduce Ru(III) and Ru(IV),<sup>92</sup> always depending on the nature of the ligands, while molecular dioxygen and cytochrome oxidase can oxidize Ru(II) in certain complexes.<sup>93-95</sup>

The redox potential of ruthenium compounds can be exploited to improve the effectiveness of Ru-based drugs in the clinic.<sup>90, 91</sup> In many cases the altered metabolism associated with cancer and microbial infection results in lower oxygen concentration (hypoxia) in these tissues in comparison to healthy ones.<sup>96</sup> In a healthy cell the reduction of Ru(III) to Ru(II) by glutathione is a very slow process. Besides, the Ru(II) product is readily oxidized back to Ru(III) by the dioxygen that is present in the tissue. However, the reduction of relatively inert Ru(III) complexes by glutathione is more important in the hypoxic environment of solid tumours.<sup>97</sup>

The reduction of Ru(III) to Ru(II) can be catalysed by mitochondrial and microsomal single-electron-transfer proteins, amongst others. The mitochondrial proteins are of particular interest in drug design, as they can initiate apoptosis.<sup>90</sup>

One more property of ruthenium that makes it very appreciated in medicinal chemistry is its tendency to selectively bind biomolecules, which partly accounts for the low toxicity of ruthenium drugs.<sup>90, 91</sup> Transferrin and albumin are two proteins used by mammals to solubilise and transport iron, thereby reducing its toxicity. The ability of some ruthenium drugs to bind to transferrin has been proven.<sup>97-101</sup> Since rapidly dividing cells, such as microbially infected or cancer cells, have a greater requirement of iron, they increase the number of transferrin receptors on their surfaces. This implies that the amount of ruthenium taken up by these infected or cancerous cells is greater than the amount taken up by healthy cells. This selectivity of the drug towards the diseased cells accounts for a reduction on its general toxicity.

### **Anticancer activity**

Two approaches are commonly used for the design of new anticancer compounds. The trial-and-error approach consists on synthesizing as many compounds as possible that are analogous to a complex of known activity, but which has drawbacks that need to be solved. These new compounds are then tested for anticancer activity, both *in vitro* and *in vivo*.

The second approach is based on thorough studies of the properties of some particular complexes, with the final aim of reaching some knowledge about their mechanisms of action. The chemical, physical, pharmacological properties, the uptake of the drug, its biodistribution and its detoxifying processes are subject of study. This implies a multidisciplinary task in which collaboration of scientists from different fields is necessary. Step by step novel derivatives are developed as potential drugs in anticancer therapy.

The first generation of ruthenium compounds synthesized for anticancer purposes consists on a series of complexes that mimic platinum drugs and target DNA, just like cisplatin is generally accepted to do.

### 1.5. Classification of ruthenium complexes with anticancer properties

#### Ammine-chlorido derivatives

The first ruthenium complexes to be tested in search for anticancer properties were close imitators of cisplatin: several ammine and chlorido ligands were coordinated to Ru(II) and Ru(III) to form complexes with general formula  $[\text{Ru}(\text{NH}_3)_{6-x}\text{Cl}_x]^{Y+}$ . Those complexes in which the oxidation state of the ruthenium ion was (II) were expected to bind to DNA in an analogous way to cisplatin, and indeed the first experiments performed with the complexes  $[\text{Ru}(\text{II})(\text{NH}_3)_5\text{Cl}]^+$  (see Fig.1.11) and  $[\text{Ru}(\text{II})(\text{NH}_3)_5(\text{H}_2\text{O})]^{2+}$  fulfilled this expectation.<sup>102-104</sup> The cytotoxicity tests carried out with these species yielded however disappointing results. Interestingly, both *cis*- $[\text{Ru}(\text{III})(\text{NH}_3)_4\text{Cl}_2]^+$  and especially *fac*- $[\text{Ru}(\text{III})(\text{NH}_3)_3\text{Cl}_3]$  displayed a comparable antitumour activity to that of cisplatin in a few selected cell lines.<sup>99, 105</sup> It has been hypothesized that these complexes, once inside the cell, are reduced to less inert Ru(II) species, which bind to DNA after hydrolysis.<sup>92</sup> The trichlorido complex, being the most promising of all these compounds, was discarded for further investigation due to its poor water solubility.

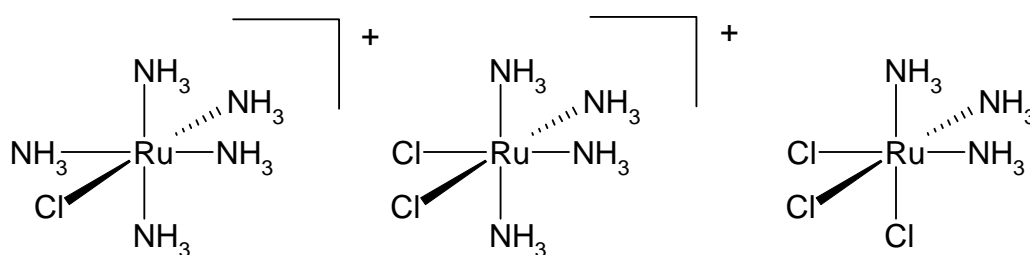


Fig.1.11. Ammine-chlorido derivatives. From left to right,  $[\text{Ru}(\text{II})(\text{NH}_3)_5\text{Cl}]^+$ , *cis*- $[\text{Ru}(\text{III})(\text{NH}_3)_4\text{Cl}_2]^+$  and *fac*- $[\text{Ru}(\text{III})(\text{NH}_3)_3\text{Cl}_3]$ .

#### Dimethylsulfoxide complexes

The substitution of the ammine ligands by dmsu molecules yields compounds with improved solubility. Both *cis*- and *trans*- $[\text{Ru}(\text{II})\text{Cl}_2(\text{dmsu})_4]$  (see Fig.1.12) were shown to be able to coordinate to guanine residues of DNA via the N7 position.<sup>106</sup> The better activity displayed by the *trans* complex with respect to its *cis* analogue, both *in vitro* and *in vivo*, in cytotoxicity tests, was explained by means of differences in kinetics. This *trans* isomer also seemed to overcome cisplatin resistance, as seen in the case of the P388 leukaemia cell line.<sup>107</sup> This observation, together with the fact that *trans*- $[\text{Ru}(\text{II})\text{Cl}_2(\text{dmsu})_4]$  shows a good

antimetastatic activity,<sup>107</sup> suggests that the *trans*-ruthenium complexes could be an interesting alternative to cisplatin, by acting through a different mechanism of action.

A series of dimethyl sulfoxide-ruthenium complexes was designed, which were inspired on the above-mentioned promising compound. Noteworthy are the compounds  $\text{Na}\{\text{trans}[\text{Ru}(\text{III})\text{Cl}_4(\text{dms})(\text{Him})]\}$ , (Him = imidazole), nicknamed NAMI, and the more stable  $[\text{H}_2\text{Im}][\text{trans}[\text{Ru}(\text{III})\text{Cl}_4(\text{dms})(\text{Him})]]$ , also known as NAMI-A (see Fig.1.12). The dms ligand is in both cases bound via the S atom. NAMI-A is the first ruthenium complex to have ever reached clinical testing for anticancer activity, of which it has recently completed phase-I studies. Nowadays, when surgical removal of primary cancers is efficient and successful, a complex such as NAMI-A, which presents an antimetastatic activity in a broad range of tumours including lung metastasis, is becoming of utmost interest.<sup>108, 109</sup>

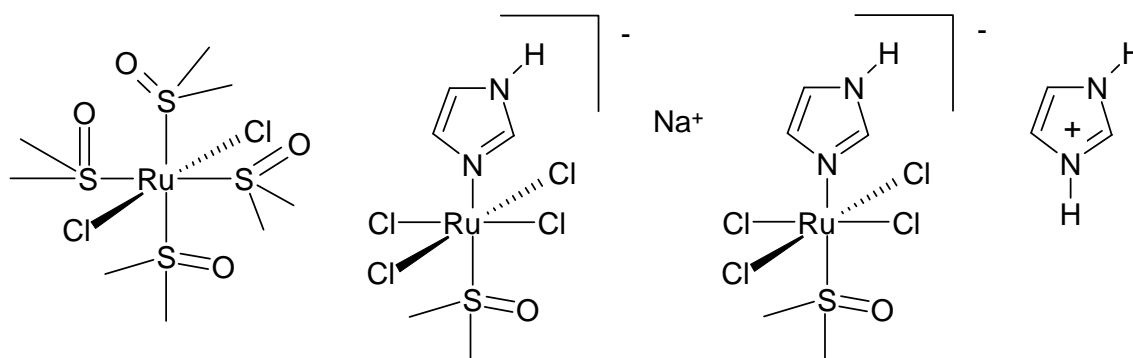


Fig.1.12. Dimethylsulfoxide complexes. From left to right,  $\text{trans}[\text{Ru}(\text{II})(\text{dms})_4\text{Cl}_2]$ ,  $\text{Na}\{\text{trans}[\text{Ru}(\text{III})\text{Cl}_4(\text{dms})(\text{Him})]\}$  (NAMI) and  $[\text{H}_2\text{Im}]\{\text{trans}[\text{Ru}(\text{III})\text{Cl}_4(\text{dms})(\text{Him})]\}$  (NAMI-A).

It is possible that these complexes are reduced to Ru(II) once inside the cell. It has been shown that NAMI loses two of its chlorido ligands, which are substituted by aqua ligands. This hydrated species could bind to several biomolecules, including DNA.<sup>110, 111</sup> However, the main mechanism of action of both NAMI and NAMI-A is thought not to be directly related to binding to DNA, but these molecules would exert their action via different ways than cisplatin.<sup>111-113</sup>

A series of NAMI-A analogues bearing a weakly basic heterocyclic nitrogen ligand *trans*- to dms was synthesized.<sup>108</sup> These complexes were found to be more stable than

NAMI-A in slightly acidic solution, and their *in vivo* effectiveness appeared to be slightly better than that of the parent compound. NAMI-A, as well as these analogues, were proven to have an effect on cell distribution among cell cycle phases. In the case of the parent compound a cell cycle arrest is induced in the G(2)-M phase, an effect which does not take place in the experiments carried out with the NAMI-A analogues.<sup>108</sup>

### Complexes with other heterocyclic ligands

Keppler and co-workers prepared a group of complexes, the so-called “Keppler-type” compounds. These are anionic ruthenium(III) complexes with monodentate heterocyclic nitrogen donor ligands, the most successful of which have the formula *trans*-[RuCl<sub>4</sub>(L)<sub>2</sub>]<sup>-</sup>, where L is imidazole (KP418) or indazole (KP1019 and KP1339), and the counterion (LH)<sup>+</sup> or Na<sup>+</sup> (see Fig.1.13). KP1019 and KP1339 were reported effective in inhibiting platinum-resistant colorectal carcinomas in rats;<sup>114</sup> KP1019 recently completed phase-I clinical trials.<sup>100</sup>

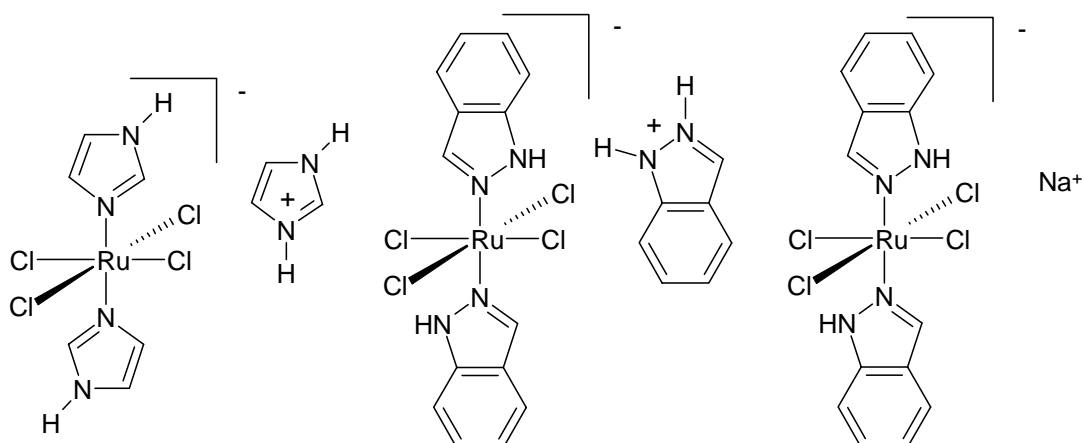


Fig.1.13. Molecular formula of the ruthenium(III) complexes imidazolium *trans*-[tetrachloridobis(imidazole)ruthenate(III)] (KP418), indazolium *trans*-[tetrachloridobis(indazole)ruthenate(III)] (KP1019) and sodium *trans*-[tetrachloridobis(indazole)ruthenate(III)] (KP1339).

The mechanism of action of these complexes is thought to differ considerably from that of cisplatin. The involvement of the “activation-by-reduction” process and the transferrin-mediated transport into the cells seem to play a very important role in the efficiency of the “Keppler-type” complexes,<sup>100, 114</sup> as in the case of NAMI-A.

Several ruthenium polypyridyl complexes (see Fig.1.14) were synthesised, their *in vitro* DNA binding was studied and their antitumour activity in murine L1210 leukaemia and human cervix carcinoma HeLa cells was investigated. The only complex of this kind which was reported to be antitumour active was *mer*-[Ru(III)(tpy)Cl<sub>3</sub>], where tpy is 2,2':6',2''-terpyridine.<sup>115</sup> This complex was also the only one of this group that showed significant bifunctional DNA binding, therefore its cytotoxicity was thought to be related to the possibility of interstrand DNA cross-link formation.<sup>116, 117</sup> Its poor water solubility, however, hampered its further progress into the clinical trials.

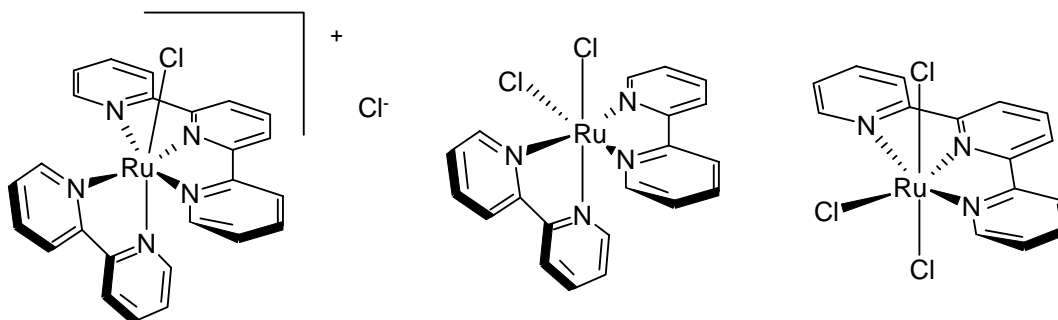


Fig.1.14. Molecular formula of the ruthenium polypyridyl complexes  
 $[Ru(II)(bpy)(tpy)Cl]Cl$ ,  $cis-[Ru(II)(bpy)_2Cl_2]$ , and  $mer-[Ru(III)(tpy)Cl_3]$   
 ( $bpy = 2,2'$ -bipyridine,  $tpy = 2,2':6',2''$ -terpyridine).

Ten years later an X-ray structure was reported of the  $cis-[Ru(II)(bpy)_2]^{2+}$  fragment ( $bpy = 2,2'$ -bipyridine) bifunctionally binding to two DNA model bases.<sup>118</sup> However, the ruthenium(II) precursor  $cis-[Ru(II)(bpy)_2Cl_2]$  had been proven mostly inactive in the above-described biological tests.<sup>115</sup> The fact that this complex can bind two model bases (after chloride removal) but it is inactive *in vitro* questions the relation that has been established between the possibility of bifunctionally binding to DNA and the cytotoxicity of ruthenium polypyridyl complexes.

As a last noteworthy example of *in vitro* antitumour-active ruthenium complexes with heterocyclic ligands, one of the isomers of  $cis-[Ru(II)(azpy)_2Cl_2]$  (see Fig.1.15), where  $azpy = 2$ -phenylazopyridine, showed a remarkably high cytotoxicity against fast-growing cell lines.<sup>119, 120</sup> The higher activity of  $cis-[Ru(II)(azpy)_2Cl_2]$  with respect to  $cis-[Ru(II)(bpy)_2Cl_2]$  has been related to a higher flexibility of the  $azpy$  ligand, which

allows an easier substitution of the chloride ligand and thus the binding of the complex to even two DNA bases.<sup>119</sup>

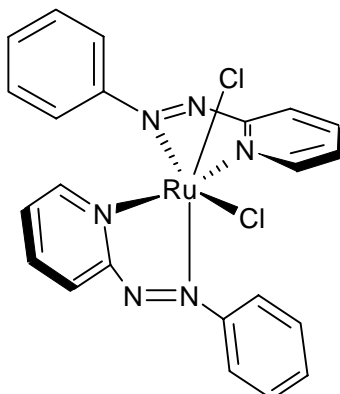


Fig.1.15. Molecular formula of the most active isomer of *cis*-[Ru(II)(azpy)<sub>2</sub>Cl<sub>2</sub>].

### Ruthenium polyaminocarboxylate complexes

There has been a wide interest in the redox properties of ruthenium(III/IV) complexes with polydentate mixed-donor ligands. Ligands like ethylenediaminetetraacetate (edta), 1,2-cyclo-hexanediaminetetraacetate (cdta), 1,2-propylendiaminetetraacetate (pdta), triethylenetriaminehexaacetate (ttha), N,N,N',N'-tetrakis(2-pyridyl)adipamide (tpda), N-hydroxyethylethylenediaminetriacetate (hedtra) and others from the H<sub>4</sub>edta family have been coordinated to ruthenium to form complexes with acid-base and redox properties that have been thoroughly studied.<sup>121-125</sup>

Some of these complexes were found to be able to bind to DNA model bases, as well as to blood proteins, such as albumin and transferrin, which suggested that they might have an antitumour activity.<sup>97, 110, 126-128</sup> While this is still under study, the complex containing cdta was the first Ru(IV) compound reported to display cytotoxic activity.<sup>129, 130</sup>

### Organoruthenium complexes

The monodentate ruthenium(II) arene complexes of the type [(η<sup>6</sup>-arene)Ru(II)(en)X][PF<sub>6</sub>], where en is ethylenediamine and X is chloride or iodide (see Fig.1.16), constitute a group that is believed to exert an antitumour action via mechanisms different from those of other ruthenium(III) complexes such as NAMI-A or KP1019.<sup>131-134</sup> The chlorido or iodido ligand is readily lost to yield the more reactive aqua species.<sup>135</sup> DNA appears to be a target for these compounds, which bind preferentially to the guanine

residues and also interact “non-covalently” via both arene intercalation and minor groove binding.<sup>136, 137</sup>

$[(\eta^6\text{-toluene})\text{Ru(II)}(\text{pta})\text{Cl}_2]$  (RAPTA-T), where pta is 1,3,5-triaza-7-phosphaadamantane (see Fig.1.16), is the parent compound from which a group of water-soluble selective DNA-binding antimetastatic drugs was synthesized.<sup>138, 139</sup> The RAPTA compounds exhibit pH dependent DNA binding, almost no toxicity towards cancer cells *in vitro* and no toxicity at all towards healthy cells, also *in vitro*. However, RAPTA-T was found to inhibit lung metastases in mice bearing a mammary carcinoma, again with only mild effects on the primary tumours. The mechanism of action of the RAPTA compounds is only starting to be investigated.<sup>140</sup>

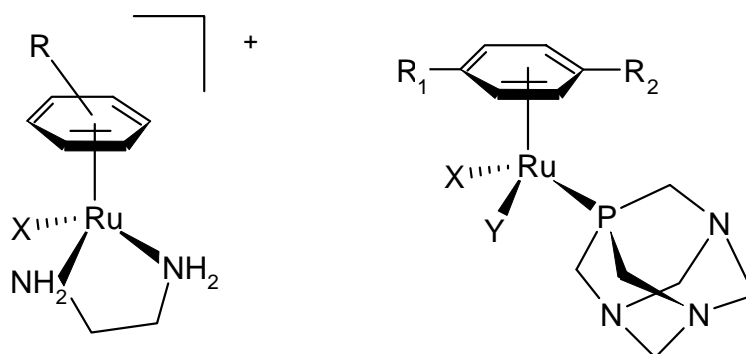


Fig.1.16. General formula of two groups of organometallic ruthenium(II) complexes with modified arene ligands. On the left,  $[(\eta^6\text{-arene})\text{Ru(II)}(\text{en})\text{X}]^+$ , where the arene can be benzene, *p*-cymene, biphenyl, 5,8,9,10-tetrahydroanthracene or 9,10-dihydroanthracene. *X* is Cl or I. On the right,  $[(\eta^6\text{-arene})\text{Ru(II)}(\text{pta})\text{XY}]$  (RAPTA complexes). *R*<sub>1</sub>, *R*<sub>2</sub> are alkyl groups; *X* and *Y* can be Cl or different  $\mu$ -dicarboxylate ligands.

### Photoreactive ruthenium compounds that induce DNA cleavage

Recently some photoreactive ruthenium(II) complexes have been under study as potential anticancer agents.<sup>91</sup> In phototherapy, a photosensitizer absorbs light and it then reacts with a targeted endogenous molecule ( $\text{O}_2$  or DNA) via energy or electron transfer.<sup>91</sup> Metal compounds such as polyazaaromatic ruthenium(II) complexes are good candidates as photosensitizers, with properties that can be modulated by introducing changes in the ligands.<sup>141</sup>

Once a photosensitizer is excited, it can react with a dioxygen molecule, leading to the production of singlet dioxygen.<sup>141</sup> This very reactive species may induce formation of

oxidizing agents, such as superoxide or hydroxyl radicals, that can damage DNA by oxidizing the guanine moiety or even cleaving the DNA strand.<sup>141</sup>

Important advances in this field are the discovery that singlet dioxygen production by  $[\text{Ru}(\text{II})(\text{bpy})_2(\text{phen})]^{2+}$  is able to block partially the activity of a bacteriophage RNA-polymerase,<sup>142</sup> as well as the encapsulation of the complex  $\{\text{Ru}(\text{II})[\text{dip}(\text{SO}_3\text{Na})_2]_3\}$ , where  $\text{dip}(\text{SO}_3\text{Na})_2$  is the sodium salt of disulfonated 4,7-diphenyl-1,10-phenanthroline, into polyacrylamide nanoparticles for use in photodynamic therapy.<sup>143</sup> The main drawbacks of the *in vivo* treatments in photodynamic therapy are collateral damages to healthy cells, acquired resistance and limitation of light penetration in tissues.<sup>143</sup>

An electron-transfer process can also be involved in phototherapy leading to DNA cleavages. Ru(II)-2,3-naphthalocyanine compounds showed activity *in vivo* against cancer cells in absence of singlet oxygen.<sup>144</sup> Besides, it has been demonstrated that a photo-induced electron transfer takes place from a guanine to the excited state of some Ru(II) complexes containing  $\pi$ -deficient ligands such as TAP (1,4,5,8-tetraazaphenanthrene), HAT (1,4,5,8,9,12-hexaazatriphenylene) or BPZ (2,2'-bipyrazine). The formation of the radical on the guanine is enough to provoke DNA cleavages.<sup>141, 145</sup>

### Dinuclear ruthenium complexes

As explained in section 1.3, several dinuclear platinum complexes have been synthesised in search for compounds that interact with DNA in a drastically different way to cisplatin. The interaction of each of these complexes with DNA, as well as its cellular processing, are expected to be unique, involving long-range intrastrand cross-links upon DNA and van der Waals interactions within the minor groove, amongst others, with as final aim finding a drug capable of overcoming cisplatin resistance.

Although the electrochemical and photophysical properties of several cationic ruthenium dimeric complexes with heterocyclic bridging ligands had been extensively studied in the 1970s,<sup>146</sup> the testing of this kind of complexes in the oncological field was only reported in the last decade. A group of these complexes has the general formula  $[\{\text{trans-Ru}(\text{III})\text{Cl}_2(\text{dmsO})\text{L}_1\text{L}_2\}_2(\mu\text{-L}_3)]^{m+}$ .  $\text{L}_1$ ,  $\text{L}_2$  are Cl or dmsO.  $\text{L}_3$  is a nitrogen heterocyclic ligand with at least two nitrogen atoms, like pyrazine (pyz), pyrimidine (pym), 4, 4'-bipyridine (bipy), 1,2-bis(4-pyridyl)ethane (etbipy), 1,2-bis(4-pyridyl)propane (prbipy) or *trans*-1,2-bis(4-pyridyl)ethylene (etilbipy). Finally,  $m$  is 0, 1 or 2 (see Fig.1.17). These complexes are based on the mononuclear NAMI-A.<sup>147</sup> The dinuclear complexes

obtained from this antimetastatic compound show a chemical stability that renders them very suitable for pharmacological formulation, as well as a high antimetastatic activity that indicates they could be helpful in the treatment of tumours with a high degree of metastatic diffusion, such as mammary, lung or digestive tract carcinomas.<sup>148-151</sup>

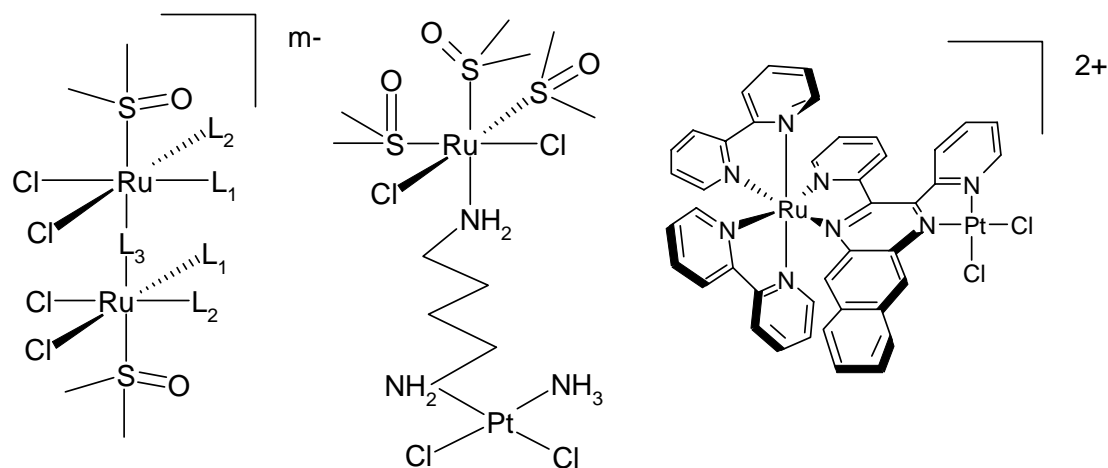


Fig.1.17. From left to right, the general formula of dinuclear Ru(III) complexes based on NAMI-A; a Ru(II)-Pt(II) heterodinuclear complex with an aliphatic linker and a Ru(II)-Pt(II) heterodinuclear complex with an intercalating linker.

*In vitro* studies carried out with these complexes showed that a G(2)-M cell cycle arrest was induced, which was dependant on the ruthenium concentration and on the cell line, while their cytotoxicity was only mild against human and murine cell lines. This behaviour is comparable to that of the parent mononuclear complex NAMI-A. Moreover the cell cycle-regulating protein cyclin B appears to be significantly modified.<sup>152</sup>

A variation of these compounds, where dmso is substituted by tetramethylene sulfoxide (tmsu) is currently under study. So far only the mononuclear compounds have been described,<sup>153, 154</sup> as well as the anionic ruthenium(III) dinuclear versions of these complexes with pyrazine as bridging ligand.<sup>155</sup>

Mixed-valent ruthenium tetracarboxylate complexes were shown to have a mild antineoplastic activity against P388 leukaemia cell lines. However, these complexes are poorly water soluble.<sup>109</sup> Mixed-valent complexes of structural formula  $[(RuL)_2(\mu-O_2CR)_4](PF_6)$  were tested for cytotoxicity against HeLa and multidrug resistant CoLo 320DM human cancer cells. L is an imidazole, a 1-methylimidazole or an aqua

ligand when R is a methyl group, and L is an ethanol when R is a ferrocenyl (Fc) or a Fc-CH=CH-. The related series of complexes with formula  $M_3[Ru_2(\mu-O_2CR)_4(H_2O)_2] \cdot 4H_2O$ , where M is  $Na^+$  when R is  $m-C_6H_4SO_3^-$  and M is  $K^+$  when R is  $p-C_6H_4SO_3^-$  were also tested for cytotoxicity against the above-mentioned HeLa and multidrug resistant CoLo 320DM human cancer cells. A few of these complexes show some cytotoxicity and, more interestingly, CoLo 320DM was found to be more sensitive to these complexes than HeLa, which is more sensitive than CoLo 320DM to cisplatin. This observation suggests that the mechanism of action of these complexes is different to that of the classical platinum drugs.<sup>156</sup>

Complexes with  $\mu$ -N,N'-diphenylformamidinate and  $\mu$ -(fluoroanilino)pyridinates have also been prepared. The compound  $\mu$ -[(F<sub>3</sub>CCO<sub>2</sub>)<sub>4</sub>(F<sub>3</sub>CCO<sub>2</sub>)Ru<sub>2</sub>] forms *cis*-[ $\mu$ -(F<sub>3</sub>CCO<sub>2</sub>)<sub>4</sub>- $\mu$ -(9EtGua)Ru<sub>2</sub>(CH<sub>3</sub>OH)<sub>2</sub>]<sup>2+</sup> where 9EtGua = 9-ethylguanine in which the guanines bridge between the two Ru(II) atoms in a N7-O6 head-to-tail fashion.<sup>99, 157</sup>

The compound  $\mu$ -O-[Ru(III)(bpy)<sub>2</sub>(H<sub>2</sub>O)<sub>2</sub>]<sub>2</sub><sup>4+</sup> is a borderline example. This dinuclear ruthenium(III) complex has been proven to be effective in double-stranded DNA cleavage. However, its action is thought to be due to the mononuclear [Ru(III)(bpy)<sub>2</sub>(H<sub>2</sub>O)<sub>2</sub>]<sup>2+</sup>, which is formed by intracellular reduction of the dinuclear complex.<sup>158, 159</sup>

The combination of metal moieties with different properties provides systems of great interest. Although the following three examples fall slightly out of the scope of the dinuclear ruthenium complexes, they are worth mentioning in relation with them. In general ruthenium complexes are less reactive than platinum compounds, and the design of ruthenium/platinum heterodinuclear complexes provides molecules that can selectively, sequentially react with particular DNA sequences and facilitate unique DNA modification.<sup>160</sup> The complex  $\{[cis, fac-Ru(II)Cl_2(dmsO)_3][\mu-NH_2(CH_2)_4NH_2][cis-PtCl_2(NH_3)]\}$  (see Fig.1.17) was the first of the series.<sup>161</sup> These anticancer compounds are suspected to exert their action via a novel mechanism of action, involving interstrand crosslinks in which each metal atom is coordinated to one strand of DNA. A second strategy is the coupling of a light absorber to a cisplatin moiety by a ligand capable of intercalative binding with DNA. The  $\{[M(bpy)_2]_2(\mu-dpb)[PtCl_2]\}$ <sup>2+</sup> complexes, where M is Ru(II) or Os(II) and dpb is 2,3-bis(2-pyridyl)benzoquinoxaline, form primarily intrastrand crosslinks, but interstrand crosslinks were also formed (see Fig.1.17).<sup>162, 163</sup> Finally, the highly flexible heterodinuclear complex [Ru(II)(tpy)]( $\mu$ -dtdeg)[PtCl]<sup>3+</sup>, where dtdeg is bis[4'-((2,2':6',2''-terpyridyl)-diethyleneglycol ether)], was synthesized.<sup>164</sup> Modifications of

the linker are currently under study in search for a derivative of this complex with an increased antitumour activity.

### **1.6. How these drugs work: mechanisms of action**

In the past two decades a new approach to treating cancer, known as targeted therapy, has started to emerge.<sup>165</sup> While classical chemotherapy involves drugs interfering with replication and mitotic processes of tumour cells, their “target” being thus DNA, a more recent strategy involves targeting cellular signalling pathways of cancer cells, yielding highly effective cancer treatments with less severe side effects.<sup>166</sup> The recent discovery of receptors and growth factors, such as epidermal growth factor receptor (EGFR), vascular endothelial growth factor (VEGF), or cyclin-dependent kinases (CDK) that are upregulated in cancer cells provides new possible targets for cancer therapy.<sup>166</sup> The high specificity of targeted therapies accounts for a more manageable toxicity profile of the drugs. Its main drawback is that most targeted therapeutic drugs are only effective in specific types of cancer (e.g. Imatinib mesylate for chronic myelogenous leukaemia, Erlotinib for advanced non-small cell lung cancer, etc), which limits their applicability.<sup>165</sup> In recent years, ruthenium-based drug research is moving from classical chemotherapy into the non-conventional approaches.

Classical ruthenium anticancer therapy is based on the capability of ruthenium to coordinatively bind to DNA via some of the nitrogen atoms of the nucleic bases, in particular via the nitrogen N7 of guanine. This is also the action expected from the first ruthenium complexes designed as anticancer drugs, the ammine-chloro derivatives. The novelty is that these complexes are thought to act as ruthenium(III) prodrugs, which would be inactive until the ruthenium gets reduced in the cytosol.<sup>92, 102-104</sup>

Binding to DNA via an additional mode was achieved when an intercalating polypyridyl ligand was added to the ruthenium system. Additional properties that make polypyridyl groups desirable ruthenium ligands are their photoluminescence, which makes them suitable as DNA probes, as well as the stability of the complexes that they can originate, amongst others.<sup>165</sup> An often encountered problem is the poor water solubility of many of these complexes.

While ruthenium(II) dimethylsulfoxide complexes were conceived as water-soluble versions of the above-mentioned ammine-chlorido derivatives, the good antimetastatic activity of *trans*-[Ru(II)Cl<sub>2</sub>(dmsO)<sub>4</sub>] soon became apparent, as well as its capability to

overcome cisplatin resistance in certain cell lines. These two observations suggested a mechanism of action different to the by then widely accepted mechanism of cisplatin.<sup>107</sup>

The use of polyaminocarboxylate ligands in metallopharmaceutical applications seemed a logical option due to their resemblance to biological molecules.<sup>167</sup> Several of these complexes turned out to be antitumour active with low systemic toxicity. Some of them were proven to bind to DNA, alter its conformation and even induce DNA cleavage.<sup>110, 168</sup> In addition, several of these complexes were found to be effective NO scavengers and protease inhibitors, thus they could be used to treat various diseases or serve as antiviral agents.<sup>169</sup>

DNA also seems to be a target for the organometallic arene-ruthenium complexes. The coordination of the ruthenium atom to the nucleic bases was seen to be enhanced through H-bonding interactions or weakened because of steric interactions, suggesting the possibility to design compounds to target specific nucleotides.<sup>170</sup> The binding of the complex to DNA appeared to be promoted by hydrophobic arene-purine base  $\pi$ - $\pi$  stacking interactions when large ring systems were used.<sup>136</sup>

Finally, the photoreactive ruthenium compounds can also be considered within the classical therapy, as well as most of the dinuclear ruthenium compounds aboved described, as their target is still DNA.

One of the most successful ruthenium-based anticancer drugs to date, NAMI-A, displays a unique behaviour. Its lack of cytotoxicity *in vitro*, together with its *in vivo* ability to reduce metastases weight while the primary tumour remains unaffected, appear to exclude DNA as the primary target. NAMI-A binds strongly to serum proteins, including the iron transporter transferrin, and it induces cell arrest in the premitotic G(2)-M phase.<sup>108</sup> Studies carried out with NAMI-A analogues suggest that the imidazole fragment is not essential for the antimetastatic activity. On the other hand, the reinforcement of the axis dmsO-Ru-N-donor ligand by using N-containing heterocycles that are less basic than imidazole reduce the loss of dmsO from the complex, increasing at the same time the antitumour action.<sup>108</sup>

The only ruthenium drug other than NAMI-A currently undergoing clinical trials, KP1019 (see Fig.1.13), is significantly cytotoxic *in vitro* against colorectal cell lines SW480 and HT29 by inducing apoptosis.<sup>114</sup> The drug was also found to be highly effective in *in vivo* tests in which cisplatin had been inactive. The mechanism of action of the “Keppler-type” complexes is thought to be due to at least two factors, namely the

“activation-by-reduction” process and the transferrin-mediated transport into the cells.<sup>100, 114</sup> KP1019 is capable of forming crosslinks with DNA that are different to those originated by cisplatin. DNA is not completely excluded as a target for KP1019. However, it induces apoptosis in colorectal cell lines mainly via the intrinsic mitochondria pathway.<sup>100, 171</sup> An increase in the number of indazole ligands of these complexes improved significantly the *in vitro* cytotoxicity in several cell lines, allegedly because the cellular uptake is facilitated and the reduction potential is increased.<sup>172</sup>

Although DNA appears to be a target for the organometallic arene-ruthenium complexes (*vide supra*), the RAPTA complexes constitute a particular case (see Fig.1.16). Parting from the observation that the complex RAPTA-T displayed a similar *in vivo* activity to NAMI-A, albeit with lower systemic toxicity, a group of derivatives from this parent compound was synthesised, which were then tested *in vitro* for interactions with different biological molecules and *in vivo* for antitumour and antimetastatic activity.<sup>140, 173</sup> Several of these complexes showed a reduction in lung metastases in mice, while leaving the primary tumour mostly unaffected. Moreover some specific protein-binding interactions were detected.<sup>140, 173</sup> A proteomic-based analytical approach based on 2D PAGE and laser-ablation inductively-coupled mass spectrometry (ICP-MS) appears to be a promising tool to identify the specific proteins interacting with ruthenium-based drugs.<sup>174-176</sup>

In conclusion, ruthenium drugs are particularly important in the clinic due to their low toxicity. These complexes appear in some cases to function in a different way to classical chemotherapies. For this reason the conventional tests used to screen new compounds for anticancer activity should be treated with caution, and new assays for potential drug candidates are needed. Methods are required to rapidly locate drug interactions with key protein targets. Finally, even when metal drugs are not found directly active, they may interact with the proteins that regulate apoptosis, thereby modifying cell behaviour.

### ***1.7. Aim and scope of this thesis***

The existence of two common approaches for the design of new anticancer drugs has been mentioned in section 1.4. The first method, often known as “trial-and-error”, is based on the synthesis and testing of libraries of closely-related complexes. This thesis is based on the second approach, which parts from the synthesis of very few compounds. These are thoroughly studied in order to gain some insight about the way they function and, subsequently, how they can be improved.

The subject is first introduced earlier in **Chapter 1** with an overview about medicinal inorganic chemistry, in particular about platinum and ruthenium anticancer agents. Special attention is given to the mechanisms of action of these antitumour drugs, as well as the structure-activity relationships that are known to date.

A group of ruthenium(II) polypyridyl complexes is presented in **Chapter 2**. A complete description is given of the synthesis and characterization by several methods of three compounds derived from the cytotoxic, but poorly water-soluble complexes, Ru(III)(tpy)Cl<sub>3</sub> and  $\alpha$ -Ru(II)(azpy)<sub>2</sub>Cl<sub>2</sub>.

With the purpose of proving or discarding DNA as a potential target of the newly-synthesised complexes, a study was carried out, which is included in **Chapter 3**. NMR is used as a basic tool to follow the reaction between each of the complexes and a DNA model base, allowing identifying kinetic differences amongst the three proposed compounds. A conformational investigation of the so-called ruthenium–model base adduct was found to be of theoretical interest.

Other modes of interaction between ruthenium complexes and DNA were looked into with the help of circular and linear dichroism. The question “is there a correlation between these interactions and the antitumour activity of the selected ruthenium(II) polypyridyl complexes?” has been dealt with in **Chapter 4**. The synthesis and characterisation of a ruthenium(II) homodinuclear complex are described. This compound, together with a few previously-known ruthenium(II) polypyridyl complexes, is investigated in the search for some structure-activity relationships.

In **Chapter 5** some suggestions for future directions in this work are given. The synthesis of a new ruthenium(II) homodinuclear complex, which is closely related to the other compounds herein described, raised several new questions.

**Chapter 6** offers a summary and discussion of the results presented in this thesis.

Finally, a study carried out in relation with the work included in **Chapter 3**, in this case excluding the metal atom, is briefly described in the **Appendix**.

Parts of this thesis have been published<sup>177-179</sup> or submitted for publication.<sup>180</sup>

## 1.8. References

1. Orvig, C.; Abrams, M. J., *Chem. Rev.* **1999**, *99*, 2201-2203.
2. Raymond, K. N., *Bioinorganic chemistry II*. Washington, **1977**.
3. Dixon, N. E.; Gazzola, C.; Blakeley, R. L.; Zerner, B., *J. Am. Chem. Soc.* **1975**, *97*, 4131-4133.

4. Kendrick, M. J.; May, M. T.; Plishka, M. J.; Robinson, K. D., Metals in biological systems. Chichester, **1992**.
5. Antman, K. H., *Oncologist* **2001**, *6*, 1-2.
6. Waxman, S.; Anderson, K. C., *Oncologist* **2001**, *6*, 3-10.
7. Lloyd, N. C.; Morgan, H. W.; Nicholson, B. K.; Ronimus, R. S., *Angew. Chem.-Int. Edit.* **2005**, *44*, 941-944.
8. Guo, Z. J.; Sadler, P. J., *Angew. Chem.-Int. Edit.* **1999**, *38*, 1513-1531.
9. Peyrone, M., *Ann. Chemie Pharm.* **1845**, *51*, 1-29.
10. Rosenberg, B.; van Camp, L.; Trosko, J. E.; Mansour, V. H., *Nature* **1969**, *222*, 385-386.
11. Rosenberg, B.; van Camp, L.; Krigas, T., *Nature* **1965**, *205*, 698-699.
12. Reedijk, J., *Pure Appl. Chem.* **1987**, *59*, 181-192.
13. Wittgen, B. P. H.; Kunst, P. W. A.; Perkins, W. R.; Lee, J. K.; Postmus, P. E., *J. Aerosol Med.-Depos. Clear. Eff. Lung* **2006**, *19*, 385-391.
14. Ishida, S.; Lee, J.; Thiele, D. J.; Herskowitz, I., *Proc. Natl. Acad. Sci. U. S. A.* **2002**, *99*, 14298-14302.
15. Jamieson, E. R.; Lippard, S. J., *Chem. Rev.* **1999**, *99*, 2467-2498.
16. Fichtinger-Schepman, A. M. J.; van der Veer, J. L.; den Hartog, J. H. J.; Lohman, P. H. M.; Reedijk, J., *Biochemistry* **1985**, *24*, 707-713.
17. Eastman, A., *Biochemistry* **1986**, *25*, 3912-3915.
18. Lee, K. B.; Wang, D.; Lippard, S. J.; Sharp, P. A., *Proc. Natl. Acad. Sci. U. S. A.* **2002**, *99*, 4239-4244.
19. Naser, L. J.; Pinto, A. L.; Lippard, S. J.; Essigmann, J. M., *Biochemistry* **1988**, *27*, 4357-4367.
20. Maeda, Y.; Nunomura, K.; Ohtsubo, E., *J. Mol. Biol.* **1990**, *215*, 321-329.
21. Kagemoto, A.; Takagi, H.; Naruse, K.; Baba, Y., *Thermochim. Acta* **1991**, *190*, 191-201.
22. Poklar, N.; Pilch, D. S.; Lippard, S. J.; Redding, E. A.; Dunham, S. U.; Breslauer, K. J., *Proc. Natl. Acad. Sci. U. S. A.* **1996**, *93*, 7606-7611.
23. Yang, D. Z.; van Boom, S. S. G. E.; Reedijk, J.; van Boom, J. H.; Wang, A. H. J., *Biochemistry* **1995**, *34*, 12912-12920.
24. Takahara, P. M.; Rosenzweig, A. C.; Frederick, C. A.; Lippard, S. J., *Nature* **1995**, *377*, 649-652.
25. den Hartog, J. H. J.; Altona, C.; van Boom, J. H.; van der Marel, G. A.; Haasnoot, C. A. G.; Reedijk, J., *J. Biomol. Struct. Dyn.* **1985**, *2*, 1137-1155.
26. den Hartog, J. H. J.; Altona, C.; van der Marel, G. A.; Reedijk, J., *Eur. J. Biochem.* **1985**, *147*, 371-379.
27. Herman, F.; Kozelka, J.; Stoven, V.; Guittet, E.; Girault, J. P.; Huynh-Dinh, T.; Igolen, J.; Lallemand, J. Y.; Chottard, J. C., *Eur. J. Biochem.* **1990**, *194*, 119-133.
28. Sherman, S. E.; Gibson, D.; Wang, A. H. J.; Lippard, S. J., *Science* **1985**, *230*, 412-417.
29. Admiraal, G.; van der Veer, J. L.; de Graaff, R. A. G.; den Hartog, J. H. J.; Reedijk, J., *J. Am. Chem. Soc.* **1987**, *109*, 592-594.
30. Sherman, S. E.; Gibson, D.; Wang, A. H. J.; Lippard, S. J., *J. Am. Chem. Soc.* **1988**, *110*, 7368-7381.
31. Legendre, F.; Bas, V.; Kozelka, J.; Chottard, J. C., *Chem.-Eur. J.* **2000**, *6*, 2002-2010.
32. Ohndorf, U. M.; Rould, M. A.; He, Q.; Pabo, C. O.; Lippard, S. J., *Nature* **1999**, *399*, 708-712.
33. Setlow, R. B.; Carrier, W. L., *Proc. Natl. Acad. Sci. U. S. A.* **1964**, *51*, 226-231.

34. Boyce, R. P.; Howard-Flanders, P., *Proc. Natl. Acad. Sci. U. S. A.* **1964**, *51*, 293-300.
35. Sancar, A., *Science* **1994**, *266*, 1954-1956.
36. Wozniak, K.; Blasiak, J., *Acta Biochim. Pol.* **2002**, *49*, 583-596.
37. Cohen, S. M.; Jamieson, E. R.; Lippard, S. J., *Biochemistry* **2000**, *39*, 8259-8265.
38. Wei, M.; Cohen, S. M.; Silverman, A. P.; Lippard, S. J., *J. Biol. Chem.* **2001**, *276*, 38774-38780.
39. Jung, Y. W.; Mikata, Y.; Lippard, S. J., *J. Biol. Chem.* **2001**, *276*, 43589-43596.
40. Yarnell, A. T.; Oh, S.; Reinberg, D.; Lippard, S. J., *J. Biol. Chem.* **2001**, *276*, 25736-25741.
41. Barnes, K. R.; Lippard, S. J., *Metal ions in biological systems*. Basel, **2004**; Vol. 42, p 158-159.
42. Brown, S. J.; Kellett, P. J.; Lippard, S. J., *Science* **1993**, *261*, 603-605.
43. Huang, J. C.; Zamble, D. B.; Reardon, J. T.; Lippard, S. J.; Sancar, A., *Proc. Natl. Acad. Sci. U. S. A.* **1994**, *91*, 10394-10398.
44. Wei, M.; Burenkova, O.; Lippard, S. J., *J. Biol. Chem.* **2003**, *278*, 1769-1773.
45. Altaha, R.; Liang, X.; Yu, J. J.; Reed, E., *Int. J. Mol. Med.* **2004**, *14*, 959-970.
46. Brabec, V.; Kaspárková, J., *Drug Resist. Update* **2005**, *8*, 131-146.
47. Thatcher, N.; Lind, M., *Semin. Oncol.* **1990**, *17*, 40-48.
48. Alberts, D. S.; Green, S.; Hannigan, E. V.; Otoole, R.; Stocknovack, D.; Anderson, P.; Surwit, E. A.; Malvlya, V. K.; Nahhas, W. A.; Jolles, C. J., *J. Clin. Oncol.* **1992**, *10*, 706-717.
49. Uchida, N.; Takeda, Y.; Kasai, H.; Maekawa, R.; Sugita, K.; Yoshioka, T., *Anticancer Res.* **1998**, *18*, 3375-3379.
50. Lebwohl, D.; Canetta, R., *Eur. J. Cancer* **1998**, *34*, 1522-1534.
51. Hasegawa, Y.; Takanashi, S.; Okudera, K.; Aoki, M.; Basaki, K.; Kondo, H.; Takahata, T.; Yasui-Furukori, N.; Tateishi, T.; Abe, Y.; Okumura, K., *Jpn. J. Clin. Oncol.* **2004**, *34*, 647-653.
52. Kawase, S.; Okuda, T.; Ikeda, M.; Ishihara, S.; Itoh, Y.; Yanagawa, S.; Ishigaki, T., *Gynecol. Oncol.* **2006**, *102*, 493-499.
53. Takaoka, E. I.; Kawai, K.; Ando, S.; Shimazui, T.; Akaza, H., *Jpn. J. Clin. Oncol.* **2006**, *36*, 60-63.
54. Sato, Y.; Takayama, T.; Sagawa, T.; Okamoto, T.; Miyanishi, K.; Sato, T.; Araki, H.; Iyama, S.; Abe, S.; Murase, K.; Takimoto, R.; Nagakura, H.; Hareyama, M.; Kato, J.; Niitsu, Y., *Cancer Chemother. Pharmacol.* **2006**, *58*, 570-576.
55. Shirai, T.; Hirose, T.; Noda, M.; Ando, K.; Lshida, H.; Hosaka, T.; Ozawa, T.; Okuda, K.; Ohnishi, T.; Ohmori, T.; Horichi, N.; Adachi, M., *Lung Cancer* **2006**, *52*, 181-187.
56. Shinohara, N.; Harabayashi, T.; Suzuki, S.; Nagao, K.; Nagamori, S.; Matsuyama, H.; Naito, K.; Nonomura, K., *J. Clin. Oncol.* **2006**, *24*, 236S-236S.
57. Misset, J. L., *Br. J. Cancer* **1998**, *77*, 4-7.
58. Kelland, L. R.; Abel, G.; McKeage, M. J.; Jones, M.; Goddard, P. M.; Valenti, M.; Murrer, B. A.; Harrap, K. R., *Cancer Res.* **1993**, *53*, 2581-2586.
59. Choi, S.; Filotto, C.; Bisanzo, M.; Delaney, S.; Lagasee, D.; Whitworth, J. L.; Jusko, A.; Li, C. R.; Wood, N. A.; Willingham, J.; Schwenker, A.; Spaulding, K., *Inorg. Chem.* **1998**, *37*, 2500-2504.
60. Lemma, K.; Berglund, J.; Farrell, N.; Elding, L. I., *J. Biol. Inorg. Chem.* **2000**, *5*, 300-306.
61. [http://www.gpc-biotech.com/en/anticancer\\_programs/satraplatin/](http://www.gpc-biotech.com/en/anticancer_programs/satraplatin/), GPC-Biotech, Anticancer Programs. In **2007**.

62. Bengtson, E. M.; Rigas, J. R., *Drugs* **1999**, *58*, 57-69.
63. Holford, J.; Sharp, S. Y.; Murrer, B. A.; Abrams, M.; Kelland, L. R., *Br. J. Cancer* **1998**, *77*, 366-373.
64. Treat, J.; Schiller, J.; Quoix, E.; Mauer, A.; Edelman, M.; Modiano, M.; Bonomi, P.; Ramlau, R.; Lemarie, E., *Eur. J. Cancer* **2002**, *38*, S13-S18.
65. Gelmon, K. A.; Vandenberg, T. A.; Panasci, L.; Norris, B.; Crump, M.; Douglas, L.; Walsh, W.; Matthews, S. J.; Seymour, L. K., *Ann. Oncol.* **2003**, *14*, 543-548.
66. Gelmon, K. A.; Stewart, D.; Chi, K. N.; Chia, S.; Cripps, C.; Huan, S.; Janke, S.; Ayers, D.; Fry, D.; Shabbits, J. A.; Walsh, W.; McIntosh, L.; Seymour, L. K., *Ann. Oncol.* **2004**, *15*, 1115-1122.
67. Gore, M. E.; Atkinson, R. J.; Thomas, H.; Cure, H.; Rischin, D.; Beale, P.; Bougnoux, P.; Dirix, L.; Smit, W. M., *Eur. J. Cancer* **2002**, *38*, 2416-2420.
68. Bierbach, U.; Qu, Y.; Hambley, T. W.; Peroutka, J.; Nguyen, H. L.; Doedee, M.; Farrell, N., *Inorg. Chem.* **1999**, *38*, 3535-3542.
69. Farrell, N.; Ha, T. T. B.; Souchard, J. P.; Wimmer, F. L.; Cros, S.; Johnson, N. P., *J. Med. Chem.* **1989**, *32*, 2240-2241.
70. van Beusichem, M.; Farrell, N., *Inorg. Chem.* **1992**, *31*, 634-639.
71. Farrell, N.; Kelland, L. R.; Roberts, J. D.; van Beusichem, M., *Cancer Res.* **1992**, *52*, 5065-5072.
72. Zou, Y.; van Houten, B.; Farrell, N., *Biochemistry* **1993**, *32*, 9632-9638.
73. Montero, E. I.; Díaz, S.; González-Vadillo, A. M.; Pérez, J. M.; Alonso, C.; Navarro-Ranninger, C., *J. Med. Chem.* **1999**, *42*, 4264-4268.
74. Montero, E. I.; Pérez, J. M.; Schwartz, A.; Fuertes, M. A.; Malinge, J. M.; Alonso, C.; Leng, M.; Navarro-Ranninger, C., *Chembiochem* **2002**, *3*, 61-67.
75. Kaspárková, J.; Marini, V.; Najajreh, Y.; Gibson, D.; Brabec, V., *Biochemistry* **2003**, *42*, 6321-6332.
76. Kaspárková, J.; Nováková, O.; Marini, V.; Najajreh, Y.; Gibson, D.; Pérez, J. M.; Brabec, V., *J. Biol. Chem.* **2003**, *278*, 47516-47525.
77. Coluccia, M.; Nassi, A.; Loseto, F.; Boccarelli, A.; Mariggio, M. A.; Giordano, D.; Intini, F. P.; Caputo, P.; Natile, G., *J. Med. Chem.* **1993**, *36*, 510-512.
78. Boccarelli, A.; Intini, F. P.; Sasanelli, R.; Sivo, M. F.; Coluccia, M.; Natile, G., *J. Med. Chem.* **2006**, *49*, 829-837.
79. Brabec, V.; Neplechova, K.; Kaspárková, J.; Farrell, N., *J. Biol. Inorg. Chem.* **2000**, *5*, 364-368.
80. Natile, G.; Coluccia, M., *Metal ions in biological systems*. Basel, **2004**; Vol. 42, p 239-240.
81. Mellish, K. J.; Barnard, C. F. J.; Murrer, B. A.; Kelland, L. R., *Int. J. Cancer* **1995**, *62*, 717-723.
82. Farrell, N., *Metal ions in biological systems*. Basel, **2004**; Vol. 42, p 251-296.
83. Qu, Y.; Rauter, H.; Fontes, A. P. S.; Bandarage, R.; Kelland, L. R.; Farrell, N., *J. Med. Chem.* **2000**, *43*, 3189-3192.
84. Wheate, N. J.; Collins, J. G., *Coord. Chem. Rev.* **2003**, *241*, 133-145.
85. Komeda, S.; Lutz, M.; Spek, A. L.; Chikuma, M.; Reedijk, J., *Inorg. Chem.* **2000**, *39*, 4230-4236.
86. Komeda, S.; Lutz, M.; Spek, A. L.; Chikuma, M.; Reedijk, J., *Inorg. Chem.* **2000**, *39*, 4382-4382.
87. Manzotti, C.; Pratesi, G.; Menta, E.; Di Domenico, R.; Cavalletti, E.; Fiebig, H. H.; Kelland, L. R.; Farrell, N.; Polizzi, D.; Supino, R.; Pezzoni, G.; Zunino, F., *Clin. Cancer Res.* **2000**, *6*, 2626-2634.

88. Zanzi, I.; Srivastava, S. C.; Meinken, G. E.; Robeson, W.; Mausner, L. F.; Fairchild, R. G.; Margouleff, D., *Nucl. Med. Biol.* **1989**, *16*, 397-403.
89. Srivastava, S. C., *Semin. Nucl. Med.* **1996**, *26*, 119-131.
90. Allardyce, C. S.; Dyson, P. J., *Platinum Metals Rev.* **2001**, *45*, 62-69.
91. Lentzen, O.; Moucheron, C.; Kirsch-De Mesmaeker, A., *Metallotherapeutic drugs & metal-based diagnostic agents*. John Wiley & Sons, Ltd: West Sussex, **2005**; p 359-378.
92. Clarke, M. J.; Bitler, S.; Rennert, D.; Buchbinder, M.; Kelman, A. D., *J. Inorg. Biochem.* **1980**, *12*, 79-87.
93. Stanbury, D. M.; Haas, O.; Taube, H., *Inorg. Chem.* **1980**, *19*, 518-524.
94. Stanbury, D. M.; Mulac, W. A.; Sullivan, J. C.; Taube, H., *Inorg. Chem.* **1980**, *19*, 3735-3740.
95. Stanbury, D. M.; Gaswick, D.; Brown, G. M.; Taube, H., *Inorg. Chem.* **1983**, *22*, 1975-1982.
96. Galeotti, T.; Cittadini, A.; Neri, G.; Scarpa, A., *Membrane in cancer cells*. New York, **1988**; Vol. 551.
97. Clarke, M. J., *Coord. Chem. Rev.* **2003**, *236*, 209-233.
98. Smith, C. A.; Sutherland-Smith, A. J.; Keppler, B. K.; Kratz, F.; Baker, E. N., *J. Biol. Inorg. Chem.* **1996**, *1*, 424-431.
99. Clarke, M. J.; Zhu, F. C.; Frasca, D. R., *Chem. Rev.* **1999**, *99*, 2511-2533.
100. Hartinger, C. G.; Zorbas-Seifried, S.; Jakupec, M. A.; Kynast, B.; Zorbas, H.; Keppler, B. K., *J. Inorg. Biochem.* **2006**, *100*, 891-904.
101. Polec-Pawlak, K.; Abramski, J. K.; Semenova, O.; Hartinger, C. G.; Timerbaev, A. R.; Keppler, B. K.; Jarosz, M., *Electrophoresis* **2006**, *27*, 1128-1135.
102. Clarke, M. J.; Buchbinder, M.; Kelman, A. D., *Inorg. Chim. Acta* **1978**, *27*, L87-L88.
103. Clarke, M. J.; Jansen, B.; Marx, K. A.; Kruger, R., *Inorg. Chim. Acta* **1986**, *124*, 13-28.
104. Rodriguez-Bailey, V. M.; La Chance-Galang, K. J.; Doan, P. E.; Clarke, M. J., *Inorg. Chem.* **1997**, *36*, 1873-1883.
105. Durig, J. R.; Danneman, J.; Behnke, W. D.; Mercer, E. E., *Chem.-Biol. Interact.* **1976**, *13*, 287-294.
106. Alessio, E.; Mestroni, G.; Nardin, G.; Attia, W. M.; Calligaris, M.; Sava, G.; Zorzet, S., *Inorg. Chem.* **1988**, *27*, 4099-4106.
107. Coluccia, M.; Sava, G.; Loseto, F.; Nassi, A.; Boccarelli, A.; Giordano, D.; Alessio, E.; Mestroni, G., *Eur. J. Cancer* **1993**, *29A*, 1873-1879.
108. Bergamo, A.; Gava, B.; Alessio, E.; Mestroni, G.; Serli, B.; Cocchietto, M.; Zorzet, S.; Sava, G., *Int. J. Oncol.* **2002**, *21*, 1331-1338.
109. Kostova, I., *Curr. Med. Chem.* **2006**, *13*, 1085-1107.
110. Gallori, E.; Vettori, C.; Alessio, E.; González-Vilchez, F.; Vilaplana, R.; Orioli, P.; Casini, A.; Messori, L., *Arch. Biochem. Biophys.* **2000**, *376*, 156-162.
111. Messori, L.; Orioli, P.; Vullo, D.; Alessio, E.; Iengo, E., *Eur. J. Biochem.* **2000**, *267*, 1206-1213.
112. Barca, A.; Pani, B.; Tamaro, M.; Russo, E., *Mutat. Res.-Fundam. Mol. Mech. Mutagen.* **1999**, *423*, 171-181.
113. Sanna, B.; Debidda, M.; Pintus, G.; Tadolini, B.; Posadino, A. M.; Bennardini, F.; Sava, G.; Ventura, C., *Arch. Biochem. Biophys.* **2002**, *403*, 209-218.
114. Kapitza, S.; Pongratz, M.; Jakupec, M. A.; Heffeter, P.; Berger, W.; Lackinger, L.; Keppler, B. K.; Marian, B., *J. Cancer Res. Clin. Oncol.* **2005**, *131*, 101-110.
115. Nováková, O.; Kaspárková, J.; Vrána, O.; van Vliet, P. M.; Reedijk, J.; Brabec, V., *Biochemistry* **1995**, *34*, 12369-12378.

116. van Vliet, P. M.; Haasnoot, J. G.; Reedijk, J., *Inorg. Chem.* **1994**, *33*, 1934-1939.
117. van Vliet, P. M.; Toekimin, S. M. S.; Haasnoot, J. G.; Reedijk, J.; Nováková, O.; Vrána, O.; Brabec, V., *Inorg. Chim. Acta* **1995**, *231*, 57-64.
118. Zobi, F.; Hohl, M.; Zimmermann, W.; Alberto, R., *Inorg. Chem.* **2004**, *43*, 2771-2772.
119. Velders, A. H.; Kooijman, H.; Spek, A. L.; Haasnoot, J. G.; de Vos, D.; Reedijk, J., *Inorg. Chem.* **2000**, *39*, 2966-2967.
120. Hotze, A. C. G.; Velders, A. H.; Ugozzoli, F.; Biagini-Cingi, M.; Manotti-Lanfredi, A. M.; Haasnoot, J. G.; Reedijk, J., *Inorg. Chem.* **2000**, *39*, 3838-3844.
121. Scherzer, J.; Clapp, L. B., *J. Inorg. Nucl. Chem.* **1968**, *30*, 1107-1109.
122. Matsubara, T.; Creutz, C., *Inorg. Chem.* **1979**, *18*, 1956-1966.
123. Taqui-Khan, M. M.; Ramachandraiah, G., *Inorg. Chem.* **1982**, *21*, 2109-2111.
124. Taqui-Khan, M. M., *Pure Appl. Chem.* **1983**, *55*, 159-164.
125. Vilaplana-Serrano, R.; Basallote, M. G.; Ruiz-Valero, C.; Gutiérrez-Puebla, E.; González-Vilchez, F., *J. Chem. Soc.-Chem. Commun.* **1991**, 100-101.
126. González-Vilchez, F.; Vilaplana, R.; Blasco, G.; Messori, L., *J. Inorg. Biochem.* **1998**, *71*, 45-51.
127. Chatterjee, D.; Ward, M. S.; Shepherd, R. E., *Inorg. Chim. Acta* **1999**, *285*, 170-177.
128. Shepherd, R. E.; Chen, Y.; Kortés, R. A.; Ward, M. S., *Inorg. Chim. Acta* **2000**, *303*, 30-39.
129. Vilaplana, R. A.; González-Vilchez, F.; Gutiérrez-Puebla, E.; Ruiz-Valero, C., *Inorg. Chim. Acta* **1994**, *224*, 15-18.
130. Chatterjee, D.; Sengupta, A.; Mitra, A.; Basak, S., *Inorg. Chim. Acta* **2005**, *358*, 2954-2959.
131. Morris, R. E.; Aird, R. E.; Murdoch, P. D.; Chen, H. M.; Cummings, J.; Hughes, N. D.; Parsons, S.; Parkin, A.; Boyd, G.; Jodrell, D. I.; Sadler, P. J., *J. Med. Chem.* **2001**, *44*, 3616-3621.
132. Aird, R. E.; Cummings, J.; Ritchie, A. A.; Muir, M.; Morris, R. E.; Chen, H.; Sadler, P. J.; Jodrell, D. I., *Br. J. Cancer* **2002**, *86*, 1652-1657.
133. Nováková, O.; Chen, H. M.; Vrána, O.; Rodger, A.; Sadler, P. J.; Brabec, V., *Biochemistry* **2003**, *42*, 11544-11554.
134. Nováková, O.; Kaspárková, J.; Bursova, V.; Hofr, C.; Vojtiskova, M.; Chen, H. M.; Sadler, P. J.; Brabec, V., *Chem. Biol.* **2005**, *12*, 121-129.
135. Wang, F.; Chen, H. M.; Parsons, S.; Oswald, L. D. H.; Davidson, J. E.; Sadler, P. J., *Chem.-Eur. J.* **2003**, *9*, 5810-5820.
136. Chen, H. M.; Parkinson, J. A.; Parsons, S.; Coxall, R. A.; Gould, R. O.; Sadler, P. J., *J. Am. Chem. Soc.* **2002**, *124*, 3064-3082.
137. Wang, F. Y.; Bella, J.; Parkinson, J. A.; Sadler, P. J., *J. Biol. Inorg. Chem.* **2005**, *10*, 147-155.
138. Allardyce, C. S.; Dyson, P. J.; Ellis, D. J.; Heath, S. L., *Chem. Commun.* **2001**, 1396-1397.
139. Ang, W. H.; Daldini, E.; Scolaro, C.; Scopelliti, R.; Juillerat-Jeannerat, L.; Dyson, P. J., *Inorg. Chem.* **2006**, *45*, 9006-9013.
140. Dyson, P. J.; Sava, G., *Dalton Trans.* **2006**, 1929-1933.
141. Armitage, B., *Chem. Rev.* **1998**, *98*, 1171-1200.
142. Pauly, M.; Kayser, I.; Schmitz, M.; Dicato, M.; Del Guerzo, A.; Kolber, I.; Moucheron, C.; Kirsch-De Mesmaeker, A., *Chem. Commun.* **2002**, 1086-1087.
143. Moreno, M. J.; Monson, E.; Reddy, R. G.; Rehemtulla, A.; Ross, B. D.; Philbert, M.; Schneider, R. J.; Kopelman, R., *Sens. Actuator B-Chem.* **2003**, *90*, 82-89.

144. Vollano, J. F.; Bossard, G. E.; Martellucci, S. A.; Darkes, M. C.; Abrams, M. J.; Brooks, R. C., *J. Photochem. Photobiol. B-Biol.* **1997**, *37*, 230-235.
145. Ortman, I.; Moucheron, C.; Kirsch-De Mesmaeker, A., *Coord. Chem. Rev.* **1998**, *168*, 233-271.
146. Creutz, C.; Taube, H., *J. Am. Chem. Soc.* **1973**, *95*, 1086-1094.
147. Iengo, E.; Mestroni, G.; Geremia, S.; Calligaris, M.; Alessio, E., *J. Chem. Soc.-Dalton Trans.* **1999**, 3361-3371.
148. Alessio, E.; Iengo, E.; Zorzet, S.; Bergamo, A.; Coluccia, M.; Boccarelli, A.; Sava, G., *J. Inorg. Biochem.* **2000**, *79*, 173-177.
149. Serli, B.; Iengo, E.; Gianferrara, T.; Zangrando, E.; Alessio, E., *Metal-Based Drugs* **2001**, *8*, 9-18.
150. Bergamo, A.; Stocco, G.; Casarsa, C.; Cocchietto, M.; Alessio, E.; Serli, B.; Zorzet, S.; Sava, G., *Int. J. Oncol.* **2004**, *24*, 373-379.
151. Mestroni, G.; Alessio, E.; Sava, G.; Iengo, E.; Zorzet, S.; Bergamo, A. US Patent 6921824. **2005**.
152. Bergamo, A.; Stocco, G.; Gava, B.; Cocchietto, M.; Alessio, E.; Serli, B.; Iengo, E.; Sava, G., *J. Pharmacol. Exp. Ther.* **2003**, *305*, 725-732.
153. Srivastava, R. S.; Fronczek, F. R., *Inorg. Chim. Acta* **2001**, *322*, 32-36.
154. Wu, A.; Kennedy, D. C.; Patrick, B. O.; James, B. R., *Inorg. Chem.* **2003**, *42*, 7579-7586.
155. Srivastava, R. S.; Fronczek, F. R.; Romero, L. M., *Inorg. Chim. Acta* **2004**, *357*, 2410-2414.
156. Aquino, M. A. S., *Coord. Chem. Rev.* **2004**, *248*, 1025-1045.
157. Dunbar, K. R.; Matonic, J. H.; Saharan, V. P.; Crawford, C. A.; Christou, G., *J. Am. Chem. Soc.* **1994**, *116*, 2201-2202.
158. Grover, N.; Welch, T. W.; Fairley, T. A.; Cory, M.; Thorp, H. H., *Inorg. Chem.* **1994**, *33*, 3544-3548.
159. Grover, N.; Ciftan, S. A.; Thorp, H. H., *Inorg. Chim. Acta* **1995**, *240*, 335-338.
160. Brabec, V.; Nováková, O., *Drug Resist. Update* **2006**, *9*, 111-122.
161. van Houten, B.; Illenye, S.; Qu, Y.; Farrell, N., *Biochemistry* **1993**, *32*, 11794-11801.
162. Milkevitch, M.; Shirley, B. W.; Brewer, K. J., *Inorg. Chim. Acta* **1997**, *264*, 249-256.
163. Milkevitch, M.; Storrie, H.; Brauns, E.; Brewer, K. J.; Shirley, B. W., *Inorg. Chem.* **1997**, *36*, 4534-4538.
164. van der Schilden, K.; García, F.; Kooijman, H.; Spek, A. L.; Haasnoot, J. G.; Reedijk, J., *Angew. Chem.-Int. Edit.* **2004**, *43*, 5668-5670.
165. Ang, W. H.; Dyson, P. J., *Eur. J. Inorg. Chem.* **2006**, 4003-4018.
166. Sebolt-Leopold, J. S.; English, J. M., *Nature* **2006**, *441*, 457-462.
167. Chatterjee, D.; Mitra, A.; De, G. S., *Platinum Metals Rev.* **2006**, *50*, 2-12.
168. Grguric-Sipka, S. R.; Vilaplana, R. A.; Pérez, J. M.; Fuertes, M. A.; Alonso, C.; Álvarez, Y.; Sabo, T. J.; González-Vilchez, F., *J. Inorg. Biochem.* **2003**, *97*, 215-220.
169. Chatterjee, D.; Mitra, A.; Sengupta, A.; Saha, P.; Chatterjee, M., *Inorg. Chim. Acta* **2006**, *359*, 2285-2290.
170. Fernández, R.; Melchart, M.; Habtemariam, A.; Parsons, S.; Sadler, P. J., *Chem.-Eur. J.* **2004**, *10*, 5173-5179.
171. Malina, J.; Nováková, O.; Keppler, B. K.; Alessio, E.; Brabec, V., *J. Biol. Inorg. Chem.* **2001**, *6*, 435-445.
172. Jakupec, M. A.; Reisner, E.; Eichinger, A.; Pongratz, M.; Arion, V. B.; Galanski, M.; Hartinger, C. G.; Keppler, B. K., *J. Med. Chem.* **2005**, *48*, 2831-2837.

173. Scolaro, C.; Bergamo, A.; Brescacin, L.; Delfino, R.; Cocchietto, M.; Laurency, G.; Geldbach, T. J.; Sava, G.; Dyson, P. J., *J. Med. Chem.* **2005**, *48*, 4161-4171.
174. Allardyce, C. S.; Dyson, P. J.; Abou-Shakra, F. R.; Birtwistle, H.; Coffey, J., *Chem. Commun.* **2001**, 2708-2709.
175. Allardyce, C. S.; Dyson, P. J.; Ellis, D. J.; Salter, P. A.; Scopelliti, R., *J. Organomet. Chem.* **2003**, *668*, 35-42.
176. Khalaila, I.; Bergamo, A.; Bussy, F.; Sava, G.; Dyson, P. J., *Int. J. Oncol.* **2006**, *29*, 261-268.
177. Corral, E.; Hotze, A. C. G.; Tooke, D. M.; Spek, A. L.; Reedijk, J., *Inorg. Chim. Acta* **2006**, *359*, 830-838.
178. Corral, E.; Kooijman, H.; Spek, A. L.; Reedijk, J., *New J. Chem.* **2007**, *31*, 21-24.
179. Corral, E.; Hotze, A. C. G.; Magistrato, A.; Reedijk, J., *Inorg. Chem.* **2007**, *46*, 6715-6722.
180. Corral, E.; Hotze, A. C. G.; den Dulk, H.; Hannon, M. J.; Reedijk, J., **2007**, *to be submitted for publication in J. Biol. Inorg. Chem.*

## 2. Ruthenium polypyridyl complexes containing the bischelating ligand 2,2'-azobispyridine. Synthesis, characterization and crystal structures\*

Three ruthenium polypyridyl compounds of structural formula  $[\text{Ru}(\text{apy})(\text{tpy})\text{L}](\text{ClO}_4)_{(2-n)}$  (apy = 2,2'-azobispyridine; tpy = 2,2':6',2''-terpyridine; L = Cl<sup>-</sup>, H<sub>2</sub>O, CH<sub>3</sub>CN) (**1a-c**) were synthesized and crystallized. These complexes were fully characterized by means of 1D and 2D <sup>1</sup>H NMR spectroscopy, as well as mass spectrometry and elemental analysis. Although in theory two isomers are possible, i.e. the one in which the central N atom in tpy is trans to the azo N in apy and the one in which the former is trans to the pyridine N in apy, in all cases only the latter was observed. The molecular structures of the compounds were elucidated by single-crystal X-ray diffraction.

---

\* This chapter is based on Corral, E.; Hotze, A.C.G.; Tooke, D.M.; Spek, A.L.; Reedijk, J., *Inorg. Chim. Acta*, **2006**, 359, 830-838.

## 2.1. Introduction

Recently a large interest has grown in ruthenium polypyridyl complexes as a possible alternative to the use of classical platinum chemotherapy.<sup>1</sup> Some examples of these compounds are Ru(tpy)Cl<sub>3</sub> and  $\alpha$ -[Ru(azpy)<sub>2</sub>Cl<sub>2</sub>] (azpy = 2-phenylazopyridine). Ru(tpy)Cl<sub>3</sub> shows a pronounced *in vitro* cytotoxicity and exhibits antitumor activity.<sup>2</sup> The compound  $\alpha$ -[Ru(azpy)<sub>2</sub>Cl<sub>2</sub>] has been reported to show a remarkably high cytotoxicity, even more pronounced than cisplatin in most of the tested cell lines.<sup>3, 4</sup> The increased amount of possible binding modes of ruthenium polypyridyl complexes to DNA as compared to those of the first generations of platinum drugs, including intercalation of the ligands between two parallel base pairs, could be crucial in order to overcome resistance to cisplatin.<sup>5</sup> In addition, a number of ruthenium complexes, such as NAMI-A, [H<sub>2</sub>im][*trans*-Ru(III)Cl<sub>4</sub>(dmsO)(Him)] (Him = imidazole; dmsO = dimethylsulfoxide), have shown to display an antimetastatic activity, which has not been observed in the case of the routinely used platinum compounds.<sup>6, 7</sup>

In this chapter, the synthesis and characterization of a group of the above-mentioned ruthenium polypyridyl complexes are described. Taking Ru(tpy)Cl<sub>3</sub> as the starting building block in the synthesis, the second moiety of choice is 2,2'-azobispyridine (apy), a didentate polypyridyl ligand. First described by Kirpal in 1927,<sup>8</sup> the availability of two possible coordination sites has made it attractive in the synthesis of multiple dinuclear complexes, most of which were symmetric, as reviewed by Kaim.<sup>9</sup> On the other hand apy is structurally related to 2-phenylazopyridine (azpy), a ligand present in the recently reported cytotoxic bis(2-phenylazo)pyridine ruthenium(II) compounds, such as the above-mentioned  $\alpha$ -[Ru(azpy)<sub>2</sub>Cl<sub>2</sub>].<sup>3, 4</sup>

The X-ray structures of the three newly prepared complexes are presented, which provide interesting observations by comparison with each other, as well as with other already reported related structures.<sup>10-13</sup> These results indicate a powerful possibility to tune the sixth coordination site and tailor-make complexes that display varying properties, thereby fulfilling different requirements.

## 2.2. Experimental

### Materials and reagents

2,2'-Azobispyridine (apy) and Ru(tpy)Cl<sub>3</sub> were synthesized according to the literature methods.<sup>8, 14</sup> LiCl, NaClO<sub>4</sub> (both Merck), NaClO, AgNO<sub>3</sub>, (both Acros), tpy (Aldrich) and

RuCl<sub>3</sub>·3H<sub>2</sub>O (Johnson & Matthey) were used as supplied. All other chemicals and solvents were reagent grade commercial materials and used as received, without further purification.

### **Physical measurements**

C, H and N determinations were performed on a Perkin Elmer 2400 Series II analyzer. Mass spectra were obtained with a Finnigan MAT TSQ-700 mass spectrometer equipped with a custom-made electrospray interface (ESI). FTIR spectra were obtained on a Perkin Elmer Paragon 1000 FTIR spectrophotometer equipped with a Golden Gate ATR device, using the diffuse reflectance technique (res. 4 cm<sup>-1</sup>). NMR spectra were recorded on a Bruker DPX-300 spectrometer operating at a frequency of 300 MHz, on a Bruker AV-500, at a frequency of 500 MHz, and on a Bruker DMX-400, at a frequency of 400 MHz. Chemical shifts were calibrated against tetramethylsilane (TMS).

### **X-ray structural determination**

X-ray intensities were measured on a Nonius KappaCCD diffractometer with rotating anode and Mo K $\alpha$  radiation (graphite monochromator,  $\lambda = 0.71073$  Å) at a temperature of 150(2) K. A multi-scan absorption correction was applied using MULABS<sup>15</sup> (**1a**) or SADABS<sup>16</sup> (**1b** and **1c**). The structures were solved with the program DIRDIF,<sup>17</sup> and refined using the program SHELXL-97<sup>18</sup> against F<sup>2</sup> of all reflections up to a resolution of  $(\sin\theta/\lambda)_{\max} = 0.65$ . The perchlorate anion containing Cl(2) in **1b** was refined using a disorder model, with final occupancies of 88% and 12%. All other non hydrogen atoms were freely refined with anisotropic displacement parameters. The H atoms on the water molecules in **1b** were found in a difference map, and refined with isotropic displacement parameters. All other H atoms were placed in geometrically idealized positions [ $d(C - H) = 0.98$ Å for methyl H atoms and 0.95Å for other H atoms] and constrained to ride on their parent atoms, with  $U_{\text{iso}}(\text{H}) = 1.5U_{\text{eq}}(\text{C})$  for methyl H atoms and  $U_{\text{iso}}(\text{H}) = 1.2U_{\text{eq}}(\text{C})$  for all other H atoms. The structure calculations, space group determination, validation and drawings were performed with the program PLATON.<sup>19</sup> Further experimental details are given in Table 2.1. Crystallographic data (excluding structure factors) for the structures reported in this chapter have been deposited at the Cambridge Crystallographic Data Centre as numbers CCDC 266695-266697.

Table 2.1. Crystal data and structure refinement details for  $[Ru(apy)(tpy)Cl](ClO_4)$  (**1a**),  $[Ru(apy)(tpy)(H_2O)](ClO_4)_2 \cdot 2H_2O$  (**1b**) and  $[Ru(apy)(tpy)(CH_3CN)](ClO_4)_2$  (**1c**)

	<b>1a</b>	<b>1b</b>	<b>1c</b>
Formula	$C_{25}H_{19}N_7O_4RuCl_2$	$C_{25}H_{25}N_7O_{11}RuCl_2$	$C_{27}H_{22}N_8O_8RuCl_2$
Formula weight	653.44	771.49	758.50
Crystal colour	Dark (purple)	Dark (purple)	Dark (purple)
Crystal size (mm <sup>3</sup> )	0.08 x 0.20 x 0.23	0.03 x 0.09 x 0.24	0.15 x 0.20 x 0.30
Crystal system	Monoclinic	Triclinic	Triclinic
Space group	Pc (No.7)	P-1 (No. 2)	P-1 (No. 2)
$a$ (Å)	8.6951(5)	10.9876(9)	11.2566(7)
$b$ (Å)	9.8750(5)	11.5675(5)	11.6870(8)
$c$ (Å)	14.7384(7)	12.8188(15)	12.0681(9)
$\alpha$ (°)	90	79.141(7)	94.444(6)
$\beta$ (°)	97.810(4)	70.879(7)	113.183(5)
$\gamma$ (°)	90	84.259(6)	91.415(5)
$V$ (Å <sup>3</sup> )	1253.76(11)	1510.5(2)	1452.40(18)
$Z$	2	2	2
$D_{calc}$ (g/cm <sup>3</sup> )	1.731	1.696	1.734
$\mu$ (Mo K $\alpha$ )(mm <sup>-1</sup> )	0.887	0.767	0.790
Transmission range	0.63-0.93	0.76-0.98	0.72-0.89
Total/unique reflections	33311/5711	41476/6905	40042/6634
$R_1$	0.0316	0.0379	0.0289
$\omega R_2$	0.0785	0.0825	0.0688
S	1.041	1.03	1.043
Npar	352	485	416
Residual density (e/Å <sup>3</sup> )	-0.49/1.14	-0.63/1.56	-0.80/1.03

### Synthesis and characterization of the $[Ru(\text{apy})(\text{tpy})L](\text{ClO}_4)_{(2-n)}$ compounds

The synthesis of the three complexes was accomplished in three steps, analogously to the synthesis of their related azpy complexes,<sup>10</sup> as described in detail below (see Fig.2.1).

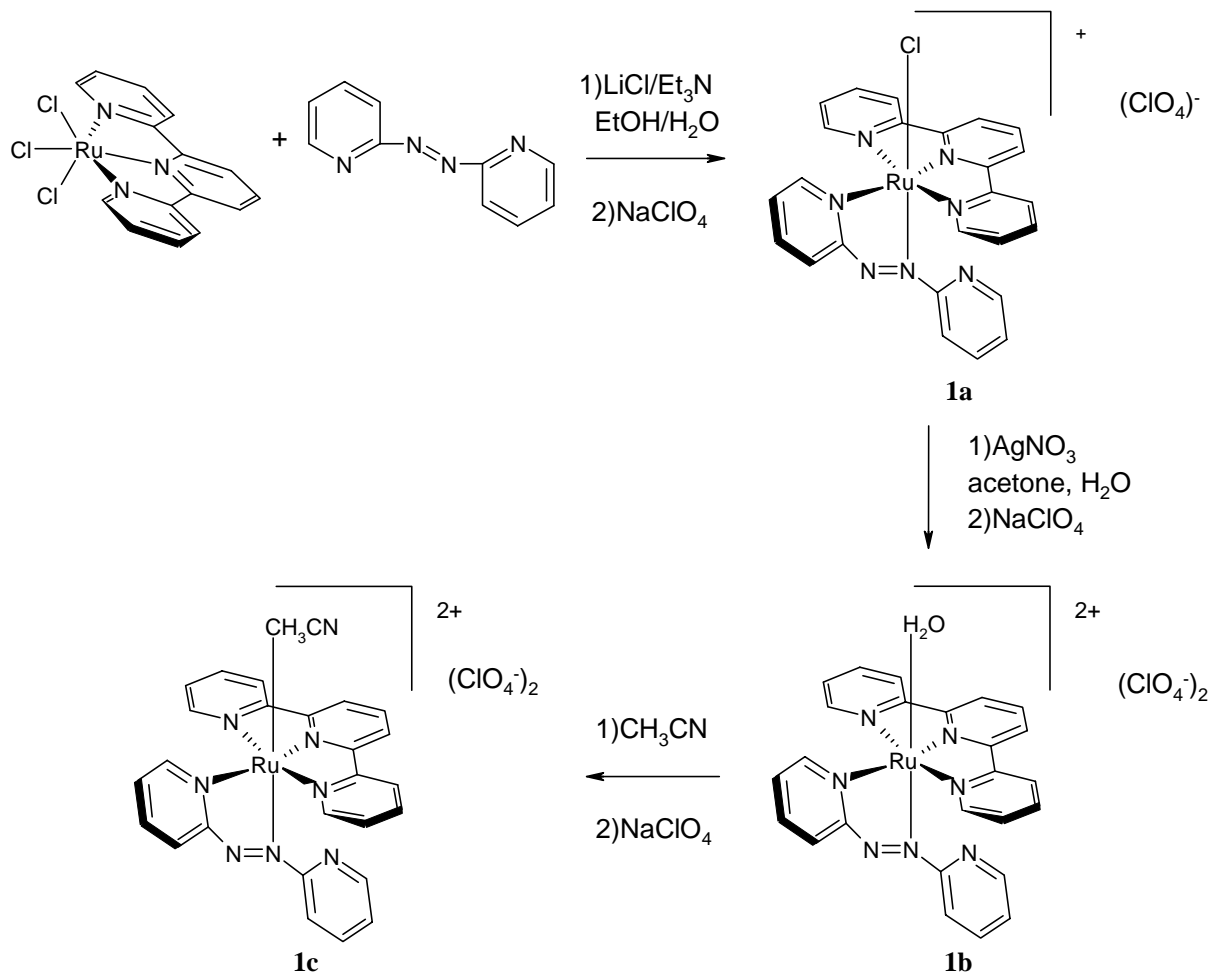


Fig.2.1. Scheme of the synthesis of the  $[Ru(\text{apy})(\text{tpy})L](\text{ClO}_4)_{(2-n)}$  compounds.

**Caution:** Although no problems were encountered in the synthesis and handling of the materials described below, those containing perchlorate are potentially explosive and should be handled with care.

*Chloro(2,2'-azobispyridine)(2,2':6',2''-terpyridine)ruthenium(II) perchlorate,  $[Ru(\text{apy})(\text{tpy})\text{Cl}](\text{ClO}_4)$  (**1a**)*

$\text{LiCl}$  (300 mg, 7.08 mmol) was dissolved in 45 ml of ethanol-water (3:1). Triethylamine (0.096 ml, 0.68 mmol) was added, followed by  $Ru(\text{tpy})\text{Cl}_3 \cdot 3\text{H}_2\text{O}$  (300 mg, 0.68 mmol) and 2,2'-azobispyridine (apy; 189 mg, 1.02 mmol). The mixture was refluxed for one hour, after which the hot solution was filtered to remove any insoluble material. The

filtrate was left to cool down to RT. By addition of a saturated aqueous solution of NaClO<sub>4</sub> (15 ml), a dark crystalline solid appeared. The crystals obtained were found to be suitable for X-ray diffraction measurements. The product was collected by filtration, washed with little ice-cold water and dried *in vacuo* over P<sub>4</sub>O<sub>10</sub>. Yield: 211 mg (47%). *Anal.* Calc. for C<sub>25</sub>H<sub>19</sub>N<sub>7</sub>O<sub>4</sub>Cl<sub>2</sub>Ru: C, 45.9; H, 2.9; N, 15.0%. Found: C, 45.2; H, 2.9; N, 14.8%. *m/z* (ESIMS) 553.0 ([Ru(apy)(tpy)Cl]<sup>+</sup>, 100%). <sup>1</sup>H NMR (DMSO-*d*<sub>6</sub>): δ (ppm): 9.83 (1H, d, 4.61 Hz); 8.93 (1H, d, 7.90 Hz); 8.63 (3H, m); 8.45 (1H, t, 7.86 Hz); 8.27 (2H, m); 8.10 (2H, t, 6.57 Hz); 7.82 (1H, d, 3.57 Hz); 7.72 (1H, t, 7.71 Hz); 7.41 (2H, t, 6.09 Hz); 7.31 (1H, t, 4.72 Hz); 7.22 (2H, d, 4.46 Hz); 7.12 (1H, d, 8.07 Hz).

*Aqua(2,2'-azobispyridine)(2,2':6',2''-terpyridine)ruthenium(II) diperchlorate dihydrate, [Ru(apy)(tpy)(H<sub>2</sub>O)](ClO<sub>4</sub>)<sub>2</sub>·2H<sub>2</sub>O (1b)*

To a stirred solution of [Ru(apy)(tpy)Cl](ClO<sub>4</sub>) (170 mg, 0.26 mmol) in 30 ml of acetone-water (1:5), 1 equivalent of AgNO<sub>3</sub> (44 mg, 0.26 mmol) was added. The mixture was refluxed for one hour, then left to cool down to RT. AgCl was filtered off, together with any possible rests of unreacted starting material. Finally a saturated aqueous solution of NaClO<sub>4</sub> (10 ml) was added and the solution was left overnight at 4 °C. The product was collected by filtration, washed with little ice-cold water and dried *in vacuo* over P<sub>4</sub>O<sub>10</sub>. Yield: 153 mg (76%). *Anal.* Calc. for C<sub>25</sub>H<sub>25</sub>N<sub>7</sub>O<sub>11</sub>Cl<sub>2</sub>Ru: C, 38.9; H, 3.3; N, 12.7%. Found: C, 39.1; H, 3.0; N, 12.9%. *m/z* (ESIMS) 259.2 ([Ru(apy)(tpy)]<sup>2+</sup>, 100%). <sup>1</sup>H NMR (DMSO-*d*<sub>6</sub>): δ (ppm): 9.46 (1H, d, 5.11 Hz); 9.01 (1H, d, 7.82 Hz); 8.67 (3H, m); 8.55 (1H, t, 8.09 Hz); 8.36 (2H, m); 8.19 (2H, t, 7.83 Hz); 7.84 (1H, d, 4.70 Hz); 7.75 (1H, t, 7.67 Hz); 7.50 (2H, m); 7.34 (3H, m); 7.14 (1H, d, 8.00 Hz).

*Acetonitrile(2,2'-azobispyridine)(2,2':6',2''-terpyridine)ruthenium(II) diperchlorate, [Ru(apy)(tpy)(CH<sub>3</sub>CN)](ClO<sub>4</sub>)<sub>2</sub> (1c)*

[Ru(apy)(tpy)(H<sub>2</sub>O)](ClO<sub>4</sub>)<sub>2</sub> (56 mg, 0.08 mmol) was dissolved in 9 ml CH<sub>3</sub>CN. The solution was refluxed for 30 minutes. The volume of the solution was reduced 5 to 6 times under reduced pressure before adding a saturated aqueous solution of NaClO<sub>4</sub> (2.8 ml). A dark crystalline solid appeared overnight at 4 °C, from which a single crystal suitable for X-ray diffraction measurements was extracted. The product was collected by filtration, washed with little ice-cold water and dried *in vacuo* over P<sub>4</sub>O<sub>10</sub>. Yield: 45 mg (78 %). *Anal.* Calc. for C<sub>27</sub>H<sub>22</sub>N<sub>8</sub>O<sub>8</sub>Cl<sub>2</sub>Ru: C, 42.8; H, 2.9; N, 14.8%. Found: C, 42.8; H, 2.9; N, 15.0%. *m/z* (ESIMS) 279.8 ([Ru(apy)(tpy)(CH<sub>3</sub>CN)]<sup>2+</sup>, 100%); 259.2 ([Ru(apy)(tpy)]<sup>2+</sup>, 30%). <sup>1</sup>H NMR (CDCl<sub>3</sub>): δ (ppm): 9.67 (1H, d, 5.17 Hz); 8.93 (1H, d, 7.91 Hz); 8.50 (1H, t, 7.64

Hz); 8.38 (3H, m); 8.28 (1H, m); 8.18 (1H, t, 6.00 Hz); 8.06 (2H, t, 9.16 Hz); 7.80 (1H, d, 3.66 Hz); 7.70 (1H, t, 7.82 Hz); 7.36 (4H, m); 7.27 (2H, m).

### **2.3. Results and discussion**

#### **Synthesis and characterization of the [Ru(apy)(tpy)L](ClO<sub>4</sub>)<sub>(2-n)</sub> compounds**

The synthesis of [Ru(apy)(tpy)Cl](ClO<sub>4</sub>) takes place in a one-pot reaction from the previously synthesized Ru(tpy)Cl<sub>3</sub>·3H<sub>2</sub>O and 2,2'-azobispyridine (apy). The presence of both triethylamine and lithium chloride is needed. The first of these compounds acts as a reducing agent of Ru(III) to Ru(II), helping in the dissociation of the chlorido from Ru(tpy)Cl<sub>3</sub>·3H<sub>2</sub>O, whereas LiCl is used to prevent any dissociation of Cl<sup>-</sup> from the product.

AgNO<sub>3</sub> in an aqueous solution is required to substitute the chlorido ligand, which is filtered off in the form of the insoluble salt AgCl, by an aqua ligand. The latter is easily substituted by acetonitrile by simply refluxing for a short time in that solvent.

The possibility to synthesize a complex in which the sixth coordination position can be occupied by ligands with different lability, which also have an influence in the solubility, provides with a choice to fulfill the requirements of each situation. DNA is thought to be the ultimate target of platinum drugs and of some antitumor-active ruthenium compounds.<sup>1</sup> The kinetics of the reaction of the complex with DNA are expected to be different in each case. Therefore the kinetics can be optimized by simply tuning the sixth coordination site.

Crystallization turned out to be the most appropriate method found for the purification of these three new compounds. For that purpose, perchlorate was found to be the ideal counter ion, which not only allowed obtaining the compounds in high purity, but also crystals suitable for X-ray diffraction analysis.

The composition and structures of these three complexes are confirmed by elemental analysis, mass spectrometry, infrared spectroscopy and <sup>1</sup>H NMR spectroscopy. The microanalytical data are consistent with the empirical formulas C<sub>25</sub>H<sub>19</sub>N<sub>7</sub>O<sub>4</sub>RuCl<sub>2</sub> (**1a**), C<sub>25</sub>H<sub>21</sub>N<sub>7</sub>O<sub>9</sub>RuCl<sub>2</sub>·2H<sub>2</sub>O (**1b**) and C<sub>27</sub>H<sub>22</sub>N<sub>8</sub>O<sub>8</sub>RuCl<sub>2</sub> (**1c**). The mass spectrum of **1a** reveals the appearance of a molecular peak at *m/z* (ESIMS) 553.0, which corresponds to the expected cation [Ru(apy)(tpy)Cl]<sup>+</sup>. In the case of **1b** the aqua ligand is dissociated, therefore the molecular peak appears at *m/z* (ESIMS) 259.2, which corresponds to the species [Ru(apy)(tpy)]<sup>2+</sup>. This peak was also found in the case of **1c**, however the molecular peak was found at *m/z* (ESIMS) 279.8, corresponding to the cation [Ru(apy)(tpy)(CH<sub>3</sub>CN)]<sup>2+</sup>.

The infrared spectra of the three complexes are almost identical. The only remarkable difference is the presence of a broad, weak peak at 3000-3500  $\text{cm}^{-1}$  in the spectrum of **1b**, which appears not only as a consequence of the aqua ligand, but also of the water molecules in the lattice structure of the compound, *vide infra*. The presence of perchlorate as a counterion is confirmed by the very strong, broad peak at 1070-1090  $\text{cm}^{-1}$  and the strong, sharp peak at around 620  $\text{cm}^{-1}$ . Further the spectrum is complicated, with many peaks in the fingerprint area. A weak, broad peak around 3090  $\text{cm}^{-1}$ , characteristic of aromatic C-H stretching, as well as a sharp peak of medium intensity around 1600  $\text{cm}^{-1}$ , characteristic of aromatic ring stretchings, and an intense, sharp peak at 765-767  $\text{cm}^{-1}$ , characteristic of ring deformations and C-H out-of-plane deformations, appear as expected from a structure including aromatic rings. Two sharp peaks of medium intensity appear at 1448  $\text{cm}^{-1}$  and 1300  $\text{cm}^{-1}$ , respectively. These signals are the result of the N=N stretching vibration, indicating the presence of an azo group in the molecule. A Ru-Cl stretching mode would be expected in the area around 300  $\text{cm}^{-1}$ .<sup>20</sup> However, this is a too crowded area with bands therefore no conclusions can be drawn.

Finally, the solution geometry can be accurately assigned by means of 2D  $^1\text{H}$  NMR spectroscopy. Together with the NOE couplings, the COSY couplings between the peaks unmistakably confirm that the central nitrogen atom in tpy is trans to the pyridine N in apy in the three complexes (*vide infra*).

### X-ray structural determinations

Plots of the structures of the cations of  $[\text{Ru}(\text{apy})(\text{tpy})\text{L}](\text{ClO}_4)_{(2-n)}$  ( $\text{L} = \text{Cl}^-, \text{H}_2\text{O}, \text{CH}_3\text{CN}$ ) are given in Fig.2.2.

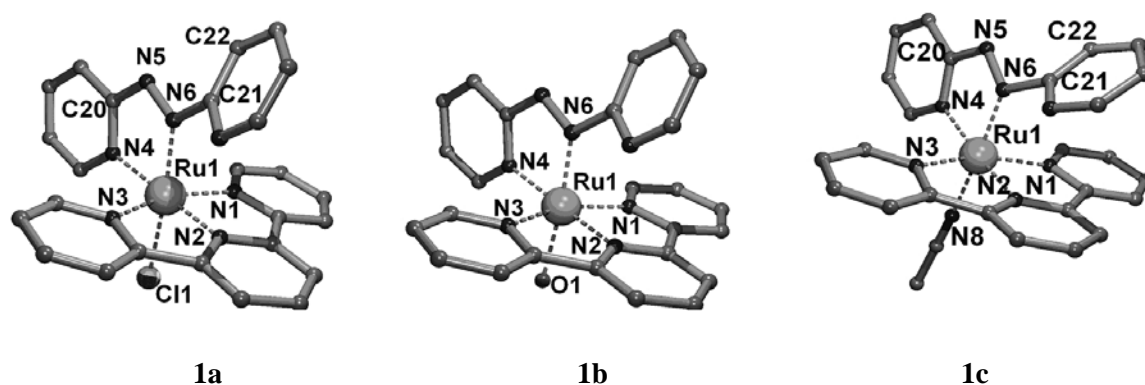


Fig.2.2. PLATON projections of the cations  $[\text{Ru}^{\text{II}}(\text{apy})(\text{tpy})\text{L}]^{m+}$  ( $\text{L} = \text{Cl}^-, \text{H}_2\text{O}, \text{CH}_3\text{CN}$ ) (**1a-c**), with numbering of major atoms. Hydrogen atoms and counter ions have been omitted for clarity.

The apy ligand could theoretically yield two different isomers of  $[\text{Ru}(\text{apy})(\text{tpy})\text{L}]^{(2-n)+}$ , the one in which the azo nitrogen of apy is trans to the pyridine nitrogen of tpy and the one in which the azo nitrogen is trans to the sixth coordination position, that is to say, to the chloro in **1a**, the aqua in **1b** and the acetonitrile in **1c**. However, the only observed isomer is in all three cases the latter. A similar arrangement has been reported for the 2-phenylazopyridine (azpy) analogues.<sup>10, 12, 13</sup>

The Ru-N(azo) bond distance is shorter than that of Ru-N(pyridine) in all three cases (see Table 2.2). This result is consistent with literature observations for the azpy analogues<sup>10, 12, 13</sup> and can be explained by the stronger  $\pi$ -backbonding,  $d\pi(\text{Ru}) \rightarrow \pi^*(\text{azo})$ . The bite angle of the apy ligand is between 76.2 (**1a**) and 76.8 (**1b**), comparable to the azpy ligand in  $[\text{Ru}(\text{azpy})(\text{tpy})\text{Cl}]\text{Cl}$ .<sup>13</sup> The tpy ligand is coordinated in such a way that the distance between the ruthenium and the central N is shorter than the distances between the ruthenium and the extreme N atoms. This characteristic was also observed in the above mentioned azpy analogues,<sup>10, 12, 13</sup> whereas in the starting complex  $\text{Ru}(\text{tpy})\text{Cl}_3$  these three bond lengths are equivalent.<sup>11</sup> Finally the tpy ligand is planar whereas the apy ligand is not. The latter consists of two planes: that of the coordinating pyridine ring and the one of the non-coordinating pyridine ring. The lack of coplanarity reduces the delocalization through the apy ligand. The dihedral angle between these two planes is 33.52(19)° for **1a**, 32.52(16)° for **1b** and 53.56(10)° in the case of **1c**.

#### *Packing in the crystal lattice*

Three-dimensional packing of the three complexes is depicted in Figs.2.3-2.5. Hydrogen bonding plays an important role in the crystal structure of complex **1b** (Fig.2.4), the only one in which classical hydrogen bonds are formed. These occur between the hydrogen atoms of the aqua ligand and the oxygen atoms of both the water molecules and one perchlorate counter ion, between the hydrogen atoms of the water molecules and the oxygen atoms of perchlorate and also between the former and the oxygen atoms of other water molecules.

$\pi$ - $\pi$  stacking is observed between the pyridine rings in all three complexes. In both **1a** and **1b** (Fig.2.3 and Fig.2.4), this stacking occurs between a pyridine ring of a tpy ligand and the opposite pyridine ring of the tpy ligand coordinated to the adjacent molecule, as well as between pyridine rings of adjacent apy ligands. Complex **1c** only displays  $\pi$ - $\pi$  stacking between opposite tpy pyridine rings.

Table 2.2. Selected distances (Å) and angles (°) in the crystal structures of  $[Ru(apy)(tpy)Cl](ClO_4)$  (**1a**),  $[Ru(apy)(tpy)(H_2O)](ClO_4)_2 \cdot 2H_2O$  (**1b**) and  $[Ru(apy)(tpy)(CH_3CN)](ClO_4)_2$  (**1c**)

<b>1a</b>		<b>1b</b>		<b>1c</b>	
Interatomic distances (Å)		Interatomic distances (Å)		Interatomic distances (Å)	
Ru(1)-N(1)	2.060 (3)	Ru(1)-N(1)	2.075 (2)	Ru(1)-N(1)	2.0710 (18)
Ru(1)-N(2)	1.968 (3)	Ru(1)-N(2)	1.978 (2)	Ru(1)-N(2)	1.9833 (19)
Ru(1)-N(3)	2.074 (3)	Ru(1)-N(3)	2.066 (2)	Ru(1)-N(3)	2.0762 (18)
Ru(1)-N(4)	2.053 (4)	Ru(1)-N(4)	2.060 (2)	Ru(1)-N(4)	2.0512(19)
Ru(1)-N(6)	1.981 (3)	Ru(1)-N(6)	1.960 (2)	Ru(1)-N(6)	1.9744(18)
Ru(1)-Cl(1)	2.3962 (9)	Ru(1)-O(1)	2.143 (2)	Ru(1)-N(8)	2.0537 (19)
		Hydrogen bonds			
		Donor-H...Acceptor	D..A (Å)		
		O(1)-H(101)...O(3)	2.646(4)		
		O(1)-H(102)...O(11)	2.718(4)		
		O(2)-H(103)...O(6)	2.802(4)		
		O(2)-H(104)...O(7)	2.849(4)		
		O(3)-H(105)...O(2)	2.718(4)		
		O(3)-H(106)...O(8)	2.948(5)		
Angles (°)		Angles (°)		Angles (°)	
N(4)-Ru(1)-Cl(1)	96.19 (9)	N(4)-Ru(1)-O(1)	95.93 (9)	N(4)-Ru(1)-N(8)	95.06 (8)
N(4)-Ru(1)-N(6)	76.17 (13)	N(4)-Ru(1)-N(6)	76.85 (10)	N(4)-Ru(1)-N(6)	76.41 (8)
N(4)-Ru(1)-N(1)	101.00 (14)	N(4)-Ru(1)-N(1)	101.55 (9)	N(4)-Ru(1)-N(1)	97.57 (7)
N(4)-Ru(1)-N(2)	179.00 (12)	N(4)-Ru(1)-N(2)	177.95 (9)	N(4)-Ru(1)-N(2)	172.53 (7)
N(4)-Ru(1)-N(3)	100.25 (14)	N(4)-Ru(1)-N(3)	99.81 (9)	N(4)-Ru(1)-N(3)	104.05 (7)
N(6)-Ru(1)-Cl(1)	172.28 (9)	N(6)-Ru(1)-O(1)	172.78 (9)	N(6)-Ru(1)-N(8)	170.52 (8)
N(6)-Ru(1)-N(1)	92.46 (14)	N(6)-Ru(1)-N(1)	94.21 (9)	N(6)-Ru(1)-N(1)	96.53 (7)
N(6)-Ru(1)-N(2)	102.84 (12)	N(6)-Ru(1)-N(2)	101.27 (9)	N(6)-Ru(1)-N(2)	97.00 (8)
N(6)-Ru(1)-N(3)	93.97 (14)	N(6)-Ru(1)-N(3)	93.12 (9)	N(6)-Ru(1)-N(3)	89.28 (7)
N(1)-Ru(1)-Cl(1)	90.13 (10)	N(1)-Ru(1)-O(1)	87.21 (9)	N(1)-Ru(1)-N(8)	88.62 (7)
N(1)-Ru(1)-N(2)	79.16 (13)	N(1)-Ru(1)-N(2)	79.33 (9)	N(1)-Ru(1)-N(2)	79.49 (7)
N(1)-Ru(1)-N(3)	158.71 (15)	N(1)-Ru(1)-N(3)	158.49(9)	N(1)-Ru(1)-N(3)	158.36 (8)
N(2)-Ru(1)-Cl(1)	84.80 (9)	N(2)-Ru(1)-O(1)	85.95 (9)	N(2)-Ru(1)-N(8)	91.75 (8)
N(2)-Ru(1)-N(3)	79.62 (13)	N(2)-Ru(1)-N(3)	79.42 (9)	N(2)-Ru(1)-N(3)	79.12 (7)
N(3)-Ru(1)-Cl(1)	86.18 (10)	N(3)-Ru(1)-O(1)	88.05 (9)	N(3)-Ru(1)-N(8)	88.80 (7)
Torsion angles (°)		Torsion angles (°)		Torsion angles (°)	
N(6)-N(5)-C(20)-N(4)	-0.9 (5)	N(6)-N(5)-C(20)-N(4)	-1.3 (4)	N(6)-N(5)-C(20)-N(4)	-5.5 (3)
N(5)-N(6)-C(21)-C(22)	-31.8 (5)	N(5)-N(6)-C(21)-C(22)	-29.6 (4)	N(5)-N(6)-C(21)-C(22)	-45.0 (3)

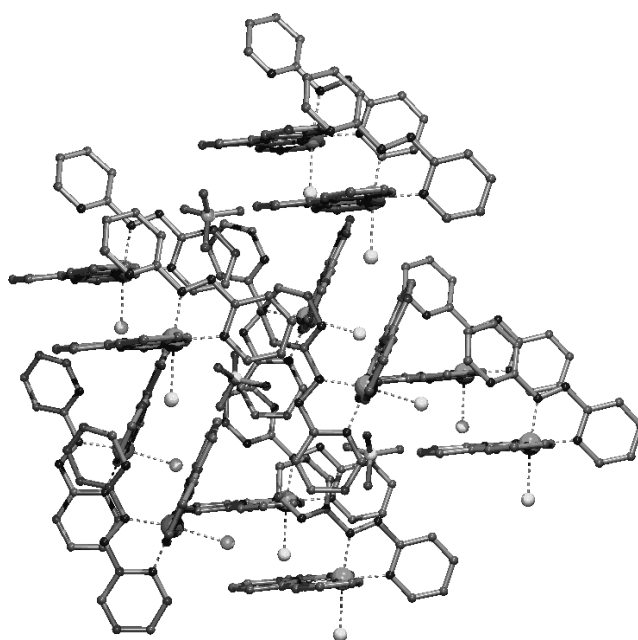


Fig.2.3. Packing of  $[Ru(apy)(tpy)Cl](ClO_4)$  (**1a**). Hydrogen atoms are omitted for clarity.

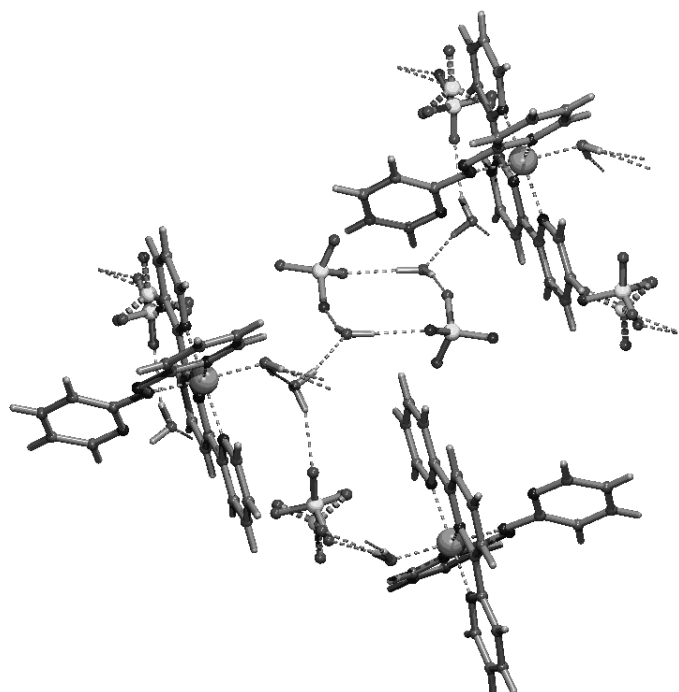


Fig.2.4. Hydrogen bonding in  $[Ru(apy)(tpy)(H_2O)](ClO_4)_2 \cdot 2 H_2O$  (**1b**).

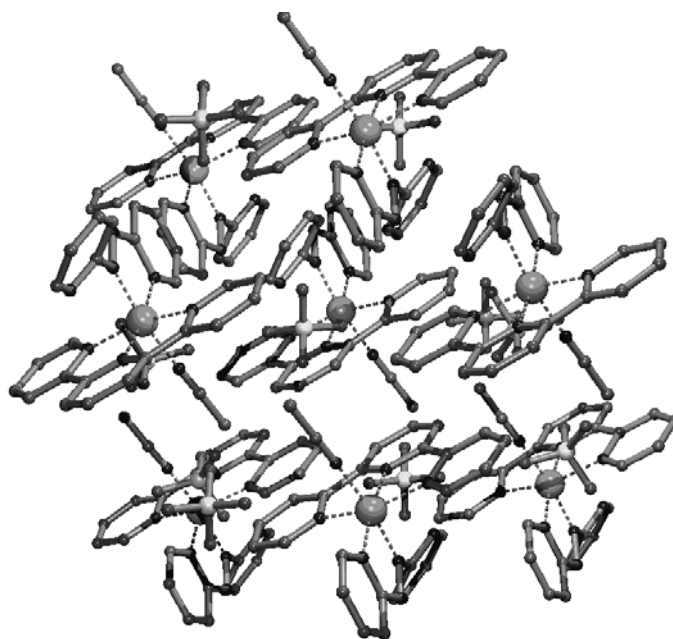


Fig.2.5. Packing of  $[Ru(apy)(tpy)(CH_3CN)](ClO_4)_2$  (**1c**). Hydrogen atoms are omitted for clarity.

### $^1H$ NMR characterization of the $[Ru(apy)(tpy)L](ClO_4)_{(2-n)}$ compounds

The  $^1H$  NMR spectra of compounds **1a**, **1b** and **1c** were recorded at 298 K in DMSO- $d_6$ , DMSO- $d_6$  and  $CD_3CN$ , respectively. In all three cases four sets of peaks were observed in the aromatic region. The hydrogen atoms present in the coordinated pyridine ring will be from now on referred to as NA, where N is a number that indicates the position of the hydrogen in the ring. Analogously, the hydrogen atoms in the non-coordinated pyridine ring will be called NA'; the hydrogen atoms in the extreme pyridine rings in tpy, NT and finally the ones in the central pyridine ring in tpy, NT' (see Fig.2.6 for the numbering). The aromatic region of the  $^1H$ - $^1H$  COSY and NOESY spectra of **1a** in DMSO- $d_6$  at 298K are shown in Fig.2.7. Some assignments are indicated in the figure.

The most deshielded peak in the aromatic region of the  $^1H$  NMR spectrum of **1a** appears at 9.83 ppm and corresponds to the 6A atom. This proton appears at such a low field, because it is close in space to a chlorine atom and also attached to a carbon adjacent to a coordinated nitrogen atom. This last fact determines that the  $J$  coupling of this doublet is smaller than that of the one situated directly upfield, which can be assigned as 3A, as explained below. The 2D COSY connectivities result in the assignment of 5A, 4A and 3A, at 8.27 ppm, 8.45 ppm and 8.93 ppm, respectively.

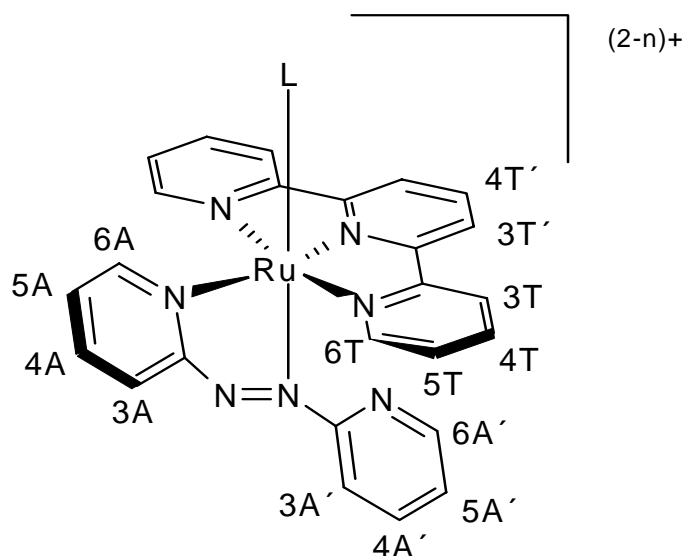


Fig.2.6.  $[Ru(apy)(tpy)L](ClO_4)_{(2-n)}$  compounds. Proton numbering scheme for  $^1H$  NMR spectra.

The 2D NOESY spectrum shows a clear crosspeak between the 6A signal and that appearing at 7.22 ppm. Since it is known from the X-ray structure that 6A and 6T are close to each other in space, the signal at 7.22 ppm is assigned to the 6T atom. Once 6T is known, 5T, 4T and 3T can be assigned from the interactions shown in the COSY spectrum. Theoretically a NOESY peak should appear between 3T and 3T', but this was not observed due to overlap. The set 6A', 5A', 4A', 3A' appears much more upfield than 6A, 5A, 4A, 3A and can be assigned analogously. In this case, 6A' is also more deshielded than 3A'.

The  $^1H$  NMR spectra of **1b** and **1c** were assigned using the same methodology. The aromatic region of the  $^1H$ - $^1H$  COSY and NOESY spectra of **1b** in DMSO- $d_6$  are shown in Fig.2.8. Analogous 2D NMR spectra of **1c** in CD $_3$ CN at 298K can be found in Fig.2.9. The peaks corresponding to 3T' and 4T' appear overlapping those of 3T and 5A, respectively, in the case of complexes **1a** and **1b**. This can be seen from the integral values, as well as the COSY interactions. In the spectrum of **1c** the signals corresponding to 3T', 4T' and 3T are overlapped, forming a multiplet of intensity four.

The peak corresponding to 5A' in complex **1b** overlaps with 6T; 3A' and 5A' are overlapping with each other in complex **1c**, resulting in a multiplet of intensity two. The chemical shift values of all the above-mentioned protons are listed in Table 2.3.

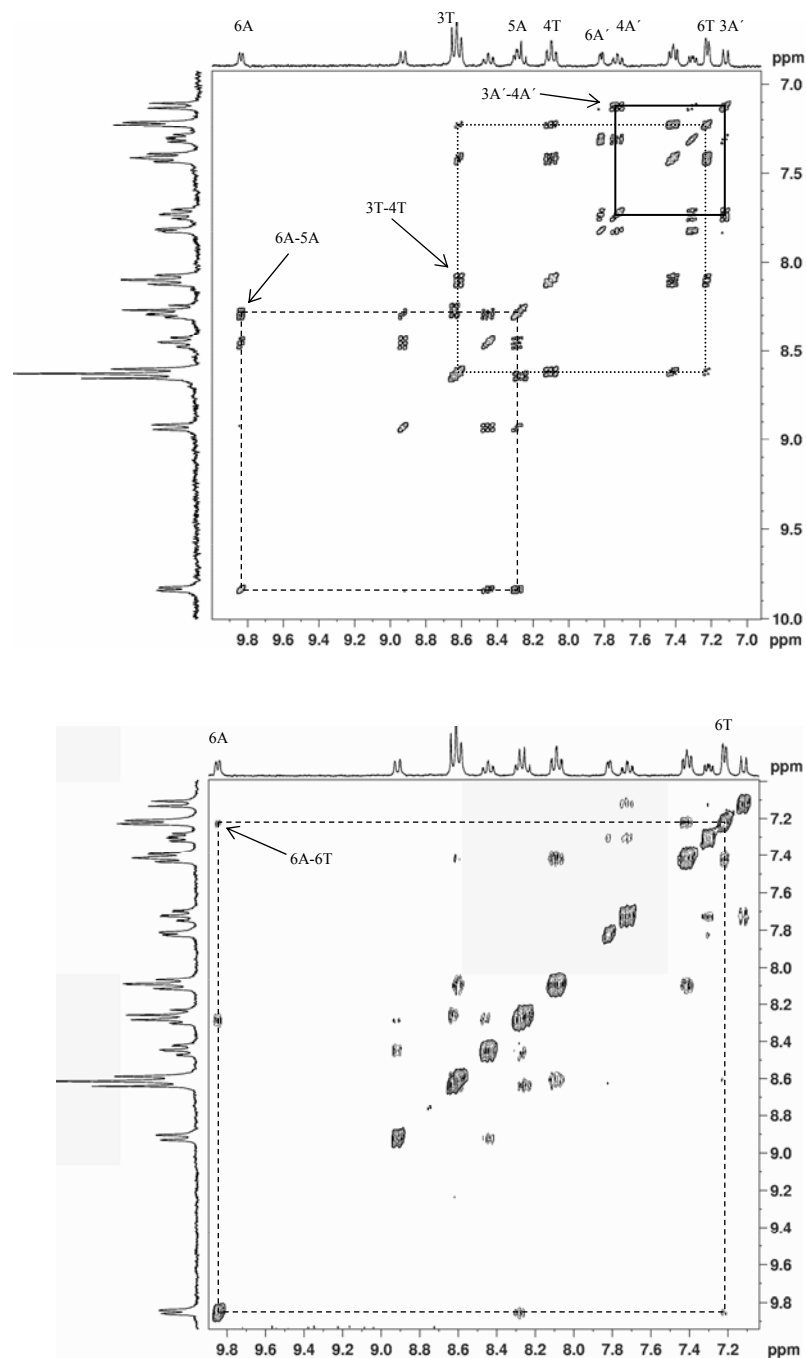


Fig.2.7. Aromatic region of the  $^1\text{H}$ - $^1\text{H}$  COSY (above) and NOESY (below) spectra of **1a** in  $\text{DMSO-d}_6$  at 298K, with some assignments. In the COSY spectrum, the dashed lines indicate the 6A-5A(-4A-3A) COSY cross peaks. The dotted lines show the 3T-4T(-5T-6T) COSY cross peaks. The solid lines indicate the 3A'-4A'(-5A'-6A') COSY cross peaks. Arrows show the COSY cross peaks between 6A and 5A, 3T and 4T, 3A' and 4A', respectively. In the NOESY spectrum, the 6A-6T NOE is signalled.

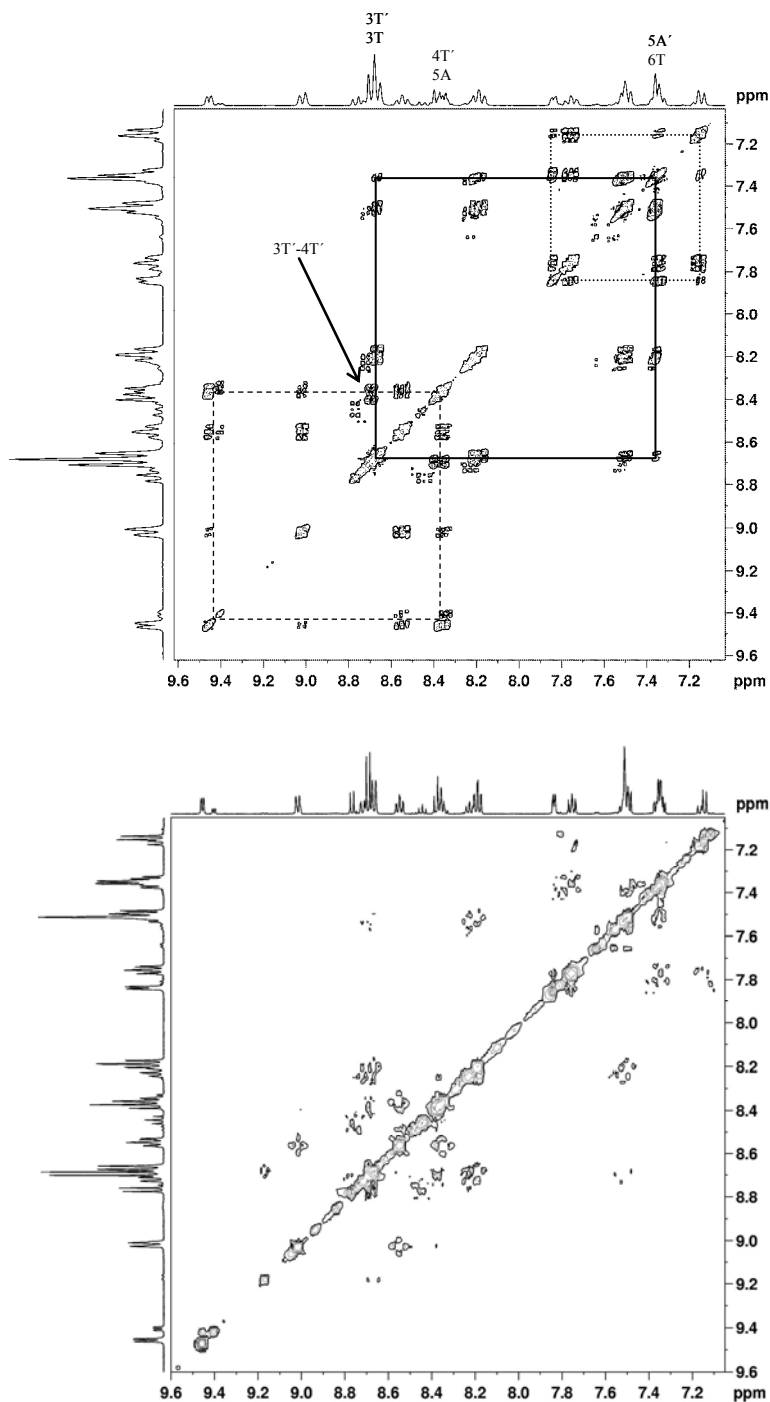


Fig.2.8. Aromatic region of the  $^1\text{H}$ - $^1\text{H}$  COSY (above) and NOESY (below) spectra of **1b** in  $\text{DMSO-d}_6$  at 298K, with some assignments. In the COSY spectrum, the dashed lines show the 6A-5A(-4A-3A) COSY cross peaks. The dotted lines show the 3T-4T(-5T-6T) COSY cross peaks. The solid lines indicate the 3A'-4A'(-5A'-6A') COSY cross peaks. An arrow shows the COSY cross peak between 3T' and 4T'. Substitution of  $\text{H}_2\text{O}$  by dmsO has occurred to some extent.

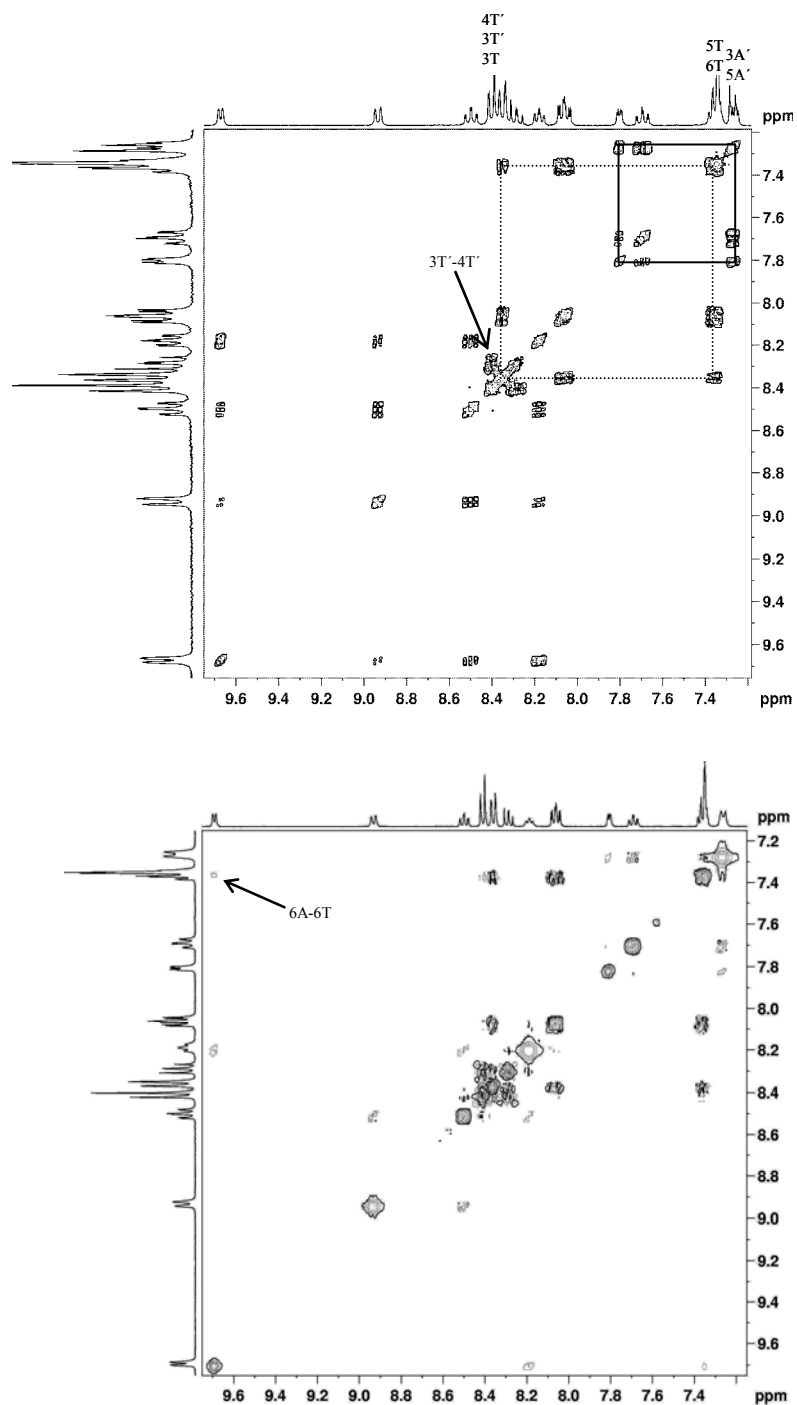


Fig.2.9. Aromatic region of the  $^1\text{H}$ - $^1\text{H}$  COSY (above) and NOESY (below) spectra of **1c** in  $\text{CD}_3\text{CN}$  at 298K, with some assignments. In the COSY spectrum, the dotted lines show the 3T-4T(-5T-6T) COSY cross peaks. The solid lines indicate the 3A'-4A'(-5A'-6A') COSY cross peaks. An arrow shows the COSY cross peak between 3T' and 4T'. In the NOESY spectrum, the 6A-6T NOE is signalled.

*Table 2.3. Proton chemical shift values (ppm) for the [Ru(apy)(tpy)L](ClO<sub>4</sub>)<sub>(2-n)</sub> complexes **1a-1c**. **1a** and **1b** were taken in DMSO-*d*<sub>6</sub>; **1c** was taken in CD<sub>3</sub>CN, all of them at 298K.*

Complex	3A	4A	5A	6A	3A'	4A'	5A'	6A'	3T	4T	5T	6T	3T'	4T'
<b>1a</b>	8.93	8.45	8.27	9.83	7.12	7.72	7.31	7.82	8.63	8.10	7.41	7.22	8.63	8.27
<b>1b</b>	9.01	8.55	8.36	9.46	7.14	7.75	7.34	7.84	8.67	8.19	7.50	7.34	8.67	8.36
<b>1c</b>	8.93	8.50	8.18	9.67	7.27	7.70	7.27	7.80	8.38	8.06	7.36	7.36	8.38	8.38

#### 2.4. Concluding remarks

A family of ruthenium polypyridyl compounds of formula [Ru(apy)(tpy)L](ClO<sub>4</sub>)<sub>(2-n)</sub> (apy = 2,2'-azobispyridine; tpy = 2,2':6',2''-terpyridine; L = Cl<sup>-</sup>, H<sub>2</sub>O, CH<sub>3</sub>CN) (**1a-c**) was successfully synthesized and characterized. The study of their crystal structures revealed *trans* azo-nitrogen coordination similar to that reported for 2-phenylazopyridine, and π-π stacking between the pyridine rings.

The potential interest of these complexes is multiple. They have been designed to be similar to Ru(tpy)Cl<sub>3</sub>, a compound with anticancer activity, but with the disadvantage of a poor water-solubility. The [Ru(apy)(tpy)L](ClO<sub>4</sub>)<sub>(2-n)</sub> complexes show an improved solubility. Moreover the ligand apy is structurally related to azpy, which is present in recently reported cytotoxic ruthenium complexes.<sup>3, 4</sup> Therefore it is of interest to find out how these compounds interact with DNA model bases and DNA, since the anticancer properties of a number of platinum and ruthenium complexes are generally accepted to be related to their binding to the DNA of cancerous cells.<sup>1</sup> In a subsequent study calf-thymus DNA, as well as a series of both cisplatin-resistant and non-resistant cancerous cell lines will be treated with the [Ru(apy)(tpy)L](ClO<sub>4</sub>)<sub>(2-n)</sub> complexes to test factors such as the DNA binding and the *in vitro* anticancer activity of such compounds (see chapter 4 of this thesis).

#### 2.5. References

1. Reedijk, J., *Proc. Natl. Acad. Sci. U. S. A.* **2003**, *100*, 3611-3616.
2. Nováková, O.; Kaspárková, J.; Vrána, O.; van Vliet, P. M.; Reedijk, J.; Brabec, V., *Biochemistry* **1995**, *34*, 12369-12378.
3. Velders, A. H.; Kooijman, H.; Spek, A. L.; Haasnoot, J. G.; de Vos, D.; Reedijk, J., *Inorg. Chem.* **2000**, *39*, 2966-2967.

4. Hotze, A. C. G.; Caspers, S. E.; de Vos, D.; Kooijman, H.; Spek, A. L.; Flamigni, A.; Bacac, M.; Sava, G.; Haasnoot, J. G.; Reedijk, J., *J. Biol. Inorg. Chem.* **2004**, *9*, 354-364.
5. Mishra, L.; Yadaw, A. K.; Sinha, R.; Singh, A. K., *Indian J. Chem. Sect A-Inorg. Bio-Inorg. Phys. Theor. Anal. Chem.* **2001**, *40*, 913-928.
6. Sava, G.; Pacor, S.; Bergamo, A.; Cocchietto, M.; Mestroni, G.; Alessio, E., *Chem.-Biol. Interact.* **1995**, *95*, 109-126.
7. Sava, G.; Clerici, K.; Capozzi, I.; Cocchietto, M.; Gagliardi, R.; Alessio, E.; Mestroni, G.; Perbellini, A., *Anti-Cancer Drugs* **1999**, *10*, 129-138.
8. Kirpal, A.; Reiter, E., *Ber. Deut. Chem. Ges.* **1927**, *60B*, 664.
9. Kaim, W., *Coord. Chem. Rev.* **2001**, *219*, 463-488.
10. Pramanik, N. C.; Pramanik, K.; Ghosh, P.; Bhattacharya, S., *Polyhedron* **1998**, *17*, 1525-1534.
11. Laurent, F.; Plantalech, E.; Donnadiou, B.; Jiménez, A.; Hernández, F.; Martínez-Ripoll, M.; Biner, M.; Llobet, A., *Polyhedron* **1999**, *18*, 3321-3331.
12. Mondal, B.; Walawalkar, M. G.; Lahiri, G. K., *J. Chem. Soc.-Dalton Trans.* **2000**, 4209-4217.
13. Hansongnern, K.; Saeteaw, U.; Mostafa, G.; Jiang, Y. C.; Lu, T. H., *Anal. Sci.* **2001**, *17*, 683-684.
14. Adcock, P. A.; Keene, F. R.; Smythe, R. S.; Snow, M. R., *Inorg. Chem.* **1984**, *23*, 2336-2343.
15. Blessing, R. H., *Acta Crystallogr. Sect. A* **1995**, *51*, 33-38.
16. Sheldrick, G. M. *SADABS. Program for Empirical Absorption Correction, Bruker AXS, Karlsruhe, Germany*, **2004**.
17. Beurskens, P. T.; Beurskens, G.; de Gelder, R.; Garcia-Granda, S.; Gould, R. O.; Israel, R.; Smits, J. M. M. *The DIRDIF-99 Program System, Crystallography Laboratory, University of Nijmegen, The Netherlands*, **1999**.
18. Sheldrick, G. M. *SHELXL97. Program for Crystal Structure Refinement, University of Göttingen, Germany*, **1997**.
19. Spek, A. L., *J. Appl. Crystallogr.* **2003**, *36*, 7-13.
20. Goswami, S.; Chakravarty, A. R.; Chakravorty, A., *Inorg. Chem.* **1982**, *21*, 2737-2742.

### 3. Interaction between the DNA model base 9-ethylguanine and a group of ruthenium polypyridyl complexes: kinetics and conformational temperature dependence<sup>\*</sup>

The binding capability of three ruthenium polypyridyl compounds of structural formula  $[\text{Ru}(\text{apy})(\text{tpy})\text{L}](\text{ClO}_4)_{(2-n)}$  (**1a-c**; apy = 2,2'-azobispyridine; tpy = 2,2':6',2''-terpyridine; L = Cl<sup>-</sup>, H<sub>2</sub>O, CH<sub>3</sub>CN) to a fragment of DNA was studied. The interaction between each of these complexes and the DNA model base 9-ethylguanine (9-EtGua) was followed by means of <sup>1</sup>H NMR studies. DFT calculations were carried out to explore the preferential ways of coordination between the ruthenium complexes and guanine. The ruthenium–9-ethylguanine adduct formed was isolated and fully characterized using different techniques. A variable-temperature <sup>1</sup>H NMR experiment was carried out, which showed that while the 9-ethylguanine fragment was rotating fast at high temperature, a loss of symmetry was suffered by the model base adduct as the temperature was lowered, indicating restricted rotation of the guanine residue.

---

<sup>\*</sup> This chapter is based on Corral, E.; Hotze, A.C.G.; Magistrato, A.; Reedijk, J., *Inorg. Chem.*, **2007**, *46*, 6715-6722.

### 3.1. Introduction

As discussed in chapter 2, recent studies concerning some ruthenium polypyridyl complexes suggest that such compounds could be an alternative to the use of the classic platinum anticancer drugs.<sup>1</sup> An example of this type of complexes is Ru(tpy)Cl<sub>3</sub>, which shows a remarkable in vitro cytotoxicity and exhibits antitumour activity.<sup>2</sup>  $\alpha$ -[Ru(azpy)<sub>2</sub>Cl<sub>2</sub>] was reported to show a very high cytotoxicity, which was found to be even more pronounced than the cytotoxicity showed by cisplatin in most of the applied cell lines.<sup>3, 4</sup>

The ultimate target of this kind of compounds is generally accepted to be DNA.<sup>5</sup> Ruthenium polypyridyl complexes bind to DNA in a variety of covalent and non-covalent modes. One of the most likely ways of interaction between the two molecules appears to be the coordination of the ruthenium centre to a DNA base.<sup>6-9</sup>

Various groups have tried to correlate DNA binding of a potential metallodrug to its anticancer activity.<sup>10-20</sup> The models vary from simple model bases, of which the preferred ones are the 9-alkylguanines, to oligonucleotides and larger DNA pieces.

NMR spectroscopy can be an important tool that allows studying whether the metal complex reacts with the model base and, if this reaction occurs, how it develops in time, as well as the structure of the formed products. Further, the experimental conditions can be tuned to resemble physiological conditions as closely as possible.

In the current investigation a series of complexes with formula [Ru(apy)(tpy)L](ClO<sub>4</sub>)<sub>(2-n)</sub> (**1a-c**; apy = 2,2'-azobispyridine; tpy = 2,2':6',2''-terpyridine; L = Cl<sup>-</sup>, H<sub>2</sub>O, CH<sub>3</sub>CN) was selected (see Fig.2.2).

These complexes are very similar to each other,<sup>21</sup> except for the relative lability of the ligand occupying the sixth coordination position. The labilities of the three chosen ligands should, in principle, be large enough to allow coordination of the complex to the model base, albeit their different sizes, shapes, charges and binding affinities suggest this process could happen following different kinetics in each case. Intercalation of the polypyridyl ligands between DNA base pairs could also be a possible way of interaction of these complexes with DNA.

The reaction between each of the complexes and the model base 9-ethylguanine was studied. The 9-ethylguanine adduct that resulted in all cases (**1d**; see Fig.3.1) was isolated and completely characterized. Conformational studies were carried out by means of variable temperature and 2D NMR studies. Structural and electronic properties of the analogous guanine adduct were calculated by DFT calculations.

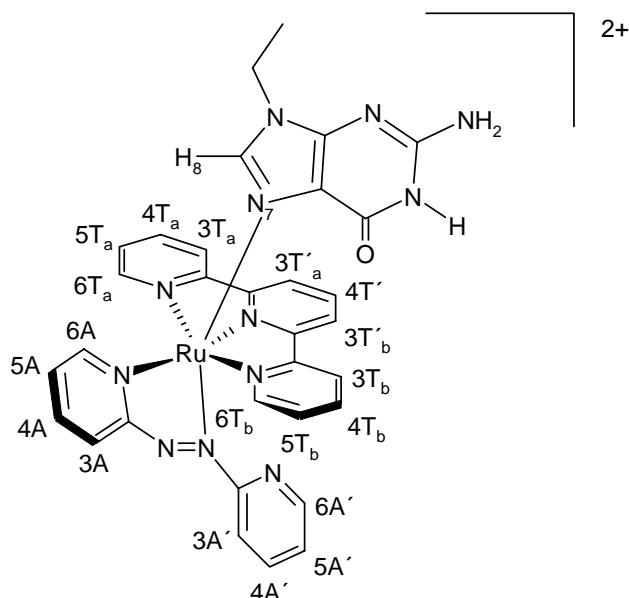


Fig.3.1. Schematic structure of  $[Ru(apy)(tpy)(9-EtGua)]^{2+}$  (**1d**). A few selected atoms have been labeled, for use in NMR assignments. The sub indexes “a” and “b” are only used in the low-temperature spectra. Under low-temperature conditions the protons in the external rings of tpy are not equivalent due to the slow rotation of 9-EtGua on the NMR time scale. As a consequence of this rotation, ring “a” becomes “b” and vice versa.

### 3.2. Experimental

#### Materials and reagents

2,2'-azobispyridine (apy),  $Ru(tpy)Cl_3$ ,  $[Ru(apy)(tpy)Cl](ClO_4)$ ,  $[Ru(apy)(tpy)(H_2O)](ClO_4)_2 \cdot 2H_2O$  and  $[Ru(apy)(tpy)(CH_3CN)](ClO_4)_2$  were synthesized according to the literature methods.<sup>21-23</sup> LiCl, NaClO<sub>4</sub> (both Merck), NaClO, AgNO<sub>3</sub> (both Acros), tpy (Aldrich),  $RuCl_3 \cdot 3H_2O$  (Johnson & Matthey), and 9-EtGua (Sigma) were used as supplied. All other chemicals and solvents were reagent grade commercial materials and used as received.

#### Physical measurements

C, H and N determinations were performed on a Perkin Elmer 2400 Series II analyzer. Mass spectra were obtained with a Finnigan Aqa mass spectrometer equipped with an electrospray ionization source (ESI). FTIR spectra were obtained on a Perkin Elmer Paragon 1000 FTIR spectrophotometer equipped with a Golden Gate ATR device, using the diffuse reflectance technique (res. 4 cm<sup>-1</sup>). NMR spectra were recorded on a Bruker DPX-300 spectrometer operating at a frequency of 300 MHz, at a temperature of 310 K; on a Bruker Avance-400, at a frequency of 400 MHz and 328 K, and on a Bruker DRX-500

spectrometer operating at a frequency of 500 MHz, at a variable temperature. Chemical shifts were calibrated against tetramethylsilane (TMS).

### **[Ru(apy)(tpy)(9-EtGua)]<sup>2+</sup> titration**

The pH titrations were carried out at 310 K in D<sub>2</sub>O, by adjustments with DCl and NaOD without the use of any buffer. The pH values were not corrected for the H/D isotope effect. The pH meter was calibrated with Fisher certified buffer solutions of pH 4.00, 7.00 and 10.00.

### **Synthesis and characterization of [Ru(apy)(tpy)(9-EtGua)](ClO<sub>4</sub>)<sub>2</sub>**

[Ru(apy)(tpy)(H<sub>2</sub>O)](ClO<sub>4</sub>)<sub>2</sub>·2H<sub>2</sub>O (15 mg, 0.019 mmol) and 9-EtGua (4 mg, 0.022 mmol) were vigorously refluxed in 5 mL EtOH abs for 24 hours. The mixture was left to cool down to r.t. The product was collected by filtration, washed with a small amount (about 2 mL) of ice-cold water and ether and dried in vacuo over silica (yield 82%). C<sub>32</sub>H<sub>28</sub>N<sub>12</sub>O<sub>9</sub>Cl<sub>2</sub>Ru (%) calcd C, 42.9; H, 3.1; N, 18.7. Found: C, 42.7; H, 2.7; N, 18.8. ESI-MS: *m/z* 697.1 ([Ru(apy)(tpy)(9-EtGua - H)]<sup>+</sup>); 348.7 ([Ru(apy)(tpy)(9-EtGua)]<sup>2+</sup>). <sup>1</sup>H NMR (300 MHz, D<sub>2</sub>O, 310 K): δ (ppm)= 9.21 (d, 1H, 5.20 Hz); 8.92 (d, 1H, 8.22 Hz); 8.48 (t, 1H, 8.00 Hz); 8.37 (m, 3H); 8.20 (t, 1H, 8.06 Hz); 8.11 (m, 3H); 7.92 (d, 1H, 4.99 Hz); 7.64 (m, 3H); 7.41 (dd, 2H, *J*<sub>1</sub> = 8.70 Hz, *J*<sub>2</sub> = 14.92 Hz); 7.30 (dd, 1H, *J*<sub>1</sub> = 4.28 Hz, *J*<sub>2</sub> = 6.86 Hz); 6.81 (s, 1H); 6.52 (d, 1H, 7.98 Hz); 3.83 (dd, 2H, *J*<sub>1</sub> = 7.21 Hz, *J*<sub>2</sub> = 14.47 Hz); 1.07 (t, 3H, 7.27 Hz).

### **Computational Details**

DFT calculations<sup>24</sup> were performed using the program CPMD<sup>25</sup> with a plane waves (PW) basis set up to an energy cut-off of 70 Ry. Core/valence interactions were described using norm conserving pseudopotentials of the Martins-Troullier type.<sup>26</sup> Integration of the non-local parts of the pseudopotential was obtained via the Kleinman-Bylander scheme<sup>27</sup> for all of the atoms except ruthenium, for which a Gauss-Hermite numerical integration scheme was used. For ruthenium a semicore pseudopotential was adopted as described in literature<sup>28</sup> that also incorporates scalar relativistic effects. The gradient corrected Becke exchange functional and the Perdew correlation functional (BP) were used.<sup>29, 30</sup> Isolated system conditions<sup>31</sup> were applied. Calculations were performed in an orthorhombic cell of edge *a* =30, *b*=29, *c*=36 a.u. Geometries have been relaxed by iterating geometry optimization runs (based on a conjugate gradient procedure) and molecular dynamics (MD)

runs at 0 K up to a gradient of  $5.0 \times 10^{-5}$  a.u. A fictitious electron mass of 900 a.u., and a time step of 0.1205 fs were used in the MD runs.

Four possible conformers of Ru(apv)(tpy)(Gua) were found, which differ in the orientation of the guanine above the plane of the ligands.

### 3.3. Results and discussion

#### <sup>1</sup>H NMR studies of the interaction between three ruthenium polypyridyl complexes and 9-ethylguanine

The reaction between the ruthenium polypyridyl complex  $[\text{Ru}(\text{apv})(\text{tpy})(\text{H}_2\text{O})]^{2+}$  and the DNA model base 9-ethylguanine was studied by <sup>1</sup>H NMR at a 1:2 ratio (see Fig.3.2). The conditions of the experiment were chosen to be as close as possible to physiological conditions, using D<sub>2</sub>O as a solvent and a temperature of 310 K. The reaction was studied for 24 hours, during which the pH was seen to remain neutral.

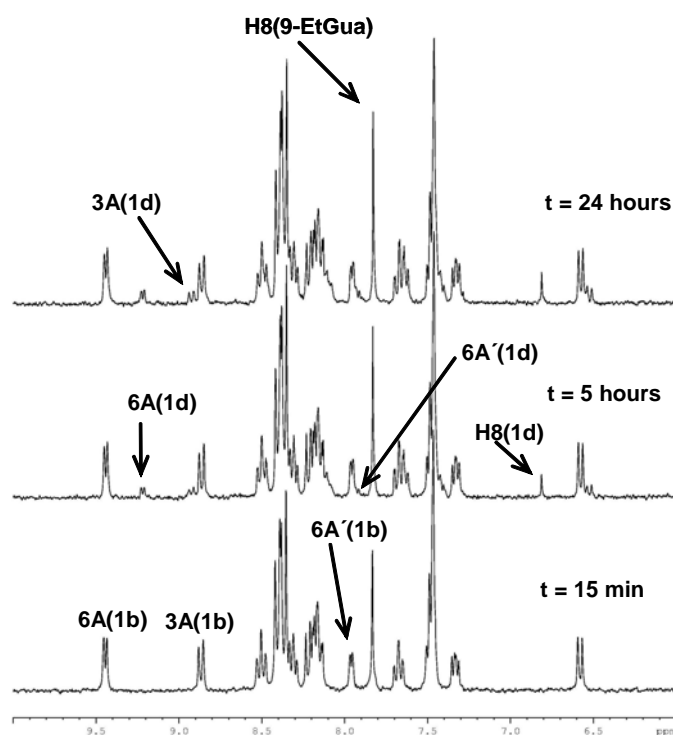


Fig.3.2. <sup>1</sup>H NMR study over 24 h of the reaction between the ruthenium polypyridyl complex  $[\text{Ru}(\text{apv})(\text{tpy})(\text{H}_2\text{O})]^{2+}$  (**1b**) and the DNA model base 9-ethylguanine in D<sub>2</sub>O at a 1:2 ratio. Some selected peaks have been labeled with their assignments.

The signals appearing in this experiment could be unambiguously assigned by comparison with the  $^1\text{H}$  NMR spectrum of the isolated model base adduct  $[\text{Ru}(\text{apy})(\text{tpy})(9\text{-EtGua})](\text{ClO}_4)_2$  (**1d**), which had been synthesized and characterized by several techniques, *vide infra*. Although the peaks corresponding to 9-ethylguanine ( $\text{CH}_3$  at 1.07 ppm,  $\text{CH}_2$  at 3.83 ppm and H8 at 6.81 ppm) were found to be shifted with respect to the free base, the peak of choice for the kinetic studies was that corresponding to the proton 6A. This significantly deshielded proton presented a different chemical shift for each of the four complexes (**1a-d**), which allowed us to easily distinguish each species in solution as well as to measure the ratio between them.

The model base 9-ethylguanine was observed to react with the ruthenium complex to give the adduct  $[\text{Ru}(\text{apy})(\text{tpy})(9\text{-EtGua})]^{2+}$ . This reaction occurred during the first 5 hours when a ruthenium compound–9-EtGua ratio of 1:2 was used. No further changes were observed. Despite the two-fold excess of 9-EtGua, only 20% of the ruthenium complex reacted to yield the adduct.

The same experiment was carried out starting from the complex  $[\text{Ru}(\text{apy})(\text{tpy})(\text{CH}_3\text{CN})](\text{ClO}_4)_2$  (**1c**; see Fig.3.3). In this case the acetonitrile complex was observed to hydrolyze to produce the cation  $[\text{Ru}(\text{apy})(\text{tpy})(\text{H}_2\text{O})]^{2+}$ , besides reacting with 9-ethylguanine as described above. After the 5 hours needed by the model base adduct to reach its maximum concentration in the experiment described above, 15% of the ruthenium could be found in the form of the 9-EtGua adduct in this second case. The 20% obtained in the first experiment was obtained in this second experiment after 8 hours. The reaction went on until the maximum fraction of adduct was reached. In a total of 18 hours from the start of the reaction, 30% of the ruthenium was found to be in the form of  $[\text{Ru}(\text{apy})(\text{tpy})(9\text{-EtGua})]^{2+}$ .

The different kinetics followed by complexes **1b** and **1c** can be understood in terms of the geometry of the labile ligand. That is, while  $\text{H}_2\text{O}$  is angular and forms hydrogen bonds,  $\text{CH}_3\text{CN}$  is linear and it does not form any hydrogen bonds, offering less sterical hindrance for an attack by 9-EtGua.

Despite the excess of 9-EtGua used for the experiment, most of the ruthenium compounds appears in the form of the aqua or the acetonitrile compound. This suggests the formation of a very slow equilibrium between **1d** and each of the other involved Ru species.

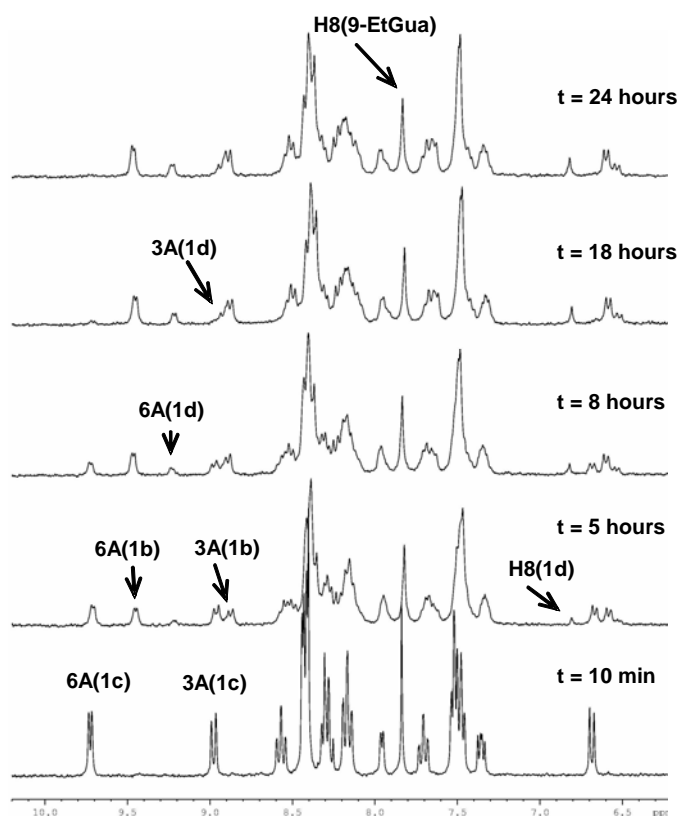


Fig.3.3.  $^1\text{H}$  NMR study over 24 h of the reaction between the ruthenium polypyridyl complex  $[\text{Ru}(\text{apy})(\text{tpy})(\text{CH}_3\text{CN})]^{2+}$  (**1c**) and the DNA model base 9-ethylguanine in  $\text{D}_2\text{O}$  at a 1:2 ratio. Some selected peaks have been labeled with their assignments.

The reaction between  $[\text{Ru}(\text{apy})(\text{tpy})\text{Cl}]^+$  and 9-ethylguanine proceeded much slower than the other two Ru precursors described above. Due to the lower solubility of the ruthenium complex in  $\text{D}_2\text{O}$ , the results obtained in this last case were only regarded in a qualitative way.

The curve of the molar fraction of  $[\text{Ru}(\text{apy})(\text{tpy})(9\text{-EtGua})]^{2+}$  ( $\chi_E$ ) vs. time (see Fig.3.4) was fitted with eq. (1).

$$\chi_E = k (1 - e^{-k't}) \quad (1)$$

Where  $k$  is the maximum value of the molar fraction of the ruthenium-model base adduct reached. The values of  $k$  and the rate constant  $k'$  were calculated, as well as the half-life of the ruthenium-model base adduct (**1d**) in solution (see Table 3.1).

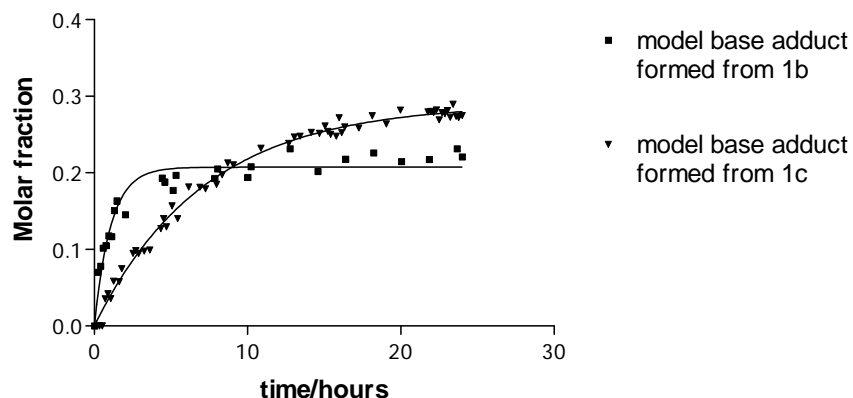


Fig.3.4. Formation of the model base adduct from two ruthenium complexes (**1b** and **1c**).  
Molar fraction of  $[\text{Ru}(\text{apy})(\text{tpy})(9\text{-EtGua})]^{2+}$  ( $\chi_E$ ) vs. time.

Table 3.1. Rate constants determined for the reaction between 9-ethylguanine and the ruthenium polypyridyl complexes  $[\text{Ru}(\text{apy})(\text{tpy})(\text{H}_2\text{O})]^{2+}$  (**1b**) and  $[\text{Ru}(\text{apy})(\text{tpy})(\text{CH}_3\text{CN})]^{2+}$  (**1c**), respectively.

Complex	Rate constant $k'$ (hours <sup>-1</sup> )	$k$	half-life of <b>1d</b> in solution (hours)
<b>1b</b>	$0.92 \pm 0.08$	$0.207 \pm 0.004$	$0.8 \pm 0.2$
<b>1c</b>	$0.139 \pm 0.004$	$0.290 \pm 0.003$	$5.0 \pm 0.3$

### DFT Calculations

Four different models of the  $[\text{Ru}(\text{apy})(\text{tpy})(\text{Gua})]^{2+}$  adduct were considered, differing in the orientation of the N1-Ru-N7-C8 torsional angles (see Fig.3.5). Structures **1d<sub>I</sub>** and **1d<sub>II</sub>** show an orientation of Gua in such a way that its keto group is wedged between the pyridine ring of apy and the pyridine ring of tpy. This orientation is analogous to that shown in the X-ray structure of the complex  $[\text{RuCl}(\text{bpy})_2(9\text{-EtGua})]^{2+}$ , where bpy is 2,2'-bipyridine.<sup>12</sup> In structure **1d<sub>III</sub>** and **1d<sub>IV</sub>**, however, the keto group is positioned above the tpy plane. The four models **1d<sub>I</sub>**-**1d<sub>IV</sub>** resulted almost isoenergetic, with relative energies  $\leq 15.9$  kJ/mol. The accuracy of these results was validated by relaxing the geometry of  $[\text{Ru}(\text{apy})(\text{tpy})(\text{H}_2\text{O})]^{2+}$  (**1b**) and by comparing it with the corresponding X-ray structure. For **1b** the largest deviation with respect to the X-ray structure<sup>21</sup> occurs for the Ru-OH<sub>2</sub>

bond  $\Delta d < 0.1 \text{ \AA}$  (4% relative error), while the overall agreement is excellent for all other coordination bond and angles.

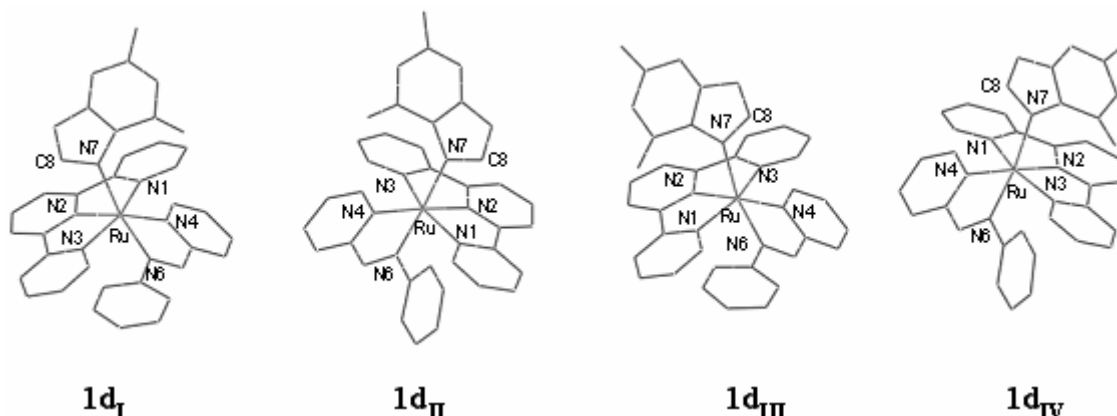


Fig. 3.5. Four models of the  $[\text{Ru}(\text{apy})(\text{tpy})(\text{Gua})]^{2+}$  adduct obtained by the DFT calculations, with numbering of major atoms as referred to in Table 3.2.

Structural parameters of the most stable isomers of  $[\text{Ru}(\text{apy})(\text{tpy})(\text{H}_2\text{O})]^{2+}$  and  $[\text{Ru}(\text{apy})(\text{tpy})(\text{Gua})]^{2+}$  are given in Table 3.2 along with an analysis of the bond ionicity (BI).<sup>32</sup> The four conformational isomers **1d<sub>I</sub>**-**1d<sub>IV</sub>** present similar coordination geometries with a small difference in the Ru-N7 bond length. The Ru-N7 varied by  $\Delta d = 0.04 \text{ \AA}$  between the most and the less thermodynamically stable conformers **1d<sub>I</sub>** and **1d<sub>IV</sub>**. The presence of the keto group of the guanine between the pyridine ring of apy and the pyridine ring of tpy in **1d<sub>I</sub>**, **1d<sub>II</sub>** or above the tpy plane in **1d<sub>III</sub>**, **1d<sub>IV</sub>** determines also a small rearrangement of the angles.

The binding of the guanine determines a small rearrangement of the apical ligands: the Ru-N7 bond shortens by  $\Delta d = 0.04 - 0.08 \text{ \AA}$  ( $\Delta\text{BI} = 0.06 - 0.08$ ) for **1d<sub>I</sub>**-**1d<sub>IV</sub>**, with respect to the Ru-OH<sub>2</sub> bond of **1b** (this might be related to the intrinsic smaller radius of N compared to O), while the Ru-N6 bond increases by  $\Delta d = +0.05 - 0.04 \text{ \AA}$  ( $\Delta\text{BI} = 0.04$ ). The coordination geometry corresponds to that of a slightly distorted octahedron that is imposed by the rigidity of the aromatic ring systems of the apy ligand.

The bond energy of the aqua ligand is exothermic by  $-78.2 \text{ kJ/mol}$ , while the binding of the guanine is exothermic by a maximum amount of  $-199.6 \text{ kJ/mol}$  in **1d<sub>I</sub>** and a minimum of  $-183.7 \text{ kJ/mol}$  in **1d<sub>IV</sub>**. The exchange reaction between water and the guanine results exothermic by  $-121.7$  to  $-105.8 \text{ kJ/mol}$  (see Table 3.2).

Table 3.2. Selected bond lengths ( $\text{\AA}$ ), angles ( $^\circ$ ) and bond ionicities (BI) of  $[\text{Ru}(\text{apy})(\text{tpy})(\text{H}_2\text{O})]^{2+}$  (**1b**) and  $[\text{Ru}(\text{apy})(\text{tpy})(\text{Gua})]^{2+}$  (**1d<sub>I</sub>**-**1d<sub>IV</sub>**) compounds. Relative energies (kJ/mol) of the conformational isomers are given, along with binding energies of water and guanine and the enthalpy for the reaction of exchange between water and guanine ligand.

Bonds	X-Ray ( <b>1b</b> )	Calculated Structure ( <b>1b</b> )	Bond Ionicity ( <b>1b</b> )	<b>1d<sub>I</sub></b>	BI <b>1d<sub>I</sub></b>	<b>1d<sub>II</sub></b>	BI <b>1d<sub>II</sub></b>	<b>1d<sub>III</sub></b>	BI <b>1d<sub>III</sub></b>	<b>1d<sub>IV</sub></b>	BI <b>1d<sub>IV</sub></b>
Ru-O,N7	2.15	2.25	0.82	2.17	0.75	2.19	0.75	2.21	0.74	2.21	0.76
Ru-N1	2.07	2.09	0.73	2.11	0.71	2.09	0.72	2.09	0.73	2.08	0.73
Ru-N2	1.98	1.98	0.71	1.98	0.76	1.98	0.75	1.98	0.70	1.98	0.70
Ru-N3	2.07	2.08	0.73	2.08	0.73	2.09	0.71	2.09	0.73	2.09	0.74
Ru-N4	2.06	2.07	0.74	2.07	0.75	2.08	0.73	2.08	0.74	2.09	0.75
Ru-N6	1.96	1.97	0.68	2.02	0.72	2.01	0.72	2.01	0.72	2.01	0.72
Angles											
N1-Ru-O,N7	87.2	87.0		89.5		85.4		85.9		93.6	
N2-Ru-O,N7	85.9	86.2		88.0		87.5		88.7		89.9	
N3-Ru-O,N7	88.0	88.3		91.0		91.9		96.4		88.9	
N4-Ru-O,N7	95.9	95.3		94.6		96.1		93.6		92.8	
N4-Ru-N6	76.8	77.2		76.2		76.7		76.4		76.2	
N6-Ru-N1	94.3	93.8		88.6		90.7		88.5		88.9	
N6-Ru-N2	101.3	101.5		100.5		100.1		101.6		101.0	
N6-Ru-N3	93.1	93.6		94.7		91.9		93.1		92.9	
N6-Ru-O,N7	172.8	172.2		169.7		172.1		167.2		169.1	
Torsional Angles											
N1-Ru-N7-C8				121.3		133.4		-44.6		-157.6	
Relative Energies				0.0		2.1		10.5		15.9	
$\Delta H$ binding wat/Gua		-78.2		-199.6		-197.5		-189.1		-183.7	
$\Delta H$ exchange wat/Gua				-121.7		-119.7		-111.3		-105.8	

**Synthesis and characterization of [Ru(apy)(tpy)(9-EtGua)](ClO<sub>4</sub>)<sub>2</sub>. pH titration.**

**Variable temperature and 2D NMR studies**

The <sup>1</sup>H NMR chemical shift values for the model base adduct [Ru(apy)(tpy)(9-EtGua)]<sup>2+</sup> (**1d**) in the aromatic region are presented in Table 3.3.

Table 3.3. Proton chemical shift values (ppm) for the complexes **1b** and **1d** in the aromatic region, taken in D<sub>2</sub>O at 310 K. The proton labels are indicated in Fig.3.1.

Complex	3A	4A	5A	6A	3A'	4A'	5A'	6A'	3T	4T	5T	6T	3T'	4T'	H8
<b>1b</b>	9.01	8.55	8.36	9.46	7.14	7.75	7.34	7.84	8.67	8.19	7.50	7.34	8.67	8.36	-----
<b>1d</b>	8.92	8.48	8.11	9.21	6.52	7.64	7.30	7.92	8.37	8.11	7.41	7.64	8.37	8.20	6.81

The coordination of 9-ethylguanine to ruthenium was proven to occur via the nitrogen N7 by a <sup>1</sup>H NMR pH titration experiment. At low pH, the N7 atom in free 9-ethylguanine is protonated. When the pH is increased, site N7 is deprotonated, causing a shift in the H8 peak toward higher field. The absence of this shift when the experiment was carried out with **1d** was sufficient to prove that the N7 position of 9-ethylguanine was coordinated to ruthenium.

When a <sup>1</sup>H NMR spectrum of **1d** was recorded at r.t., some of the peaks appeared broadened. This effect is of great interest in the study of the conformational behaviour of the adduct, as these broad resonances suggest hindered rotational behaviour of the coordinated 9-EtGua.

Subsequently, a full variable-temperature NMR study was carried out. For this purpose, the solvent was chosen to be MeOH-*d*<sub>4</sub>, as its lower freezing point than that of water allowed a more extensive study. <sup>1</sup>H NMR spectra of [Ru(apy)(tpy)(9-EtGua)]<sup>2+</sup> were recorded in MeOH-*d*<sub>4</sub> at the following temperatures: 213 K, 233 K, 253 K, 273 K, 298 K, 308 K and 318 K (see Fig.3.6). 2D NMR spectra of the compound were recorded at 213 K (see Fig.3.7) and 328 K (see Fig.3.8). The peaks of the spectra at the highest and the lowest temperatures were assigned as indicated in Table 3.4.

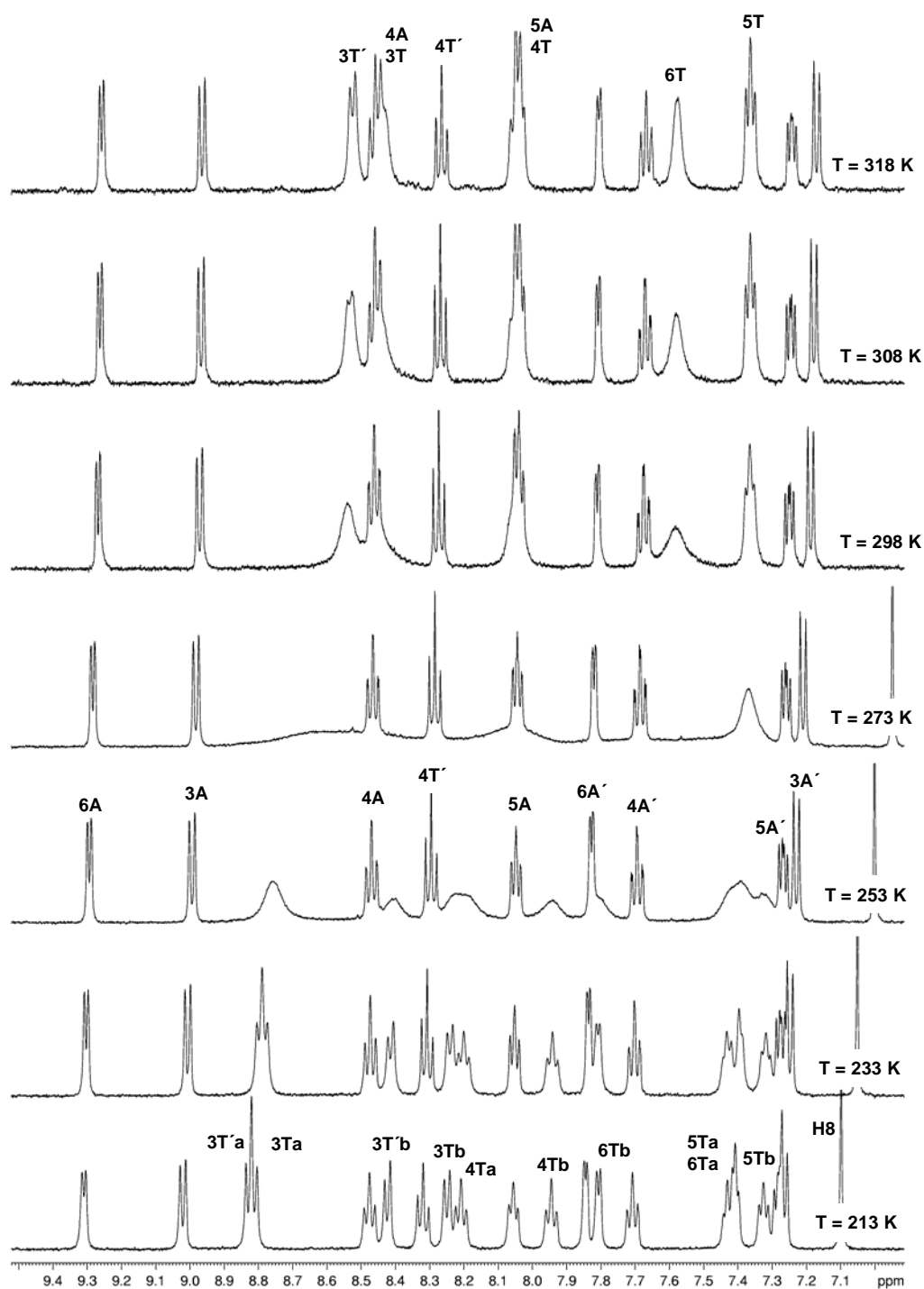


Fig.3.6.  $^1\text{H}$  NMR spectra of  $[\text{Ru}(\text{apy})(\text{tpy})(9\text{-EtGua})]^{2+}$  (**1d**) in  $\text{MeOH-d}_4$  at different temperatures in the range 213 K – 318 K, with labeled peak assignments. The peak corresponding to H8 was left out at 298, 308 and 318 K for clarity of the figure.

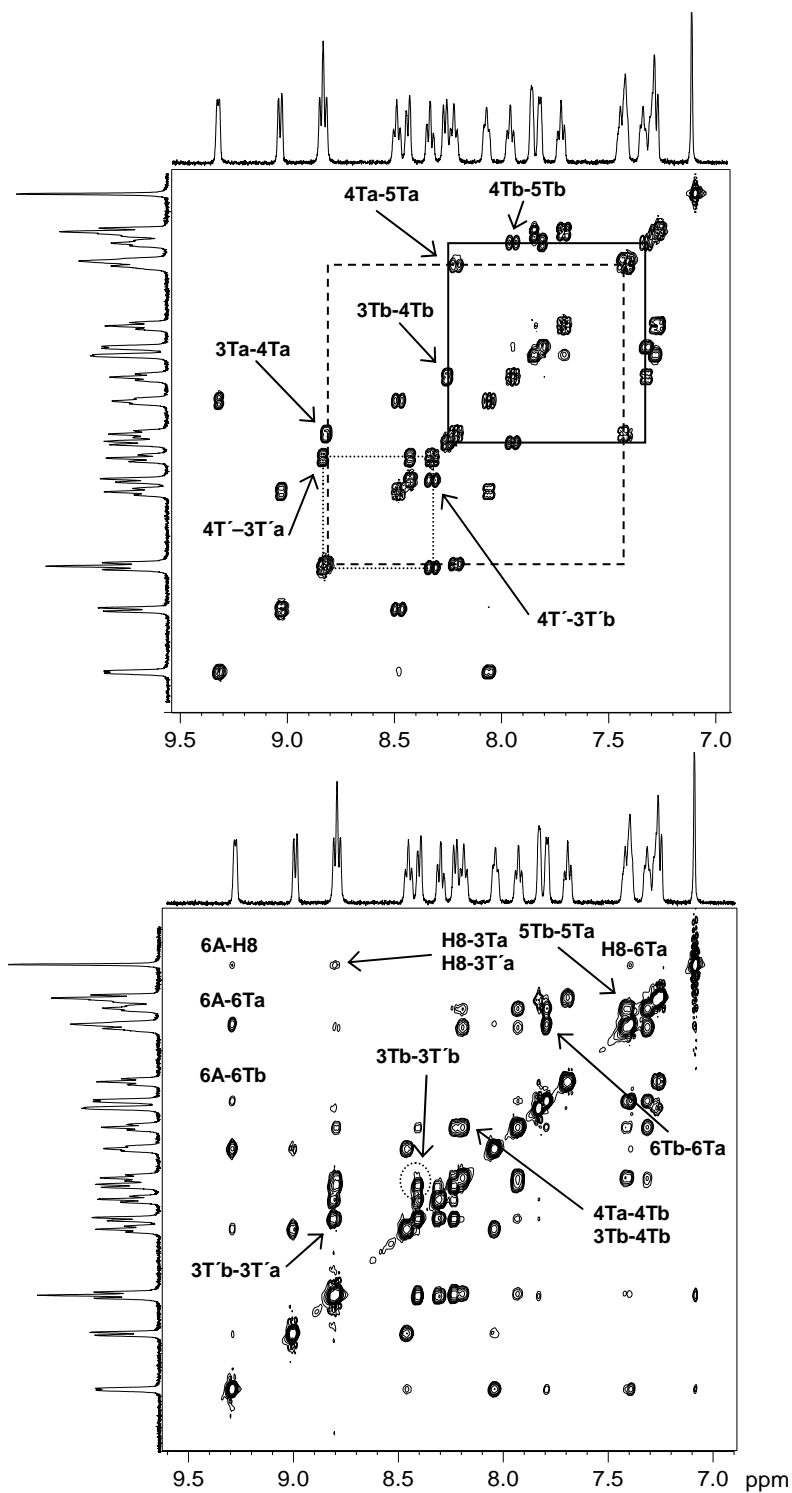


Fig.3.7. Aromatic region of the  $^1\text{H}$ - $^1\text{H}$  COSY (above) and NOESY (below) spectra of **1d** in  $\text{MeOH-d}_4$  at 213 K. In the COSY spectrum, the dashed lines indicate the 3Ta-4Ta-5Ta-6Ta cross peaks. The dotted lines show the 3T'a-4T'-3T'b cross-peaks. The solid lines indicate the 3Tb-4Tb-5Tb-6Tb cross-peaks. Some of these COSY cross-peaks are labeled. In the NOESY spectrum, a few selected cross-peaks and exchange peaks are assigned.

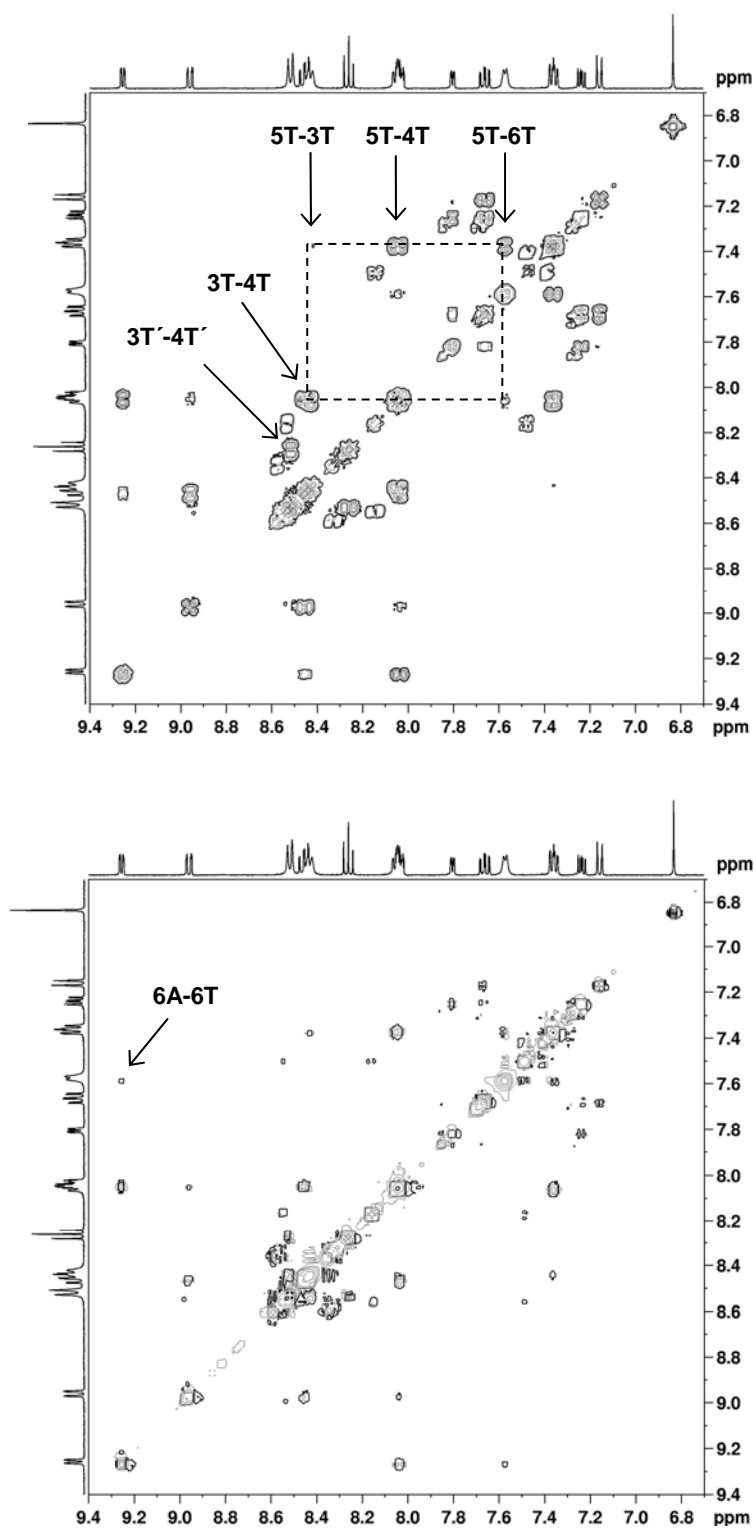


Fig.3.8. Aromatic region of the  $^1\text{H}$ - $^1\text{H}$  COSY (above) and NOESY (below) spectra of **1d** in  $\text{MeOH-d}_4$  at 328 K, with some assignments. In the COSY spectrum, the dashed lines indicate the 3T-4T-5T-6T cross-peaks. Some of these COSY cross-peaks are labeled. In the NOESY spectrum, a selected cross-peak is assigned. Decomposition of **1d** to **1b** has occurred to some extent.

*Table 3.4. Proton chemical shift values (ppm) for the complex **1d** in the aromatic region, taken in MeOH-*d*<sub>4</sub> at 213 K and 328 K. The proton labels are indicated in Fig.3.1.*

T	3A	4A	5A	6A	3A'	4A'	5A'	6A'	4T'	H8	3Ta	4Ta	5Ta	6Ta	3T'a
											3Tb	4Tb	5Tb	6Tb	3T'b
											3T	4T	5T	6T	3T'
<b>213 K</b>	9.03	8.48	8.06	9.31	7.27	7.71	7.28	7.85	8.33	7.12	8.83	8.21	7.43	7.43	8.85
											8.25	7.94	7.32	7.80	8.43
<b>328 K</b>	8.95	8.46	8.04	9.25	7.16	7.66	7.24	7.80	8.26	6.80	8.43	8.04	7.36	7.58	8.51

The shifts of the 2,2'-azobispyridine protons, as well as that of the proton labeled 4T' (see Fig.3.1) remain virtually unaltered by the temperature change. These peaks look sharp in the complete range of temperatures. If the 9-ethylguanine moiety is disregarded, all these protons lie on or close to a symmetry plane. The rest of the terpyridine protons give one set of sharp signals of intensity 2 at 318 K, which split into two sets of sharp signals of intensity 1 at 213 K. At intermediate temperatures, these terpyridine resonances appear broadened.

If one considers the 9-ethylguanine moiety to be rotating fast on the NMR time scale at high temperature, its proximity to all terpyridine protons would be equivalent. This would have the same effect if a symmetry plane were considered, formed by the apy ligand, the Ru atom, the N atom of the central terpyridine ring and 4T'. The rest of the terpyridine protons would therefore be equivalent in pairs, and one set of five sharp peaks with intensity 2 would be obtained. As described above, this is what can be seen in the experiment at 318 K (see Fig.3.6).

Upon decreasing the temperature, the protons lying on that "symmetry plane" shift slightly, while the rest of the terpyridine protons broaden first, and finally split into ten sharp peaks with intensity 1 at 213 K (see Fig.3.6). This effect is due to the 9-ethylguanine progressively slowing down its rotational movement, until it has reached a slow rotational movement on the NMR time scale. The complex has become now asymmetric and therefore each proton gives a different NMR resonance.

Since the protons of the two external pyridine rings of terpyridine are not equivalent at low temperature, the subindexes "a" and "b" were given to distinguish them. In the same way, 3T'a is closer to the "a" ring and 3T'b is closer to the "b" ring.

The NOE H8-3T'a and H8-3Ta cross-couplings (see Fig.3.7) prove that the 9-ethylguanine proton H8 is situated between the "a" and the central terpyridine rings. No NOEs are observed between H8 and 3T'b or 3Tb. Moreover, a strong NOE cross coupling can be observed between 6A and 6Ta, while the cross-coupling between 6A and 6Tb is much weaker. This difference is due to the presence of the carbonyl group between 6A and 6Tb. The proximity of the carbonyl group to 6Tb could also explain why the resonance of this proton appears 0.37 ppm downfield with respect to 6Ta. This conformation of a 9-ethylguanine adduct is analogous to that shown in the crystal structure of the complex  $[\text{RuCl}(\text{bpy})_2(9\text{-EtGua})]^{2+}$ , where bpy is 2,2'-bipyridine.<sup>12</sup>

It can be concluded from the DFT calculations that 4 conformations of the model base adduct are possible. If the torsion angle of the non-coordinated pyridine ring is neglected, only 2 conformations are possible. This is in agreement with the low-temperature  $^1\text{H}$  NMR and 2D  $^1\text{H}$ - $^1\text{H}$  NMR spectra, which show only one of these possible pair of conformers present in a methanolic solution at 213 K, with the carbonyl group being wedged between the tpy and the apy ligands (structures **1d<sub>I</sub>** and **1d<sub>II</sub>** Fig.3.5).

Exchange cross-peaks between all of the corresponding tpy resonances can be seen in the  $^1\text{H}$ - $^1\text{H}$  NOESY NMR spectrum at 213 K (see Fig.3.7). This effect suggests that the 9-ethylguanine moiety is slowly rotating on the NMR time scale around the Ru-N7 bond. The two degenerate positions (structures **1d<sub>I</sub>** and **1d<sub>II</sub>** from Fig.3.5) are equivalent in the NMR, in such a way that the "a" ring becomes "b", and *vice versa*, which explains the absence of H8-3Tb and H8-3T'b cross couplings.

It has been suggested for analogous compounds<sup>33, 34</sup> that the above-mentioned rotation of the 9-ethylguanine moiety occurs in such a way that the keto group passes over the tpy ligand, since a  $90^\circ$  rotation of the model base is hindered by the coordinated pyridine ring of, in the present case, 2,2'-azobispyridine. During this rotation the molecule passes through two energetic minima, corresponding to the conformers **1d<sub>III</sub>** and **1d<sub>IV</sub>**, which lie at higher energies than **1d<sub>I</sub>** and **1d<sub>II</sub>** (Fig.3.5). The observation of both H8-6A and H8-6Ta NOE cross-couplings supports this theory.

The model bases bound to ruthenium polypyridyl complexes, such as guanine and other smaller imidazole derivatives, were found to be: rotating fast on the NMR time scale, as observed in the cases of the smaller imidazole ligands,<sup>35-37</sup> not rotating at all, in the cases in which the model base was stabilized by hydrogen bonds and electrostatic forces,<sup>37, 38</sup> and slowly rotating, in the intermediate cases.<sup>33, 34, 36, 37</sup> The whole rotation process can be followed by variable-temperature 1D and 2D NMR, as described in this study.

### 3.4. Conclusions

The interaction between a group of ruthenium polypyridyl complexes and a DNA model base was studied. Three very similar complexes differing only in one coordination site, occupied by a leaving group, were chosen for the experiment. The three complexes were proven to bind to 9-ethylguanine, following different kinetics in each case. Both complexes  $[\text{Ru}(\text{apy})(\text{tpy})\text{Cl}]^+$  and  $[\text{Ru}(\text{apy})(\text{tpy})(\text{CH}_3\text{CN})]^{2+}$  were seen by  $^1\text{H}$  NMR to hydrolyze to give  $[\text{Ru}(\text{apy})(\text{tpy})(\text{H}_2\text{O})]^{2+}$ , besides reacting with 9-ethylguanine. The reaction from the ruthenium starting complex to the ruthenium–model base adduct is faster in the case of  $[\text{Ru}(\text{apy})(\text{tpy})(\text{CH}_3\text{CN})]^{2+}$ , and much slower in the case of the chlorido complex.

The preferential geometry of the ruthenium–model base adduct formed in all cases was inferred from DFT calculations. This 9-ethylguanine complex shows a very interesting conformational behaviour, which has been studied in full detail by means of variable-temperature  $^1\text{H}$  NMR and 2D COSY and NOESY NMR spectroscopy. At high temperatures, the 9-ethylguanine moiety is rotating fast at the NMR time scale, while at low temperatures, this model base shows a preferred orientation, with the keto group wedged between the terpyridine and the 2,2'-azobispyridine ligands. This behaviour is in agreement with the DFT calculations.

### 3.5. References

1. Reedijk, J., *Proc. Natl. Acad. Sci. U. S. A.* **2003**, *100*, 3611-3616.
2. Nováková, O.; Kaspárková, J.; Vrána, O.; van Vliet, P. M.; Reedijk, J.; Brabec, V., *Biochemistry* **1995**, *34*, 12369-12378.
3. Velders, A. H.; Hotze, A. C. G.; van Albada, G. A.; Haasnoot, J. G.; Reedijk, J., *Inorg. Chem.* **2000**, *39*, 4073-4080.
4. Hotze, A. C. G.; Caspers, S. E.; de Vos, D.; Kooijman, H.; Spek, A. L.; Flamigni, A.; Bacac, M.; Sava, G.; Haasnoot, J. G.; Reedijk, J., *J. Biol. Inorg. Chem.* **2004**, *9*, 354-364.
5. Clarke, M. J., *Coord. Chem. Rev.* **2002**, *232*, 69-93.
6. Clarke, M. J., *J. Am. Chem. Soc.* **1978**, *100*, 5068-5075.
7. Clarke, M. J.; Jansen, B.; Marx, K. A.; Kruger, R., *Inorg. Chim. Acta-Bioinorg. Chem.* **1986**, *124*, 13-28.
8. Marx, K. A.; Kruger, R.; Clarke, M. J., *Mol. Cell. Biochem.* **1989**, *86*, 155-162.
9. Mishra, L.; Yadaw, A. K.; Sinha, R.; Singh, A. K., *Indian J. Chem. Sect A-Inorg. Bio-Inorg. Phys. Theor. Anal. Chem.* **2001**, *40*, 913-928.
10. Cauci, S.; Viglino, P.; Esposito, G.; Quadrifoglio, F., *J. Inorg. Biochem.* **1991**, *43*, 739-751.
11. Grover, N.; Welch, T. W.; Fairley, T. A.; Cory, M.; Thorp, H. H., *Inorg. Chem.* **1994**, *33*, 3544-3548.
12. van Vliet, P. M.; Haasnoot, J. G.; Reedijk, J., *Inorg. Chem.* **1994**, *33*, 1934-1939.

13. Davey, J. M.; Moerman, K. L.; Ralph, S. F.; Kanitz, R.; Sheil, M. M., *Inorg. Chim. Acta* **1998**, *281*, 10-17.
14. Malina, J.; Nováková, O.; Keppler, B. K.; Alessio, E.; Brabec, V., *J. Biol. Inorg. Chem.* **2001**, *6*, 435-445.
15. Morris, R. E.; Aird, R. E.; Murdoch, P. S.; Chen, H.; Cummings, J.; Hughes, N. D.; Parsons, S.; Parkin, A.; Boyd, G.; Jodrell, D. I.; Sadler, P. J., *J. Med. Chem.* **2001**, *44*, 3616-3621.
16. Chen, H. M.; Parkinson, J. A.; Morris, R. E.; Sadler, P. J., *J. Am. Chem. Soc.* **2003**, *125*, 173-186.
17. Bacac, M.; Hotze, A. C. G.; van der Schilden, K.; Haasnoot, J. G.; Pacor, S.; Alessio, E.; Sava, G.; Reedijk, J., *J. Inorg. Biochem.* **2004**, *98*, 402-412.
18. van der Schilden, K.; García, F.; Kooijman, H.; Spek, A. L.; Haasnoot, J. G.; Reedijk, J., *Angew. Chem.-Int. Edit.* **2004**, *43*, 5668-5670.
19. Brabec, V.; Nováková, O., *Drug Resist. Update* **2006**, *9*, 111-122.
20. Dougan, S. J.; Melchart, M.; Habtemariam, A.; Parsons, S.; Sadler, P. J., *Inorg. Chem.* **2006**, *45*, 10882-10894.
21. Corral, E.; Hotze, A. C. G.; Tooke, D. M.; Spek, A. L.; Reedijk, J., *Inorg. Chim. Acta* **2006**, *359*, 830-838.
22. Kirpal, A.; Reiter, E., *Ber. Deuts. Chem. Ges.* **1927**, *60*, 664-666.
23. Adcock, P. A.; Keene, F. R.; Smythe, R. S.; Snow, M. R., *Inorg. Chem.* **1984**, *23*, 2336-2343.
24. Parr, R. G.; Yang, W., *Density-Functional Theory of atoms and molecules*. Oxford University Press: New York, 1989.
25. (a) Car, R.; Parrinello, M., *Phys. Rev. Lett.* **1985**, *55*, 2471-2474; (b) CPMD Consortium, CPMD 3.10.0, Max-Planck-Institut für Festkörperforschung and IBM Zurich Research Laboratory, [www.cpmid.org](http://www.cpmid.org); 2005.
26. Troullier, N.; Martins, J. L., *Phys. Rev. B* **1991**, *43*, 1993-2006.
27. Kleinman, L.; Bylander, D. M., *Phys. Rev. Lett.* **1982**, *48*, 1425-1428.
28. Maurer, P.; Magistrato, A.; Rothlisberger, U., *J. Phys. Chem. A* **2004**, *108*, 11494-11499.
29. Becke, A. D., *Phys. Rev. A* **1988**, *38*, 3098-3100.
30. Perdew, J. P., *Phys. Rev. B* **1986**, *33*, 8822-8824.
31. Barnett, R. N.; Landman, U., *Phys. Rev. B* **1993**, *48*, 2081-2097.
32. Based on Boys' orbitals, the bond ionicity  $BI_{AB}$  of a bond was calculated as (F. Alber, G. Folkers, P. Carloni, *J. Phys. Chem. B*, **1999**, *103*, 6121), namely  $BI_{AB} = d_A / d_{AB}$  where  $d_A$  is the distance between atom A and the Boys orbital along the AB bond and  $d_{AB}$  is the length of the bond between A and B. BIs help individuate lone pairs and provide an estimation of ionicity of chemical bonds.
33. Velders, A. H. Ruthenium complexes with heterocyclic nitrogen ligands. PhD Thesis, Leiden University, Leiden, **2000**, p 156-162.
34. van der Schilden, K. Polynuclear ruthenium and platinum polypyridyl complexes. PhD Thesis, Leiden University, Leiden, **2006**, p 77-81.
35. Velders, A. H.; Kooijman, H.; Spek, A. L.; Haasnoot, J. G.; de Vos, D.; Reedijk, J., *Inorg. Chem.* **2000**, *39*, 2966-2967.
36. Velders, A. H.; Massera, C.; Ugozzoli, F.; Biagini-Cingi, M.; Manotti-Lanfredi, A. M.; Haasnoot, J. G.; Reedijk, J., *Eur. J. Inorg. Chem.* **2002**, 193-198.
37. Velders, A. H.; Hotze, A. C. G.; Reedijk, J., *Chem.-Eur. J.* **2005**, *11*, 1325-1340.
38. Hotze, A. C. G.; Velders, A. H.; Ugozzoli, F.; Biagini-Cingi, M.; Manotti-Lanfredi, A. M.; Haasnoot, J. G.; Reedijk, J., *Inorg. Chem.* **2000**, *39*, 3838-3844.

## 4. Ruthenium polypyridyl complexes and their modes of interaction with DNA: is there a correlation between these interactions and the antitumour activity of the compounds?\*

Different ways of interaction between a group of ruthenium polypyridyl complexes and DNA were studied using various spectroscopic techniques. A group of mononuclear compounds with structural formula  $[\text{Ru}(\text{tpy})\text{L}_1\text{L}_2]^{(2-n)+}$ , where tpy = 2,2':6',2''-terpyridine, was selected. The ligand  $\text{L}_1$  is a bifunctional pyridyl ligand, with either two pyridine rings and an azo group (apy = 2,2'-azobispyridine), or one pyridine ring and an azo group (azpy = 2-phenylazopyridine) or one pyridine ring and an imino group (impy = 2-phenylpyridinylmethylene amine). The ligand  $\text{L}_2$  is a monofunctional labile ligand ( $\text{Cl}^-$ ,  $\text{H}_2\text{O}$ ,  $\text{CH}_3\text{CN}$ ). All these complexes were found to be able to coordinate to the DNA model base 9-ethylguanine by  $^1\text{H}$  NMR and MS. The closely-related dinuclear compound  $[\{\text{Ru}(\text{apy})(\text{tpy})\}_2\{\mu\text{-H}_2\text{N}(\text{CH}_2)_6\text{NH}_2\}]^{4+}$ , which has no positions available for coordination, was studied for comparison. The interactions between each of four representative complexes and calf thymus DNA were studied by circular and linear dichroism. In order to explore a possible relation between DNA-binding ability and toxicity, all these compounds were screened for *in vitro* anticancer activity in a variety of cancer cell lines, showing in some cases an activity comparable to that of cisplatin. The design of the complexes was found helpful to formulate some structure-activity relationships.

---

\* This chapter is based on Corral, E.; Hotze, A.C.G.; den Dulk, H.; Hannon, M.J.; Reedijk, J., *to be submitted for publication in J. Biol. Inorg. Chem.*

#### 4.1. Introduction

Since the appearance of cisplatin in the medical protocols for treatment of certain cancers in 1978<sup>1</sup> a great interest has grown in anticancer metallopharmaceuticals.<sup>2</sup> The clinical drawbacks of cisplatin therapy became soon apparent.<sup>3</sup> In order to design improved antitumour platinum drugs, research focused on understanding the mechanisms of action of cisplatin in the body and in the living cell. To date DNA is generally accepted to be the main target of cisplatin, which has been proven to bind most frequently to two adjacent guanine residues via their N7 position, thereby generating a kink in the DNA structure.<sup>4</sup>

During the early years of platinum drugs anticancer research was based on a few rules known as Structure-Activity Relationships (SAR's),<sup>5</sup> which dictated the geometry that a platinum complex should have in order to display anticancer activity, as well as the lability of its ligands, amongst others. However, a number of compounds were later reported that, despite violating some of these rules, still display an anticancer activity.<sup>6-16</sup>

A relatively new line of investigation focuses on ruthenium chemistry as an alternative metallopharmaceutical approach to chemotherapy,<sup>17, 18</sup> and this ruthenium anticancer chemistry has already yielded many promising results. A few compounds have been described which exhibit an activity comparable to that of cisplatin, in some cases even better.<sup>19-24</sup> In other cases the compound did not show any cytotoxicity in the parent tumor, yielding, however, an important activity against the metastases.<sup>25, 26</sup>

Discussing the mechanism of action of these ruthenium complexes and describing a few SAR's as a starting point to design improved ruthenium anticancer drugs is not straightforward. A large variety of drugs have been synthesized, with ligands such as amines, imines, dimethylsulfoxide, polypyridyl compounds, arenes, etc.<sup>17, 27, 28</sup> These different types of ruthenium complexes might follow different mechanisms of action.<sup>29</sup>

The present investigation focuses on ruthenium polypyridyl complexes with one free binding site. A series of Ru(II) complexes was selected, which contained the chelating polypyridyl ligand 2,2':6',2''-terpyridine (tpy), a bifunctional polypyridyl ligand and a labile monofunctional ligand.<sup>30-32</sup> (see Fig.4.1). The mentioned bifunctional ligand was slightly modified by substituting a pyridine ring for a phenyl ring first and then an azo group by an imino group. These variations, together with the fact that several different labile ligands were used, allowed for the proposal of some SAR's. On the other hand, the choice for tpy as a ligand was based on earlier data of Ru(tpy) complexes that display interesting anticancer properties.<sup>33</sup>

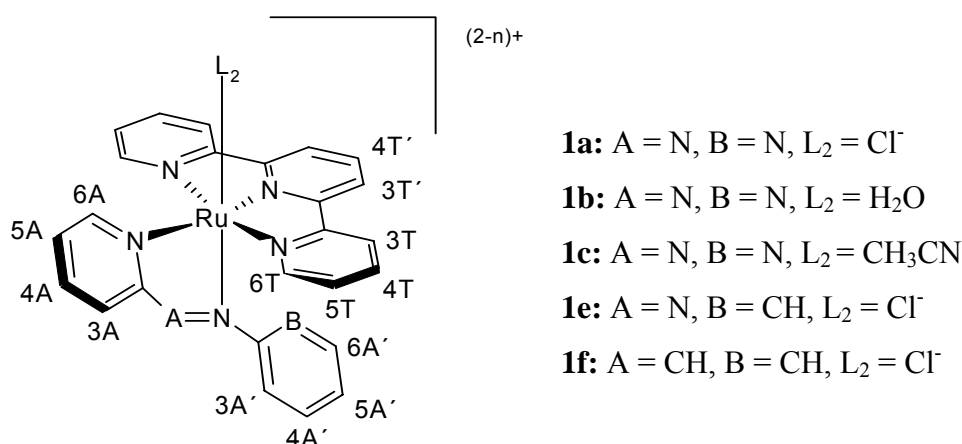


Fig.4.1. Schematic structure of  $[Ru(tpy)L_1L_2]^{(2-n)+}$  compounds (**1a-c**, **1e** and **1f**). Proton numbering scheme for use in  $^1H$  NMR spectra.

For comparison, a symmetric, homodinuclear compound has been synthesized (**1g**) (see Fig.4.2) which, unlike complexes **1a-c**, **1e** and **1f**, has no free positions available for coordination. This compound may still interact with DNA through a non-coordinative mechanism. The interactions of all these complexes with calf thymus DNA were studied by circular and linear dichroism.

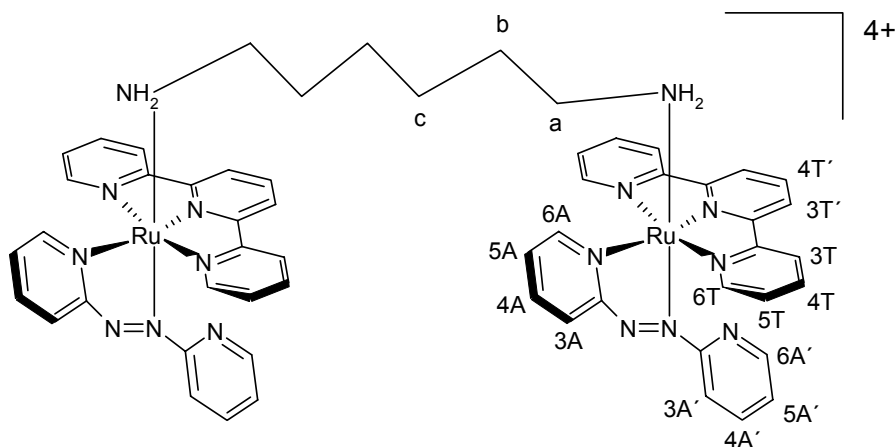


Fig.4.2. Schematic structure of the dinuclear compound  $[\{Ru(apy)(tpy)\}_2\{\mu-H_2N(CH_2)_6NH_2\}]^{4+}$  (**1g**). Proton numbering scheme for use in  $^1H$  NMR spectra.

Cytotoxicity tests were performed with the present ruthenium complexes against a series of cancerous cell lines. The new complexes show a significant cytotoxicity in several cell lines and, more interestingly, the results obtained suggest that the mechanism of action of this kind of ruthenium complexes may be quite different from that of the classical platinum anticancer agents.

## 4.2. Experimental

### Materials and reagents

2,2'-azobispyridine (apy), Ru(tpy)Cl<sub>3</sub>, [Ru(apy)(tpy)Cl](ClO<sub>4</sub>), [Ru(apy)(tpy)(H<sub>2</sub>O)](ClO<sub>4</sub>)<sub>2</sub>·2H<sub>2</sub>O, [Ru(apy)(tpy)(CH<sub>3</sub>CN)](ClO<sub>4</sub>)<sub>2</sub>, [Ru(azpy)(tpy)Cl]Cl·5H<sub>2</sub>O and [Ru(imp)(tpy)Cl](ClO<sub>4</sub>) were synthesised according to the literature methods.<sup>30-32, 34, 35</sup> LiCl, NaClO<sub>4</sub> (both Merck), NaClO, AgNO<sub>3</sub> (both Acros), tpy (Aldrich), RuCl<sub>3</sub>·3H<sub>2</sub>O (Johnson & Matthey), 9-EtGua (Sigma) and H<sub>2</sub>N(CH<sub>2</sub>)<sub>6</sub>NH<sub>2</sub> (Fluka) were used as supplied. Ultra pure water (18.2 ΩM; Aldrich) was used for the MS, CD and LD experiments. All other chemicals and solvents were reagent grade, commercial materials and used as received.

Calf-thymus DNA (*ct*-DNA) was purchased from Sigma Aldrich and used without further purification. The solid DNA salt was dissolved in ultra pure water (18.2 ΩM; Aldrich) and left at 278 K for 24 hours to fully hydrate. The resulting stock DNA solution was kept frozen and it was thawed when needed. The concentration of the DNA stock solution was determined spectroscopically, using the known molar extinction coefficient of *ct*-DNA at 258 nm:  $\epsilon_{258} = 6600 \text{ molar base}^{-1} \text{ cm}^{-1} \text{ dm}^3$ .<sup>36</sup>

A 100 mM stock solution of sodium cacodylate buffer (pH 6.8) was prepared, as well as a 1M sodium chloride stock solution, using in both cases ultra pure water (18.2 ΩM; Aldrich).

### Physical measurements

C, H and N determinations were performed on a Perkin Elmer 2400 Series II analyzer. Mass spectra were obtained with a Finnigan Aqa mass spectrometer equipped with an electrospray ionization source (ESI). NMR spectra were recorded on a Bruker DPX-300 spectrometer operating at a frequency of 300 MHz, at a temperature of 310 K, unless otherwise stated. Chemical shifts were calibrated against tetramethylsilane (TMS). CD spectra were collected in 2 mm path-length quartz cuvettes using a Jasco J-810 spectropolarimeter. Flow LD spectra were collected using a flow Couette cell in the above-mentioned spectropolarimeter. All CD and LD spectra were recorded at room temperature.

### Synthesis and characterization of $[\{\text{Ru}(\text{apy})(\text{tpy})\}_2\{\mu\text{-H}_2\text{N}(\text{CH}_2)_6\text{NH}_2\}](\text{ClO}_4)_4$

$[\text{Ru}(\text{apy})(\text{tpy})(\text{H}_2\text{O})](\text{ClO}_4)_2 \cdot 2\text{H}_2\text{O}$  (26 mg, 0.034 mmol) and  $\text{H}_2\text{N}(\text{CH}_2)_6\text{NH}_2$  (2 mg, 0.016 mmol) were dissolved in 12 mL EtOH abs:MeOH 5:1. The solution was vigorously refluxed for 15 hours. The pH remained constant around 7. The product was collected by filtration, washed with little ethanol and diethyl ether and dried *in vacuo* over silica. Yield: 20 mg (76%). Anal. Calc. for  $\text{C}_{56}\text{H}_{54}\text{N}_{16}\text{O}_{16}\text{Cl}_4\text{Ru}_2$ : C, 43.4; H, 3.5; N, 14.4%. Found: C, 43.8; H, 3.8; N, 14.5%.  $m/z$  (ESI-MS) 634.1 ( $[\{\text{Ru}(\text{apy})(\text{tpy})\}\{\text{H}_2\text{N}(\text{CH}_2)_6\text{NH}_2\}]^+$ ); 576.1 ( $[\{\text{Ru}(\text{apy})(\text{tpy})\}_2\{\mu\text{-H}_2\text{N}(\text{CH}_2)_6\text{NH}_2\}]^{2+}$ ); 317.3 ( $[\{\text{Ru}(\text{apy})(\text{tpy})\}\{\text{H}_2\text{N}(\text{CH}_2)_6\text{NH}_2\}]^{2+}$ ).  $^1\text{H}$  NMR (DMSO- $d_6$ , 298 K):  $\delta$  (ppm): 9.34 (2H, d, 4.81 Hz); 9.00 (2H, d, 8.05 Hz); 8.62 (6H, m); 8.52 (2H, t, 6.84 Hz); 8.30 (4H, m); 8.14 (4H, t, 7.24 Hz); 7.78 (2H, d, 4.83 Hz); 7.73 (2H, t, 7.76 Hz); 7.46 (4H, t, 6.12 Hz); 7.30 (6H, m); 6.98 (2H, d, 7.98 Hz); 4.92 (4H, m); 1.64 (4H, m); 1.10 (4H, m); 0.66 (4H, m).

### Interaction between ruthenium polypyridyl complexes and 9-ethylguanine

Aqueous solutions with a concentration 1.3 mM of the ruthenium compound and 2.6 mM of the DNA model base 9-ethylguanine were incubated at 310 K for 24 hours. Subsequently a mass spectrum was recorded of each of the mixtures.  $m/z$  (ESI-MS) of the mixture **1a** + 9-EtGua: 618.1  $[\text{Ru}(\text{apy})(\text{tpy})](\text{ClO}_4)^+$ ; 554.2  $[\text{Ru}(\text{apy})(\text{tpy})\text{Cl}]^+$ ; 536.3  $[\text{Ru}(\text{apy})(\text{tpy})(\text{H}_2\text{O})]^+$ ; 348.9  $[\text{Ru}(\text{apy})(\text{tpy})(9\text{-EtGua})]^{2+}$ .  $m/z$  (ESI-MS) of the mixture **1b** + 9-EtGua: 696.7  $[\text{Ru}(\text{apy})(\text{tpy})(9\text{-EtGua})]^+$ ; 617.6  $[\text{Ru}(\text{apy})(\text{tpy})](\text{ClO}_4)^+$ ; 535.7  $[\text{Ru}(\text{apy})(\text{tpy})(\text{H}_2\text{O})]^+$ ; 517.7  $[\text{Ru}(\text{apy})(\text{tpy})]^+$ ; 348.9  $[\text{Ru}(\text{apy})(\text{tpy})(9\text{-EtGua})]^{2+}$ .  $m/z$  (ESI-MS) of the mixture **1e** + 9-EtGua: 695.8  $[\text{Ru}(\text{azpy})(\text{tpy})(9\text{-EtGua})]^+$ ; 552.7  $[\text{Ru}(\text{azpy})(\text{tpy})\text{Cl}]^+$ ; 534.8  $[\text{Ru}(\text{azpy})(\text{tpy})(\text{H}_2\text{O})]^+$ ; 348.3  $[\text{Ru}(\text{azpy})(\text{tpy})(9\text{-EtGua})]^{2+}$ .  $m/z$  (ESI-MS) of the mixture **1f** + 9-EtGua: 695  $[\text{Ru}(\text{impy})(\text{tpy})(9\text{-EtGua})]^+$ ; 616  $[\text{Ru}(\text{impy})(\text{tpy})](\text{ClO}_4)^+$ ; 552  $[\text{Ru}(\text{impy})(\text{tpy})\text{Cl}]^+$ ; 534  $[\text{Ru}(\text{impy})(\text{tpy})(\text{H}_2\text{O})]^+$ ; 516  $[\text{Ru}(\text{impy})(\text{tpy})]^+$ ; 348  $[\text{Ru}(\text{impy})(\text{tpy})(9\text{-EtGua})]^{2+}$ .

Each ruthenium compound was dissolved in 600  $\mu\text{L}$   $\text{D}_2\text{O}$  and the appropriate amount of 9-ethylguanine was added to prepare solutions with a concentration 1.3 mM of the ruthenium compound and 2.6 mM of 9-ethylguanine. The interaction between each ruthenium complex,  $\text{H}_2\text{O}$  and 9-EtGua was followed by  $^1\text{H}$  NMR for 24 hours at 310 K.

### **Interaction between ruthenium polypyridyl complexes and *ct*-DNA**

Fresh samples were made with constant concentrations of DNA (300  $\mu\text{M}$  in ultrapure water for the experiments involving the complexes **1b**, **1e** and **1f** and 100  $\mu\text{M}$  for the experiment with complex **1g**), NaCl (20 mM) and sodium cacodylate buffer (1 mM), and a variation of the metal concentration using a stock solution (500  $\mu\text{M}$  in ultrapure water of the complexes **1b**, **1e** and **1f** and 300  $\mu\text{M}$  of the complex **1g**). The ratio of DNA: metal complex was decreased from 50:1 to 1.5:1 in the various samples. The CD spectra of these solutions were measured after 24 hours of incubation at 310 K. The solutions prepared with complex **1g** were also measured fresh.

For the LD measurements, a 300  $\mu\text{M}$  solution of DNA in ultrapure water containing NaCl (20 mM) and sodium cacodylate buffer (1 mM) was prepared. This solution was titrated with two stock solutions. The first solution contained each of the complexes **1b**, **1e** and **1f** in a 1000  $\mu\text{M}$  concentration in ultrapure water or complex **1g** in a 500  $\mu\text{M}$  concentration. The second stock solution contained DNA 600  $\mu\text{M}$ , NaCl (40 mM) and sodium cacodylate buffer (2 mM). The DNA, NaCl and sodium cacodylate concentrations were kept constant, while the ratio of DNA:metal complex was decreased from 20:1 to 3:1 for complexes **1b**, **1e** and **1f** or from 40:1 to 6:1 for complex **1g**.

### ***In vitro* cytotoxicity assays**

The cytotoxicity of compounds **1a-c** and **1e-g** was tested *in vitro* in a series of selected cell lines. WIDR (human colon cancer), IGROV (human ovarian cancer), M19 MEL (human melanoma), A498 (human renal cancer) and H226 (non-small human cell lung cancer) belong to the currently used anti-cancer screening panel of the National Cancer Institute, USA.<sup>37</sup> The human breast cancer cell lines MCF7 and EVSA-T are estrogen receptor (ER)+/progesterone receptor (PgR)+ and (ER)-/(PgR)-, respectively. Prior to the experiments a mycoplasma test was carried out on all cell lines and found to be negative. All cell lines were maintained in a continuous logarithmic culture in RPMI 1640 medium with Hepes and phenol red. The medium was supplemented with 10% fetal calf serum, penicillin 100 units/mL and streptomycin 100  $\mu\text{g/mL}$ . The cells were mildly trypsinized for passage and for use in the experiments. Cytotoxicity was estimated by the microculture sulforhodamine B (SRB) test.<sup>38</sup>

A2780 (human ovarian carcinoma) and A2780R cisplatin-resistant cell lines were maintained in continuous logarithmic culture in Dulbecco's modified Eagle's Medium

(DMEM) (Gibco BRL™, Invitrogen Corporation, The Netherlands) supplemented with 10% fetal calf serum (Hyclone, Perbio Science, The Netherlands), PenicillinG Sodium (100 units/ml Duchefa Biochemie BV, The Netherlands), streptomycin (100 µg/ml, Duchefa Biochemie BV, The Netherlands) and Glutamax 100x (Gibco BRL™, NL) in a humidified 7% CO<sub>2</sub>, 93% air atmosphere at 310 K. Cisplatin sensitive and resistant mouse leukemia L1210/0 and L1210/2 cells were grown under the above-mentioned conditions. The cells were harvested from logarithmic growing (confluent) monolayers. Cell viability was determined by the trypan-blue dye exclusion test.

For the cytotoxicity evaluation in the cell lines WIDR, IGROV, M19 MEL, A498, H226, MCF7 and EVSA-T, the test and reference compounds were dissolved to a concentration of 250.000 µg/mL in full medium, by 20 fold dilution of a stock solution which contained 1 mg compound/200 µL DMSO. 150 µL of trypsinized tumor cells (1500-2000 cells/well) were plated in 96-wells flatbottom microtiter plates (Falcon 3072, BD). The plates were preincubated 48 hours at 310 K, 5.5 % CO<sub>2</sub>. A three-fold dilution sequence of ten steps was then made in full medium, starting with the 250.000 µg/mL stock solution. Every dilution was used in quadruplicate by adding 50 µL to a column of four wells, resulting in a highest concentration of 62.500 mg/mL. The plates were incubated for 5 days, after which the cells were fixed with 10% trichloroacetic acid in PBS and placed at 277 K for one hour. After three washings with water the cells were stained for at least 15 minutes with 0.4% SRB dissolved in 1% acetic acid. The cells were washed with 1% acetic acid to remove the unbound stain. The plates were air-dried and the bound stain was dissolved in 150 µL of 10 mM Tris-base. The absorbance was read at 540 nm using an automated microplate reader (Labsystems Multiskan MS). Data were used for construction of concentration-response curves and determination of the IC<sub>50</sub> value by use of Deltasoft 3 software.

In the case of the cell lines A2780, A2780R, L1210/0 and L1210/2, 2000 cells/well were seeded in 100 µl of complete medium in 96-multiwell flatbottom microtiter plates (Sarstedt). The plates were incubated at 37 °C, 7% CO<sub>2</sub> for 48 h prior to drug testing to allow cell adhesion. The stock solutions of all tested compounds were freshly prepared and directly used for the dilutions. As both **1a** and  $\alpha$ -[Ru(azpy)<sub>2</sub>Cl<sub>2</sub>] are poorly water soluble and for the sake of comparison with the water-soluble compounds, a DMSO/H<sub>2</sub>O stock solution was chosen for all the tested compounds, except compound **1g**. The latter was dissolved directly in water, to avoid decomposition due to stability problems. The dilutions

(8 step dilutions) were prepared in complete medium. The range of the final tested concentrations was 0.019-0.012-0.0015-0.0009-0.0005-0.0001-0.00005-0.00001 mM in the case of  $\alpha$ -[Ru(azpy)<sub>2</sub>Cl<sub>2</sub>] and 0.17-0.11-0.06-0.04-0.01-0.003-0.001-0.0003 mM for the other compounds. Each concentration was tested in quadruplicate, using 45  $\mu$ l/well added to the 100  $\mu$ l of complete medium, plus 50  $\mu$ l of extra complete medium. In the control group only 95  $\mu$ l of complete medium were added containing the corresponding percentages of H<sub>2</sub>O and DMSO. The maximum content of DMSO in the wells was 0.96%. Parallel experiments showed that no difference in cell proliferation was observed in control groups with or without 1% DMSO. The plates were incubated for 48 h and the evaluation of cell proliferation was performed by the MTT [3-(4,5-dimethylthiazol-2-yl)-2,5-diphenyl-2H-tetrazolium bromide] colorimetric assay.<sup>39-41</sup> 50  $\mu$ l MTT solution (5 mg/ml in PBS, Sigma Chemical Co.) were added to each well and incubated for 3 hours. Formazan crystals were dissolved in 100  $\mu$ l DMSO. Optical density was measured using a microplate reader (Bio Rad) at 590 nm. IC<sub>50</sub> values were obtained by GraphPad Prism software, version 3.02, 2000.

### 4.3. Results and discussion

#### Synthesis and characterization of [ $\{\text{Ru}(\text{apy})(\text{tpy})\}_2\{\mu\text{-H}_2\text{N}(\text{CH}_2)_6\text{NH}_2\}\}(\text{ClO}_4)_4$

The anticancer activity of compounds analogous to **1a-c**, **1e** and **1f** is often hypothesized to be related to their ability to bind to DNA model bases. In order to prove this relation, an additional new compound was synthesized. [ $\{\text{Ru}(\text{apy})(\text{tpy})\}_2\{\mu\text{-H}_2\text{N}(\text{CH}_2)_6\text{NH}_2\}\}(\text{ClO}_4)_4$  (**1g**) (see Fig.4.2) was found to be pure by <sup>1</sup>H NMR and EA and fully characterized by 2D NMR and ESI Mass spectroscopy. The latter showed the intact dinuclear species and also the mononuclear fragment originating from fragmentation by the electrospray method. The <sup>1</sup>H NMR spectrum of **1g** was recorded in DMSO-*d*<sub>6</sub> because, although its solubility in water was good enough for cell testing, it was not suitable for <sup>1</sup>H NMR spectroscopy. The peak assignment was carried out with the help of 2D NMR spectra (see Table 4.1). The stability of **1g** in water was studied by dissolving the compound in this solvent, incubating the solution at 310 K for two weeks, evaporating the water and subsequently recording a <sup>1</sup>H NMR in DMSO-*d*<sub>6</sub>. The compound was proven to remain unchanged after this time.

Table 4.1. Proton chemical shift values (ppm) for the complex  $[Ru(apy)(tpy)]_2\{\mu-H_2N(CH_2)_6NH_2\}(ClO_4)_4$  (**1g**) taken in DMSO- $d_6$  at 298 K. The proton labels are indicated in Fig.4.2.

6A	3A	3T 3T'	4A	5A 4T'	4T	6A'	4A'	5T	5A' 6T	3A'	NH <sub>2</sub>	(CH <sub>2</sub> ) <sub>a</sub>	(CH <sub>2</sub> ) <sub>b</sub>	(CH <sub>2</sub> ) <sub>c</sub>
9.34	9.00	8.62	8.52	8.30	8.14	7.78	7.73	7.46	7.30	6.98	4.92	1.64	1.10	0.66

### Interaction between ruthenium polypyridyl complexes and 9-ethylguanine

A previous <sup>1</sup>H NMR study of the interaction between each of the complexes **1a-c** ( $[Ru(apy)(tpy)L_2]^{(2-n)+}$ , where L = Cl<sup>-</sup>, H<sub>2</sub>O and CH<sub>3</sub>CN, respectively) and 9-EtGua<sup>42</sup> was described in chapter 3. This study proved that these three complexes are capable of binding to the DNA model base in water at 310 K and pH = 7, albeit to a limited extent and with different kinetics in each case. Carrying out a kinetic study of these reactions was only possible for complexes **1b** and **1c**, while the low water-solubility of complex **1a** allowed only for qualitative observations to be made.

This previous study analyzed the influence of the respective leaving ligands (Cl<sup>-</sup>, H<sub>2</sub>O and CH<sub>3</sub>CN) on the reaction rate of each complex with 9-ethylguanine. In the present study a possible relationship between structure and activity is sought. For this purpose, a whole series of related compounds, which have different didentate ligands, as well as a dinuclear analogue, are taken into account.

The above-mentioned <sup>1</sup>H NMR study was carried out involving 9-ethylguanine and the complexes  $[Ru(azpy)(tpy)Cl]^+$  (**1e**) and  $[Ru(imp)(tpy)Cl]^+$  (**1f**), respectively. The hydrolysis of these complexes in the same experimental conditions and absence of the DNA model base was also followed by <sup>1</sup>H NMR. Comparison of the spectra indicated that both compounds **1e** and **1f** undergo two reactions, as it had previously been reported for the case of **1c**.<sup>42</sup> The major reaction is hydrolysis. Each complex also reacts with 9-EtGua to form a ruthenium-model base adduct. The reaction between **1e** and 9-EtGua is estimated to reach its maximum in about 2 hours, with an approximate conversion of 25%, while the complex **1f** yields as much as a 60% conversion, in a longer reaction that proceeds for about 9 hours (see Fig.4.3 and Table 4.2). The maximum conversions observed in the cases of complexes **1b** and **1c** were reported to be 20% in 5 hours and 30% in 18 hours, respectively.<sup>42</sup>

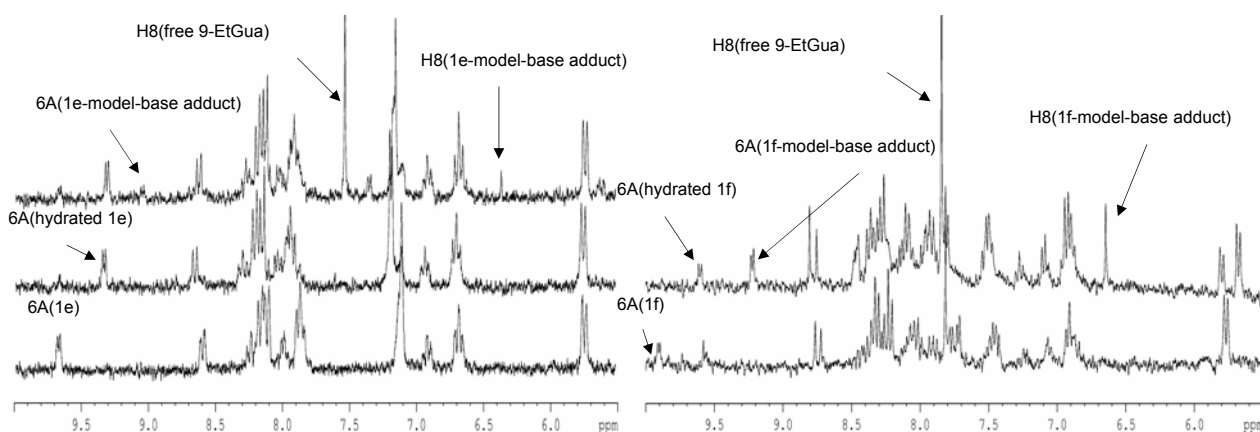


Fig. 4.3.  $^1\text{H}$  NMR studies of the reactions **1e** + 9-EtGua (left) and **1f** + 9-EtGua in  $\text{D}_2\text{O}$  (right). The spectra on the left show the complex **1e** in  $\text{D}_2\text{O}$  at time = 0 (below), the complex **1e** in  $\text{D}_2\text{O}$  at time = 24 h (centre) and the mixture **1e** + 9-EtGua at time = 24 h (above). The spectra on the right show the mixture **1f** + 9-EtGua at time = 30 min (below) and at time = 24 h (above). The peaks assigned to the proton 6A in each complex are labeled, as well as the peaks assigned to the proton H8 of 9-EtGua, both in the free ligand and in the Ru-model base adduct.

Table 4.2. Chemical shifts of the peaks assigned to the protons 6A and H8, indicative of the formation of the corresponding ruthenium-model base adducts.

Complex	6A(ppm)	H8(ppm)
Free 9-EtGua	---	7.81
<b>1b</b> (= hydrated <b>1a</b> , <b>1c</b> )	9.46	---
<b>1a-c</b> -model base adduct ( <b>1d</b> )	9.21	6.81
<b>1e</b>	9.71	---
Hydrated <b>1e</b>	9.40	---
<b>1e</b> -model base adduct	9.15	6.76
<b>1f</b>	9.90	---
Hydrated <b>1f</b>	9.57	---
<b>1f</b> -model base adduct	9.19	6.62

To confirm these results, a mixture of each of the chlorido complexes **1a**, **1d** and **1e** with 9-EtGua was incubated for 24 h at 310 K, and subsequently a mass spectrum was measured for each mixture. The spectrum of the mixture **1a** + 9-EtGua showed a peak at 348.9, which was assigned to the species  $[\text{Ru}(\text{apy})(\text{tpy})(9\text{-EtGua})]^{2+}$ . Two peaks appearing at  $m/z$  695.8 and 348.3 in the spectrum of **1e** + 9-EtGua were assigned to the species  $[\text{Ru}(\text{azpy})(\text{tpy})(9\text{-EtGua})]^+$  and  $[\text{Ru}(\text{azpy})(\text{tpy})(9\text{-EtGua})]^{2+}$ , respectively. The mass spectrum recorded from the mixture **1f** + 9-EtGua showed two peaks at  $m/z$  695 ( $[\text{Ru}(\text{impy})(\text{tpy})(9\text{-EtGua})]^+$ ) and 348 ( $[\text{Ru}(\text{impy})(\text{tpy})(9\text{-EtGua})]^{2+}$ ). The conclusion extracted from these experiments is that the ruthenium complexes **1a-c**, **1e** and **1f** have the ability to bind to the DNA model base 9-EtGua under the experimental conditions used here.

### Interaction between ruthenium polypyridyl complexes and *ct*-DNA

Circular dichroism (CD) is a well-established analytical tool for the study of conformational changes in chiral systems.<sup>43, 44</sup> A widely-studied example is DNA. Any changes in the nucleic base stacking that result in modifications in the DNA secondary structure are clearly reflected in the CD spectra.

Non-covalent (supramolecular) recognition of DNA by natural, as well as by synthetic agents occurs via several different mechanisms, which have been recently reviewed.<sup>45</sup>

As early as 1979, Lippard and co-workers were interested in the possible non-covalent interactions established between several platinum(II) compounds and DNA, particularly by intercalation.<sup>46</sup>

Since the mechanism of action of platinum anticancer complexes was generally accepted to involve an interaction with DNA, circular dichroism has often been used, in combination with other techniques, to study it.<sup>47, 48</sup> Subsequently, this method was also applied to some ruthenium complexes that had been synthesized with the aim of providing an alternative to cisplatin-based anticancer therapy.<sup>23, 49-51</sup>

In the present study, different concentrations of the ruthenium complexes **1b**, **1e**, **1f** and **1g** were mixed with *ct*-DNA and left to incubate for 24 hours at 310 K. Complex **1b** is the aqua analogue of complex **1a**; the former was preferred for this study because of its much higher water solubility. The CD spectra of all these samples were then measured (see Fig.4.4). The CD signal of pure *ct*-DNA is represented by solid lines (Fig.4.4) and it is

characteristic of B-DNA. A first glance at these curves reveals that the bands do not change their positive and negative sign, respectively, by addition of any of the ruthenium compounds under study. This observation indicates that the B-DNA structure is retained in all the studied cases.

Each of these ruthenium complexes seems to exert a slightly different interaction with DNA, as deduced from the CD signals. Both complexes **1b** and **1f** cause the negative band centred at 244 nm to diminish its intensity upon increasing the ruthenium concentration from a DNA base pairs–ruthenium complex 20:1 to 1.5:1. No effect is observed in the positive band at 275 nm. This behaviour is analogous to that reported for the monofunctional organometallic Ru(II) complex  $[(\eta^6\text{-}p\text{-cymene})\text{Ru}(\text{en})(\text{Cl})]^+$ .<sup>52</sup>

A relatively broad, positive band appears at 328 nm by addition of complex **1f**, which was not observed in any other of the measured CDs. This kind of bands has been related to either intercalation or groove binding.<sup>52</sup> These two complexes (**1b** and **1f**) appear to cause conformational changes while not significantly altering the length of the DNA chain.<sup>49, 50, 53</sup>

Low amounts of complex **1e** (ratios 20:1 to 10:1) induce significant intensity increases of both positive and negative CD bands of *ct*-DNA, in a similar way to some reported platinum(II) complexes<sup>54</sup> and to the potentially bifunctional Ru(III) complex *cis*-K[Ru(eddp)Cl<sub>2</sub>] (eddp = ethylenediamine-*N,N'*-di-3-propionate).<sup>53</sup> This observation could indicate a coordinative reaction between ruthenium and DNA. Further addition of **1e** (ratios 10:1 to 1.5) induces a notable decrease of both positive and negative CD bands due to appreciable conformational alterations of DNA. From ratio 2.5:1 to ratio 1.5:1, addition of ruthenium compound induces increase of the positive band, while keeping the decreasing tendency of the negative band.

The most dramatic effect was observed upon addition of the dinuclear complex **1g** to *ct*-DNA. The most concentrated samples showed precipitation. The remaining samples were measured to observe an important change in the CD signals. Both bands at 244 nm and 275 nm showed hyperchromic shifts; the negative band also showed a 2 nm bathochromic shift.

Since precipitation had not occurred in the fresh samples of complex **1g** with *ct*-DNA, even in the most concentrated ones, the CD spectra of the freshly-prepared solutions were also measured (see Fig.4.4). In this graph, upon increasing the ruthenium concentration, the positive band shows a hyperchromic shift first, followed by a hypochromic shift. At the same time, an important bathochromic shift (10 nm) is observed. The negative band

experiences a hyperchromic shift first, then the inverse tendency and finally the intensity of the band decreases once more. A 5 nm bathochromic shift is also observed.

The variations observed in the intensity of the CD bands of the freshly-prepared **1g** + *ct*-DNA solutions suggest a similar behaviour to **1e**, *vide supra*. Non-covalent interactions between the ruthenium complex and DNA would thus be followed by alterations of the secondary structure of the latter. In the case of the dinuclear complex **1g**, these alterations are so important that precipitation of metal-DNA adducts occurs at high ruthenium concentrations. These observations remind us of the properties reported for some metallo-supramolecular cylinders that recognize the DNA major groove, inducing DNA coiling, as can be seen in AFM images.<sup>55, 56</sup> Moreover, the dinuclear complex **1g** is presumably more hydrophobic than its mononuclear parent compound and analogues. The hydrophobic environment within the major groove should therefore favour the interactions of this species with DNA.

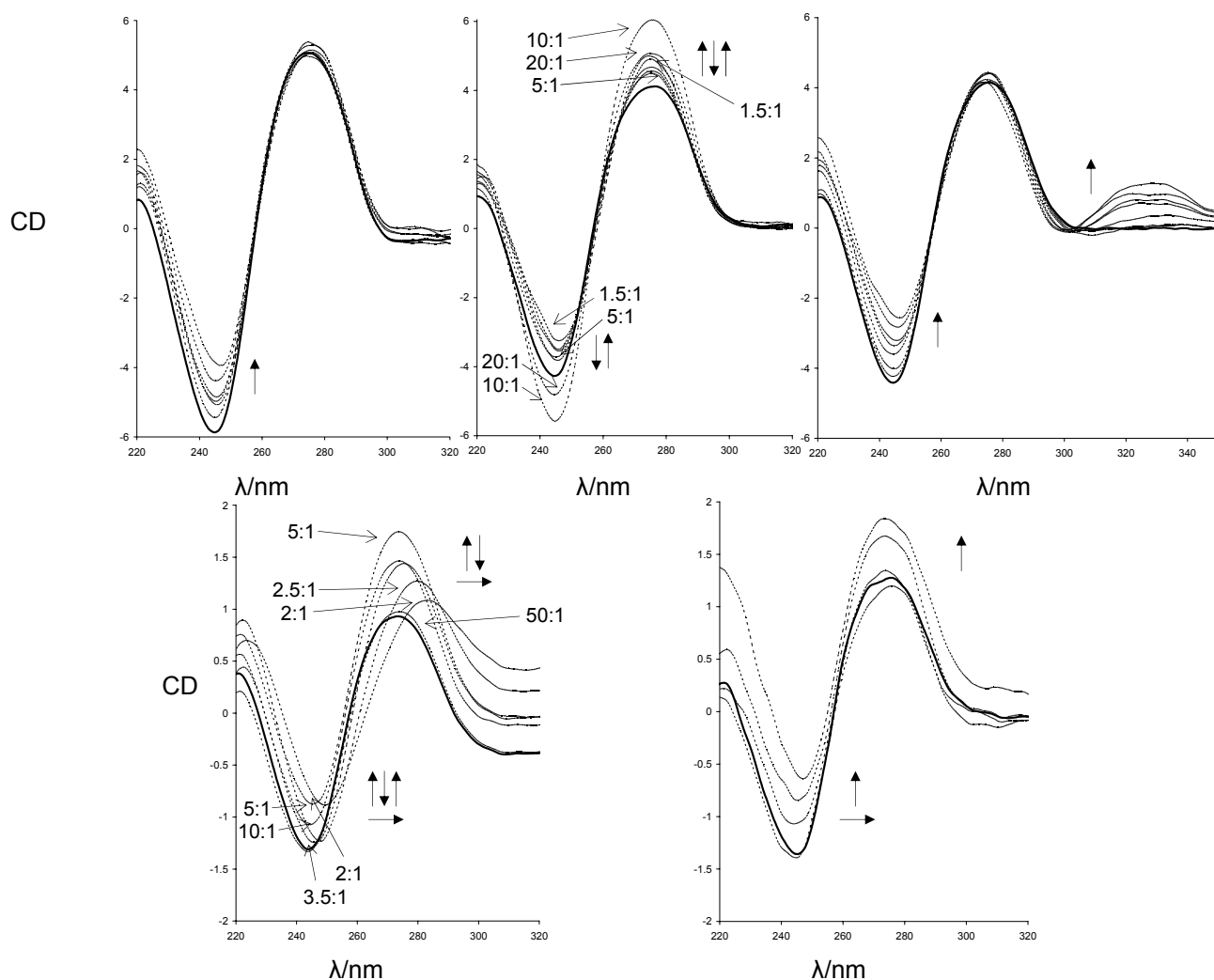


Fig.4.4. Above, circular dichroism spectra of ct-DNA 300  $\mu\text{M}$  incubated for 24h with increasing concentrations of the mononuclear ruthenium complexes **1b** (left), **1e** (centre) and **1f** (right). The DNA base pairs to ruthenium complex ratios are 20:1, 10:1, 5:1, 3:1, 2.5:1, 2:1 and 1.5:1 Below, CD spectra of ct-DNA 100  $\mu\text{M}$  with increasing concentrations of the dinuclear complex **1g**, from freshly-prepared samples (left) and from samples incubated for 24h (right). The DNA base pairs to ruthenium complex ratios are 50:1, 10:1, 5:1, 3.5:1, 2.5:1, and 2:1; the last two ratios were eliminated in the incubated sample because of precipitation. The solid line represents the ct-DNA; some of the curves are labelled with the base pairs to ruthenium complex ratios. The arrows in bold indicate a variation of the intensity of the band upon addition of ruthenium.

Linear dichroism (LD) is defined as the difference in absorption of light polarized parallel and perpendicular to an orientation axis.<sup>43, 55</sup> The DNA that is present in a sample solution located in the circular space between an outer (static) and an inner (rotating) quartz cylinders can be oriented by the viscous drag created by the rotation of one cylinder inside the other, an effect that is most efficiently achieved in a Couette cell.<sup>57</sup> This orientation along the DNA helix axis can be studied by LD. Since the base pairs are oriented perpendicular to the mentioned helix axis, a negative LD signal appears for B-DNA (see Fig.4.5, band at 258 nm).

Metallo-intercalators produce, by interaction with DNA, a significant change in this signal. For this reason LD has been used in the study of non-covalent DNA recognition by platinum(II) and copper(II) complexes<sup>58, 59</sup> and, more recently, by ruthenium antitumour complexes.<sup>52, 60</sup> This technique is typically applied in combination with other spectroscopic methods, especially circular dichroism.

The LD signal at 258 nm remained negative through all the herein described experiments, indicating that the DNA retained its B conformation. This DNA band becomes, however, less negative upon addition of the corresponding ruthenium complex in all the studied cases, indicating a reduction in the DNA orientation. This behaviour, characteristic of DNA bending or coiling, is much more pronounced in the experiment carried out with the dinuclear compound **1g**. In a similar way, this negative band has been reported to diminish its intensity by addition of complexes such as the difunctional Pt(II) complexes reported by Nordén,<sup>59</sup> or the monofunctional organometallic Ru(II) complexes reported by Sadler and Brabec.<sup>52</sup> However, the intensity decrease produced in this negative LD band by metallo-cylinders like the above-mentioned iron cylinder,<sup>55</sup> or the more recently-reported ruthenium cylinder,<sup>61</sup> is much more dramatic.

A positive induced LD band at around 330 nm can be observed in the LD series corresponding to complexes **1b** and **1g**. This band appears also in the case of **1e**, although much smaller, and it is absent in the **1f**-DNA LD spectra. The occurrence of this induced LD signal may suggest that the complex is orientated more parallel to the DNA helical axis than to the base pairs. The binding mode displayed by the complexes **1b**, **1e** and **1g** would thus be non-intercalative. In the same way, the complex **1f** would display no specific binding orientation with respect to *ct*-DNA.

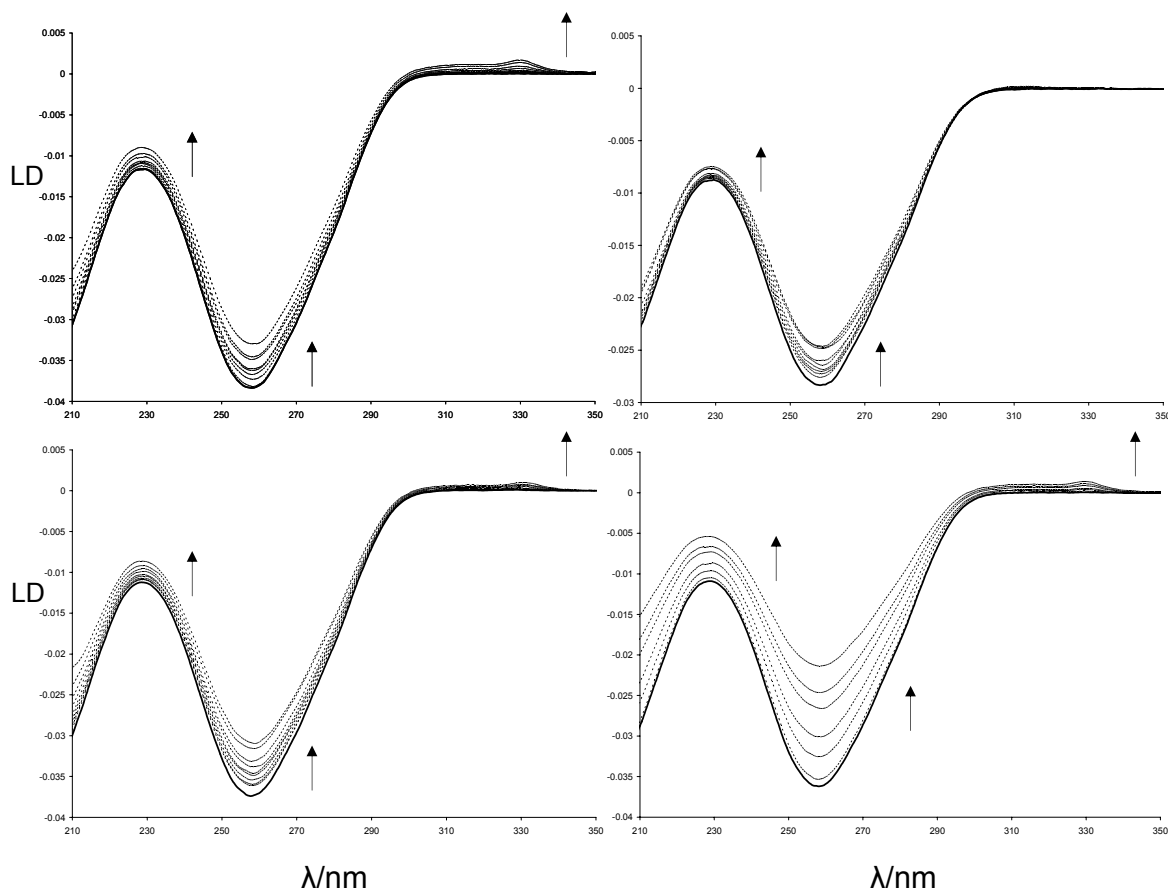


Fig.4.5. Linear dichroism spectra of *ct*-DNA 300  $\mu$ M with increasing concentrations of the ruthenium complexes **1b** (left, above), **1e** (left, below), **1f** (right, above) and **1g** (right, below). The DNA base pairs to ruthenium complex ratios are 20:1, 15:1, 10:1, 8:1, 5:1, 3.5:1, 3:1, 2.5:1 and 2:1 in the case of the mononuclear complexes (**1b**, **1e** and **1f**); for the dinuclear complex **1g**, 40:1, 20:1, 15:1, 10:1, 8:1 and 6:1. The solid line represents the *ct*-DNA. The arrows in bold indicate a variation of the intensity of the band upon addition of ruthenium.

In summary, according to the CD and LD experiments the complexes **1b** and **1e-g** cause conformational changes in the DNA molecule, although the B-DNA structure is retained in all the studied cases. Both **1b** and **1e** seem to interact with DNA via a non-intercalative way and, at high concentrations, they cause conformational changes of DNA. Complex **1g** appears to be capable of bending or coiling the DNA even at low concentrations. Finally, **1f** does not display any specific binding orientation with respect to *ct*-DNA.

### ***In vitro* cytotoxicity assays**

The cytotoxicities of the mononuclear complexes **1a-c**, **1e** and **1f** in several selected cell lines were compared, in search for differences that might arise from their structural differences. The dinuclear complex  $[\{\text{Ru}(\text{apy})(\text{tpy})\}_2\{\mu\text{-H}_2\text{N}(\text{CH}_2)_6\text{NH}_2\}](\text{ClO}_4)_4$  (**1g**) was also studied. The reasons why complex **1g** was selected are multiple. The six coordination positions of ruthenium are blocked by non-labile ligands, making **1g** unable to bind to DNA in a coordinative way. Hence, the study of this complex may give indications about the existence of a relation between DNA-binding and cytotoxicity. On the other hand the compound was chosen to be symmetrical and analogous to the mononuclear parent compounds **1a-c** to make the comparison amongst all these complexes as valid as possible. Finally the bridging ligand between the two ruthenium atoms of **1g** is a chain that is long enough to allow the complex **1g** to act as two units of the parent compound.

The analyzed compounds, including the non-coordinating homodinuclear complex **1g**, show a good to moderate activity in the EVSA-T and H226 cell lines (see Table 4.3). The same results were obtained in the A2780 normal and resistant cell lines, with only one exception. The non-azo complex **1f** showed very low or no activity at all in the tested cell lines (see Table 4.4). The most active drug in the case of the non-resistant cell line, A2780, was found to be compound **1b**. The activities in this cell line are in general worse than that of cisplatin, whereas in the resistant cell lines on average the activities are comparable to that of cisplatin. This is also displayed in the resistance factor (rf) values, which are defined as the  $\text{IC}_{50}$  value of a cisplatin-resistant cell line divided by the  $\text{IC}_{50}$  value of the corresponding cisplatin-sensitive cell line. The rf values of the active compounds for the A2780 cell lines range from 0.8-2.2, suggesting that the compounds seem unaffected by the multifactorial resistance mechanism in the resistant cell line. In the case of the murine leukaemia cell lines the compounds **1a-c** and **1e** interestingly show rather low activity in the non-resistant cell line, whereas the activity is moderate in the resistant cell line, also shown by the low rf values (0.6-1.2). This suggests that the effect of the resistance profile of the murine leukaemia cell line, if any, is actually to improve the activity of the compounds. Neither the non-azo complex (**1f**) nor the homodinuclear complex (**1g**) show any activity in the L1210 cell lines.

Table 4.3.  $IC_{50}$  values ( $\mu M$ ) of the  $[Ru(apy)(tpy)L_2]^{(2-n)+}$  complexes (**1a-c**) and their dinuclear analogue  $[\{Ru(apy)(tpy)\}_2\{\mu-H_2N(CH_2)_6NH_2\}](ClO_4)_4$  (**1g**) after a 5 days treatment in some selected cell lines. The  $IC_{50}$  values of  $\alpha-[Ru(azpy)_2Cl_2]$  and cisplatin have been included as a reference.

Tested compound	A498	EVSA-T	H226	IGRO V	M19	MCF-7	WiDR
$[Ru(apy)(tpy)Cl](ClO_4)$ ( <b>1a</b> )	>96	7	17	>96	25	13	66
$[Ru(apy)(tpy)(H_2O)](ClO_4)_2 \cdot 2H_2O$ ( <b>1b</b> )	>81	6	17	44	26	18	50
$[Ru(apy)(tpy)(CH_3CN)](ClO_4)_2$ ( <b>1c</b> )	>82	6	26	78	30	21	73
$[Ru(azpy)(tpy)Cl]Cl \cdot 5H_2O$ ( <b>1e</b> )	39	11	34	65	15	30	51
$[\{Ru(apy)(tpy)\}_2\{\mu-H_2N(CH_2)_6NH_2\}](ClO_4)_4$ ( <b>1g</b> )	>40	17	28	>40	33	>40	>40
$\alpha-[Ru(azpy)_2Cl_2]$	0.3	0.1	0.5	0.3	0.1	0.3	0.3
Cisplatin	2	1	2	0.2	3	2	2

Table 4.4.  $IC_{50}$  values ( $\mu M$ ) of the  $[Ru(tpy)L_1L_2]^{(2-n)+}$  complexes (**1a-c**, **1e** and **1f**) and the dinuclear complex  $[\{Ru(apy)(tpy)\}_2\{\mu-H_2N(CH_2)_6NH_2\}](ClO_4)_4$  (**1g**) after a 48 h treatment in some selected cell lines. The  $IC_{50}$  values of  $\alpha-[Ru(azpy)_2Cl_2]$  and cisplatin have been included as a reference.

Tested compound	A2780	A2780R	L1210/0	L1210/2
$[Ru(apy)(tpy)Cl](ClO_4)$ ( <b>1a</b> )	23	25	100	56
$[Ru(apy)(tpy)(H_2O)](ClO_4)_2 \cdot 2H_2O$ ( <b>1b</b> )	11	30	80	97
$[Ru(apy)(tpy)(CH_3CN)](ClO_4)_2$ ( <b>1c</b> )	31	28	70	40
$[Ru(azpy)(tpy)Cl]Cl \cdot 5H_2O$ ( <b>1e</b> )	19	42	42	26
$[Ru(imp)(tpy)Cl](ClO_4)$ ( <b>1f</b> )	>100	62	>100	>100
$[\{Ru(apy)(tpy)\}_2\{\mu-H_2N(CH_2)_6NH_2\}](ClO_4)_4$ ( <b>1g</b> )	33	28	>100	>100
$\alpha-[Ru(azpy)_2Cl_2]$	0.1	0.2	0.1	0.2
Cisplatin	6	25	2	24

#### **4.4. Concluding remarks**

Considering the IC<sub>50</sub> values that were found for the apy complexes **1a-c**, which are analogous to each other except for the leaving group, no correlation appears to exist between the lability of the mentioned leaving group and the cytotoxic activity of the ruthenium compound.

According to the results obtained in the experiments with 9-ethylguanine, the most rapid complex to react with the DNA model base is the azpy complex **1e**, which reaches the maximal conversion 16 hours earlier than the slowest complex, **1c**. On the other hand, the maximal amount of ruthenium-model base adduct is obtained from the impy complex **1f**.

Taking into account that the IC<sub>50</sub> values obtained for the complexes **1c** and **1e** are not the two extreme values, and that the complex giving a maximal conversion is inactive in the tested cell lines, no correlation can be established between the ability of a complex to bind to 9-ethylguanine and its cytotoxic activity.

Moreover, while the azo function is in principle unrelated to coordination to guanine, our results indicate that the presence of this functional group is necessary for cytotoxic activity. The only compound of the series lacking an azo group was found to be inactive in the tested cell lines. It is interesting to point out that the complex [Ru(bpy)(tpy)Cl]Cl, which is to some extent analogous to the complexes herein described, and which also lacks an azo group, has been reported to be inactive.<sup>33</sup>

More importantly, a relation has been found between the experiments carried out with *ct*-DNA and the activity of the compounds. The inactive compound **1f** seems to bind to *ct*-DNA, but with no specific orientation with respect to the double helix. On the other hand, the biggest changes observed in both CD and LD spectra correspond to the dinuclear complex **1g**. While this complex cannot coordinatively interact with DNA, its cytotoxic activity is comparable to those displayed by the mononuclear complexes. The CD and LD experiments show that there is indeed an interaction between DNA and **1g**, even if it is not of a coordinative nature. For other non-coordinative dinuclear compounds, this strong effect on the DNA band in LD is proven to be caused by interactions in the major groove of DNA,<sup>55, 56, 62</sup> as well as in 3-way junctions (structures that are formed at the point where 3 double-helical regions join together).<sup>45, 63</sup>

The CD experiments seem to indicate that the studied complexes cause conformational changes in the DNA. It is interesting to point out that the complex **1e** shows an effect on the positive CD band centered at 275 nm, which suggests that the azpy

complex induces changes in the DNA chain length.<sup>49, 50, 53</sup> This effect is also observed in the case of the dinuclear complex, but not in the rest of the mononuclear complexes.

#### 4.5. References

1. Loehrer, P. J.; Einhorn, L. H., *Ann. Intern. Med.* **1984**, *100*, 704-713.
2. Reedijk, J., *Curr. Opin. Chem. Biol.* **1999**, *3*, 236-240.
3. Reedijk, J., *Chem. Commun.* **1996**, 801-806.
4. Jamieson, E. R.; Lippard, S. J., *Chem. Rev.* **1999**, *99*, 2467-2498.
5. Reedijk, J., *Pure Appl. Chem.* **1987**, *59*, 181-192.
6. Bierbach, U.; Qu, Y.; Hambley, T. W.; Peroutka, J.; Nguyen, H. L.; Doedee, M.; Farrell, N., *Inorg. Chem.* **1999**, *38*, 3535-3542.
7. Farrell, N.; Ha, T. T. B.; Souchard, J. P.; Wimmer, F. L.; Cros, S.; Johnson, N. P., *J. Med. Chem.* **1989**, *32*, 2240-2241.
8. van Beusichem, M.; Farrell, N., *Inorg. Chem.* **1992**, *31*, 634-639.
9. Farrell, N.; Kelland, L. R.; Roberts, J. D.; van Beusichem, M., *Cancer Res.* **1992**, *52*, 5065-5072.
10. Coluccia, M.; Sava, G.; Loseto, F.; Nassi, A.; Boccarelli, A.; Giordano, D.; Alessio, E.; Mestroni, G., *Eur. J. Cancer* **1993**, *29A*, 1873-1879.
11. Zou, Y.; van Houten, B.; Farrell, N., *Biochemistry* **1993**, *32*, 9632-9638.
12. Montero, E. I.; Díaz, S.; González-Vadillo, A. M.; Pérez, J. M.; Alonso, C.; Navarro-Ranninger, C., *J. Med. Chem.* **1999**, *42*, 4264-4268.
13. Montero, E. I.; Pérez, J. M.; Schwartz, A.; Fuertes, M. A.; Malinge, J. M.; Alonso, C.; Leng, M.; Navarro-Ranninger, C., *ChemBiochem* **2002**, *3*, 61-67.
14. Boccarelli, A.; Intini, F. P.; Sasanelli, R.; Sivo, M. F.; Coluccia, M.; Natile, G., *J. Med. Chem.* **2006**, *49*, 829-837.
15. Kaspárková, J.; Marini, V.; Najajreh, Y.; Gibson, D.; Brabec, V., *Biochemistry* **2003**, *42*, 6321-6332.
16. Kaspárková, J.; Nováková, O.; Marini, V.; Najajreh, Y.; Gibson, D.; Pérez, J. M.; Brabec, V., *J. Biol. Chem.* **2003**, *278*, 47516-47525.
17. Clarke, M. J., *Coord. Chem. Rev.* **2003**, *236*, 209-233.
18. Kostova, I., *Curr. Med. Chem.* **2006**, *13*, 1085-1107.
19. Reedijk, J., *Proc. Natl. Acad. Sci. U. S. A.* **2003**, *100*, 3611-3616.
20. Hotze, A. C. G.; Caspers, S. E.; de Vos, D.; Kooijman, H.; Spek, A. L.; Flamigni, A.; Bacac, M.; Sava, G.; Haasnoot, J. G.; Reedijk, J., *J. Biol. Inorg. Chem.* **2004**, *9*, 354-364.
21. Velders, A. H.; Kooijman, H.; Spek, A. L.; Haasnoot, J. G.; de Vos, D.; Reedijk, J., *Inorg. Chem.* **2000**, *39*, 2966-2967.
22. Habtemariam, A.; Melchart, M.; Fernández, R.; Parsons, S.; Oswald, I. D. H.; Parkin, A.; Fabbiani, F. P. A.; Davidson, J. E.; Dawson, A.; Aird, R. E.; Jodrell, D. I.; Sadler, P. J., *J. Med. Chem.* **2006**, *49*, 6858-6868.
23. Vilaplana, R. A.; Delmani, F.; Manteca, C.; Torreblanca, J.; Moreno, J.; García-Herdugo, G.; González-Vílchez, F., *J. Inorg. Biochem.* **2006**, *100*, 1834-1841.
24. Vilaplana, R. A.; González-Vílchez, F.; Gutiérrez-Puebla, E.; Ruiz-Valero, C., *Inorg. Chim. Acta* **1994**, *224*, 15-18.
25. Sava, G.; Pacor, S.; Bergamo, A.; Cocchietto, M.; Mestroni, G.; Alessio, E., *Chem.-Biol. Interact.* **1995**, *95*, 109-126.
26. Hartinger, C. G.; Zorbas-Seifried, S.; Jakupec, M. A.; Kynast, B.; Zorbas, H.; Keppler, B. K., *J. Inorg. Biochem.* **2006**, *100*, 891-904.

27. Allardyce, C. S.; Dyson, P. J., *Platinum Metals Rev.* **2001**, *45*, 62-69.
28. Ang, W. H.; Dyson, P. J., *Eur. J. Inorg. Chem.* **2006**, 4003-4018.
29. Brabec, V.; Nováková, O., *Drug Resist. Update* **2006**, *9*, 111-122.
30. Corral, E.; Hotze, A. C. G.; Tooke, D. M.; Spek, A. L.; Reedijk, J., *Inorg. Chim. Acta* **2006**, *359*, 830-838.
31. Boelrijk, A. E. M.; Jorna, A. M. J.; Reedijk, J., *J. Mol. Catal. A-Chem.* **1995**, *103*, 73-85.
32. Hotze, A. C. G.; Faiz, J. A.; Mourtzis, N.; Pascu, G. I.; Webber, P. R. A.; Clarkson, G. J.; Yannakopoulou, K.; Pikramenou, Z.; Hannon, M. J., *Dalton Trans.* **2006**, 3025-3034.
33. Nováková, O.; Kaspárková, J.; Vrána, O.; van Vliet, P. M.; Reedijk, J.; Brabec, V., *Biochemistry* **1995**, *34*, 12369-12378.
34. Kirpal, A.; Reiter, E., *Ber. Deuts. Chem. Ges.* **1927**, *60*, 664-666.
35. Adcock, P. A.; Keene, F. R.; Smythe, R. S.; Snow, M. R., *Inorg. Chem.* **1984**, *23*, 2336-2343.
36. Reichmann, M. E.; Rice, S. A.; Thomas, C. A.; Doty, P., *J. Am. Chem. Soc.* **1954**, *76*, 3047-3053.
37. Boyd, M. R., In Status of the NCI preclinical antitumor drug discovery screen. Principles and practice of oncology, 1989; Vol. 3, pp 1-12.
38. Keepers, Y. P.; Pizao, P. E.; Peters, G. J.; van Ark-Otte, J.; Winograd, B.; Pinedo, H. M., *Eur. J. Cancer* **1991**, *27*, 897-900.
39. Alley, M. C.; Scudiero, D. A.; Monks, A.; Hursey, M. L.; Czerwinski, M. J.; Fine, D. L.; Abbott, B. J.; Mayo, J. G.; Shoemaker, R. H.; Boyd, M. R., *Cancer Res.* **1988**, *48*, 589-601.
40. Mosmann, T., *J. Immunol. Methods* **1983**, *65*, 55-63.
41. Tada, H.; Shiho, O.; Kuroshima, K.; Koyama, M.; Tsukamoto, K., *J. Immunol. Methods* **1986**, *93*, 157-165.
42. Corral, E.; Hotze, A. C. G.; Magistrato, A.; Reedijk, J., *Inorg. Chem.* **2007**, *in press*.
43. Rodger, A.; Nordén, B., Circular dichroism and linear dichroism. Oxford University Press: Oxford, 1997.
44. Kelly, S. M.; Jess, T. J.; Price, N. C., *BBA-Proteins Proteomics* **2005**, *1751*, 119-139.
45. Hannon, M. J., *Chem. Soc. Rev.* **2007**, *36*, 280-295.
46. Howegrant, M.; Lippard, S. J., *Biochemistry* **1979**, *18*, 5762-5769.
47. Brabec, V.; Kleinwächter, V.; Butour, J. L.; Johnson, N. P., *Biophys. Chem.* **1990**, *35*, 129-141.
48. Natile, G.; Marzilli, L. G., *Coord. Chem. Rev.* **2006**, *250*, 1315-1331.
49. Chen, H.; Parkinson, J. A.; Nováková, O.; Bella, J.; Wang, F. Y.; Dawson, A.; Gould, R.; Parsons, S.; Brabec, V.; Sadler, P. J., *Proc. Natl. Acad. Sci. U. S. A.* **2003**, *100*, 14623-14628.
50. Karidi, K.; Garoufis, A.; Hadjiliadis, N.; Lutz, M.; Spek, A. L.; Reedijk, J., *Inorg. Chem.* **2006**, *45*, 10282-10292.
51. Chao, H.; Yuan, Y. X.; Zhou, F.; Ji, L. N.; Zhang, J., *Transit. Met. Chem.* **2006**, *31*, 465-469.
52. Nováková, O.; Chen, H. M.; Vrána, O.; Rodger, A.; Sadler, P. J.; Brabec, V., *Biochemistry* **2003**, *42*, 11544-11554.
53. Grguric-Sipka, S. R.; Vilaplana, R. A.; Pérez, J. M.; Fuertes, M. A.; Alonso, C.; Álvarez, Y.; Sabo, T. J.; González-Vílchez, F., *J. Inorg. Biochem.* **2003**, *97*, 215-220.
54. Macquet, J. P.; Butour, J. L., *Eur. J. Biochem.* **1978**, *83*, 375-387.
55. Hannon, M. J.; Moreno, V.; Prieto, M. J.; Moldrheim, E.; Sletten, E.; Meistermann, I.; Isaac, C. J.; Sanders, K. J.; Rodger, A., *Angew. Chem.-Int. Edit.* **2001**, *40*, 880-884.

56. Meistermann, I.; Moreno, V.; Prieto, M. J.; Moldrheim, E.; Sletten, E.; Khalid, S.; Rodger, P. M.; Peberdy, J. C.; Isaac, C. J.; Rodger, A.; Hannon, M. J., *Proc. Natl. Acad. Sci. U. S. A.* **2002**, *99*, 5069-5074.
57. Rodger, A.; Marrington, R.; Geeves, M. A.; Hicks, M.; de Alwis, L.; Halsall, D. J.; Dafforn, T. R., *Phys. Chem. Chem. Phys.* **2006**, *8*, 3161-3171.
58. Nordén, B., *Inorg. Chim. Acta* **1978**, *31*, 83-95.
59. Nordén, B., *FEBS Lett.* **1978**, *94*, 204-206.
60. Coggan, D. Z. M.; Haworth, I. S.; Bates, P. J.; Robinson, A.; Rodger, A., *Inorg. Chem.* **1999**, *38*, 4486-4497.
61. Pascu, G. I.; Hotze, A. C. G.; Sánchez-Cano, C.; Kariuki, B. M.; Hannon, M. J., *Angew. Chem. Int. Ed.* **2007**, *46*, 4374-4378.
62. Uerpmann, C.; Malina, J.; Pascu, M.; Clarkson, G. J.; Moreno, V.; Rodger, A.; Grandas, A.; Hannon, M. J., *Chem.-Eur. J.* **2005**, *11*, 1750-1756.
63. Oleksi, A.; Blanco, A. G.; Boer, R.; Usón, I.; Aymamí, J.; Rodger, A.; Hannon, M. J.; Coll, M., *Angew. Chem.-Int. Edit.* **2006**, *45*, 1227-1231.

## 5. Explorations towards novel ruthenium anticancer drugs

Most of the compounds described in this thesis show a certain degree of activity in some selected cancerous cell lines. The research presented so far suggests that the mechanism of action of some of these compounds, namely the mononuclear ruthenium(II) complexes **1a-c**, **1e** and **1f**, might involve coordination to DNA. In this chapter, other alternative interaction modes with DNA are dealt with and a number of suggestions are presented for further development of this research line.

## 5.1. Alternative ways of interaction between metallodrugs and DNA

### 5.1.1. Introduction

Anticancer therapy with classical ruthenium coordination compounds is based on the capability of the metal to coordinatively bind to DNA.<sup>1</sup> These ruthenium complexes are usually bifunctional and they mostly exert their action by forming intra- or interstrand crosslinks with the DNA molecule.<sup>2</sup> On the other hand, examples of monofunctional ruthenium complexes are also known that display an anticancer activity, such as some of the complexes described in this thesis (**1a-c** and **1e**). The cytotoxicity of these monofunctional complexes could also be related to coordination to DNA.

Other ways of interaction with DNA are known, including backbone binding<sup>3</sup> and recognition of DNA junction structures.<sup>4</sup> This chapter will focus on the interactions caused by intercalation between nucleic base-pairs and on groove recognition.

#### Groove binding

The dinuclear complex  $[\{\text{Ru}(\text{apy})(\text{tpy})\}_2\{\mu\text{-H}_2\text{N}(\text{CH}_2)_6\text{NH}_2\}]^{4+}$  (**1g**), described in chapter 4, interacts with DNA presumably via electrostatic and especially via groove-binding interactions. The activity displayed by this compound in a number of cell lines is comparable to cisplatin.

Two strategies can be followed that are inspired by the above-described results. The first one consists on the synthesis of homodinuclear ruthenium(II) complexes that are first electrostatically attracted to DNA, subsequently form a coordinative interaction with the latter, and finally interact with the DNA in the same way **1g** does, *i.e.*, by groove binding (see Fig.5.1).

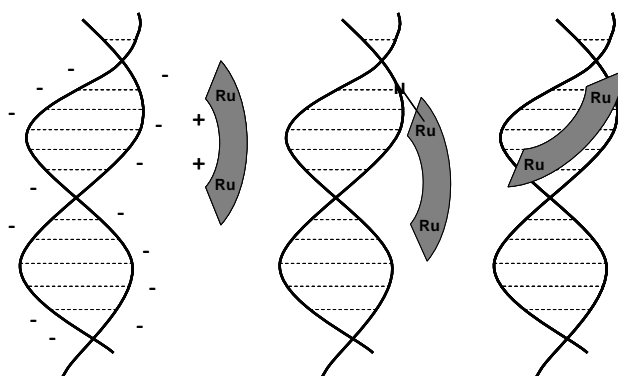


Fig.5.1. Scheme depicting a homodinuclear, positively-charged Ru(II) complex being first electrostatically attracted to DNA (left), coordinated to a nucleic base (middle) and finally binding to a DNA groove (right).

A second strategy deals with the synthesis of heterodinuclear Pt-Ru complexes using such ligands. The Pt moiety can be chosen such that it will form a coordinative interaction with DNA, like transplatin, or it could even be an intercalator, *vide infra*, such as  $[\text{Pt}(\text{tpy})]^{2+}$ .

Following the first approach, the homodinuclear ruthenium(II) compound  $[\{\text{Ru}(\text{tpy})\text{Cl}\}_2(\mu\text{-paa})](\text{BF}_4)_2$  (**1h**) was obtained, where tpy is 2,2'-6'2''-terpyridine and paa is 2-pyridinealdazine (see Fig.5.2), and some cell tests were subsequently performed (as summarized in section 5.1.2, Table 5.1).

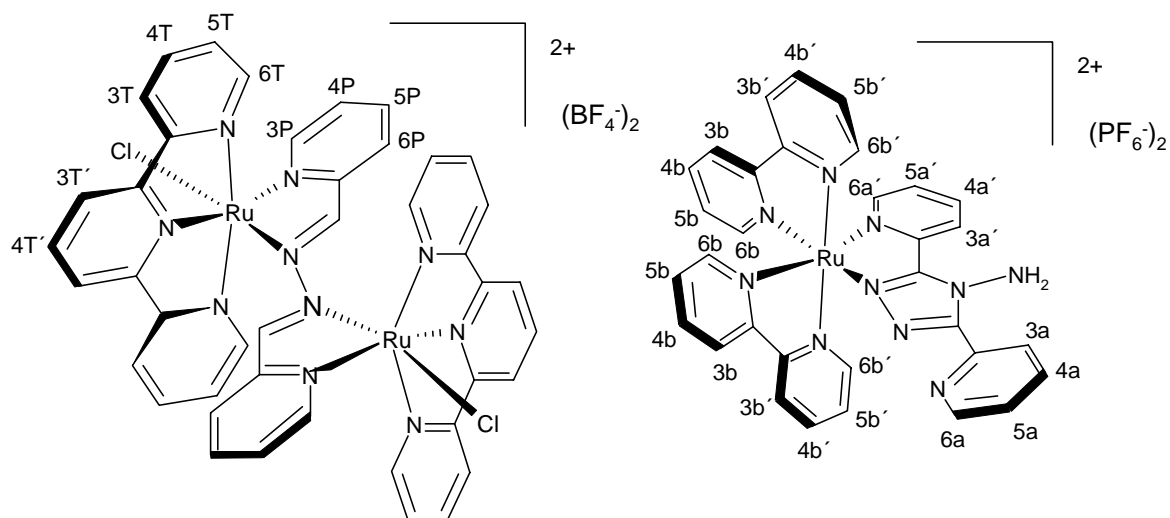


Fig.5.2. Molecular structures of  $[\{\text{Ru}(\text{tpy})\text{Cl}\}_2(\mu\text{-paa})](\text{BF}_4)_2$  (**1h**, left) and  $[\text{Ru}(\text{abpt})(\text{bpy})_2](\text{PF}_6)_2$  (**1i**, right). Proton numbering scheme as used in  $^1\text{H}$  NMR spectra.

### Intercalation

Small, planar aromatic molecules can bind DNA through intercalation, as proposed already by Lerman in 1961.<sup>5</sup> The base pairs and helical backbone extend and unwind to accommodate the molecule, which inserts into the resulting hydrophobic pocket. The intercalating surface is stabilized electronically in the helix by  $\pi$ - $\pi$  stacking with the bases, thus the intercalator is rigidly held and oriented with the planar moiety perpendicular to the helical axis.<sup>6</sup>

A decade later, the concept “metallointercalator” was introduced. The platinum(II) complexes  $[\text{Pt}(\text{tpy})(\text{SCH}_2\text{CH}_2\text{OH})]^+$  and  $[\text{Pt}(\text{tpy})\text{Cl}]^+$ , where tpy is 2,2'-6',2''-terpyridine, were proven to bind strongly to DNA by intercalation between base pairs.<sup>7</sup> Subsequently,

other aromatic ligands were made to react with platinum to generate new compounds that interact with DNA in that same way.<sup>8,9</sup>

Although in principle the square-planar geometry of platinum(II) was thought to be essential for a metallointercalator, octahedral metal centres with large planar aromatic ligands were synthesised afterwards, which also displayed intercalative interactions with the DNA helix.<sup>10, 11</sup> While one of the planar units inserts between base-pair planes, the metal and additional co-ligands interact in one of the DNA grooves.<sup>10, 11</sup> To date, many  $[\text{Ru}(\text{bpy})_2\text{L}]^{2+}$  and  $[\text{Ru}(\text{phen})_2\text{L}]^{2+}$  complexes have been described, where L is an aromatic bidentate ligand, which have been proven to interact with DNA via intercalation.<sup>12-17</sup> Even a dinuclear analogue with a large aromatic bridging ligand has been reported to very slowly bind to DNA via an intercalation process.<sup>18</sup>

It should be noted that distinguishing a groove binder from an intercalator is not straightforward, as illustrated by many discussions on the controversial case of  $[\text{Ru}(\text{phen})_3]^{2+}$ , where phen is phenantroline.<sup>6, 19-23</sup>

It may be very interesting to synthesize ruthenium(II) polypyridyl ligands containing the ligands 4-amino-3,5-bis(2-pyridinyl)-1,2,4 triazole (abpt) and 3,5-bis(2-pyridinyl)-1,2,4 triazole (Hbpt), for several reasons. Firstly, some ruthenium complexes with  $\pi$ -deficient ligands behave as photo-oxidants, giving rise to photo-induced electron-transfer processes that lead to DNA cleavage.<sup>24-27</sup> Moreover, the strong  $\sigma$ -donor properties of the triazole/triazolate groups make these ligands optimal for use as bridges in the synthesis of dinuclear and polynuclear complexes.<sup>28-31</sup>

An especially interesting feature of this kind of complexes is the luminescence displayed by some of them.<sup>32</sup> Finally, the abpt and Hbpt ligands may behave as intercalators.

The ruthenium(II) complex  $[\text{Ru}(\text{abpt})(\text{bpy})_2](\text{PF}_6)_2$  was synthesized and its anticancer activity was tested against some selected cell lines. Although this complex displayed an activity comparable to that of cisplatin in the cell line H226 and a reasonable activity in the cell line WiDR (see Tables 5.1 and 5.2), it was found to be virtually inactive in the rest of the tested cell lines. The interaction of this compound with DNA remains to be studied.

### 5.1.2. Experimental

#### Materials and reagents

2-pyridinealdazine (paa), 4-amino-3,5-bis(pyridine-2-yl)-1,2,4-triazole (abpt), Ru(tpy)Cl<sub>3</sub> and *cis*-Ru(bpy)<sub>2</sub>Cl<sub>2</sub> were synthesized following procedures described in literature.<sup>33-36</sup> 2-cyanopyridine, 2-pyridinaldehyde, hydrazine monohydrate, NH<sub>4</sub>PF<sub>6</sub> and tpy (Aldrich), LiCl (Merck), NaBF<sub>4</sub> and bpy (Acros) and RuCl<sub>3</sub>·3H<sub>2</sub>O (Johnson & Matthey) were used as supplied. All other chemicals and solvents were reagent grade commercial materials and used as received, without further purification.

#### Physical measurements

C, H and N determinations were performed on a Perkin Elmer 2400 Series II analyzer. Mass spectra were obtained with a Finnigan MAT TSQ-700 mass spectrometer equipped with a custom-made electrospray interface (ESI). NMR spectra were recorded on a Bruker DPX-300 spectrometer operating at a frequency of 300 MHz. Chemical shifts were calibrated against tetramethylsilane (TMS).

#### Synthesis and characterization of [{Ru(tpy)Cl}<sub>2</sub>(μ-paa)](BF<sub>4</sub>)<sub>2</sub> (1h)

LiCl (500 mg, 11.80 mmol) was dissolved in 80 ml of ethanol-water (3:1). Triethylamine (0.160 ml, 1.135 mmol) was added, followed by Ru(tpy)Cl<sub>3</sub> (500 mg, 1.135 mmol) and paa (360 mg, 1.715 mmol). The mixture was vigorously refluxed for 90 minutes, and the hot solution was filtered to remove any insoluble material. The brown solution was evaporated to dryness. 15 ml methanol were used to dissolve the residue, to which 35 ml of a methanolic saturated solution of NaBF<sub>4</sub> were added. The flask was left for 3 days at 4 °C. A brown precipitate had then appeared, which was filtered, washed with little ice-cold ethanol and ether and dried *in vacuo* over silica. Yield: 39 mg (3%). *Anal.* Calc. for C<sub>42</sub>H<sub>32</sub>N<sub>10</sub>B<sub>2</sub>F<sub>8</sub>Cl<sub>2</sub>Ru<sub>2</sub>: C, 44.9; H, 2.9; N, 12.5. Found: C, 42.2; H, 2.9; N, 11.7. *m/z* (ESIMS) 580.1 ([Ru(paa)(tpy)Cl]<sup>+</sup>); 475.0 ([{Ru(tpy)Cl}<sub>2</sub>(μ-paa)]<sup>2+</sup>). <sup>1</sup>H NMR (DMSO-*d*<sub>6</sub>): δ (ppm): 9.71 (2H, d, 5.49 Hz, 6P); 8.44 (8H, m, 3T, 3T'); 8.22 (2H, t, 6.93 Hz, 4P); 8.12 (4H, t, 7.12 Hz, 4T); 8.00 (4H, m, 5P, 4T'); 7.92 (2H, d, 8.06 Hz, 3P); 7.46 (4H, t, 6.24 Hz, 5T); 7.11 (4H, d, 4.83 Hz, 6T); 6.97 (2H, s, CH=).

### Synthesis and characterization of [Ru(abpt)(bpy)<sub>2</sub>](PF<sub>6</sub>)<sub>2</sub> (**1i**)

The synthesis of [Ru(abpt)(bpy)<sub>2</sub>](PF<sub>6</sub>)<sub>2</sub> was carried out as described in the literature,<sup>32</sup> with slight modifications. *cis*-Ru(bpy)<sub>2</sub>Cl<sub>2</sub> (75 mg, 0.18 mmol) and abpt (82 mg, 0.34 mmol) were dissolved in 15 ml of ethanol and refluxed for two hours. The mixture was evaporated under reduced pressure, and the obtained residue was dissolved in 2.5 ml methanol. 5 ml of a saturated solution of NH<sub>4</sub>PF<sub>6</sub> were added. An orange-red solid was collected by filtration and dried *in vacuo* over silica. Yield: 32 mg (19%). *Anal.* Calc. for C<sub>32</sub>H<sub>26</sub>N<sub>10</sub>P<sub>2</sub>F<sub>12</sub>Ru: C, 40.8; H, 2.8; N, 14.9%. Found: C, 39.9; H, 2.6; N, 14.9%. *m/z* (ESIMS) 797.1 ([Ru(abpt)(bpy)<sub>2</sub>][PF<sub>6</sub>]<sup>+</sup>), 326.1 ([Ru(abpt)(bpy)<sub>2</sub>]<sup>2+</sup>). <sup>1</sup>H NMR (MeOD-*d*<sub>4</sub>): δ (ppm): 9.13 (2H, d, 7.87 Hz, 3a); 8.75 (1H, d, 4.75 Hz, 6a'); 8.68 (2H, m, 6b'); 8.61 (2H, m, 6b); 8.11 (6H, m, 4a, 3a', 5b, 5b'); 7.93 (3H, m, 4a', 3b); 7.82 (3H, m, 6a, 3b'); 7.52 (5H, m, 5a', 4b, 4b'); 7.43 (1H, t, 6.45 Hz, 5a).

### *In vitro* cytotoxicity assays

The anticancer activity of [Ru(abpt)(bpy)<sub>2</sub>](PF<sub>6</sub>)<sub>2</sub> was tested *in vitro* in several selected cell lines, following the experimental procedure described in chapter 4 of this thesis. The results can be seen in Tables 5.1 and 5.2. Preliminary results are also given for the dinuclear complex [{Ru(tpy)Cl}<sub>2</sub>(μ-paa)](BF<sub>4</sub>)<sub>2</sub>.

### 5.1.3. Results, discussion and concluding remarks

The synthesis of groove-binder homodinuclear ruthenium(II) and heterodinuclear Pt-Ru complexes has been introduced. As a possible example of the former, the ruthenium(II) compound [{Ru(tpy)Cl}<sub>2</sub>(μ-paa)](BF<sub>4</sub>)<sub>2</sub> (**1h**) was obtained. This dinuclear compound has two leaving groups, one per ruthenium atom, therefore a coordinative interaction with DNA is also possible, and even the formation of intra- and interstrand adducts might be expected.

According to the results obtained in preliminary cell tests (see Table 5.1), complex **1h** is moderately active in the L1210/2 cell line, although it displays virtually no activity in the human ovarian cancer cell lines A2780 and A2780R, in which the homodinuclear complex **1g** was shown to be active (see Table 4.3).

The ruthenium(II) complex [Ru(abpt)(bpy)<sub>2</sub>](PF<sub>6</sub>)<sub>2</sub> (**1i**) was selected as the parent compound of a family of ruthenium(II) polypyridyl complexes to be tested for anticancer activity. Substitution of the bpy groups by other chelating polypyridyl ligands, such as 2,2':6',2''-terpyridine or phenantroline, or the more π-deficient 2,2'-bipyrazine, 1,4,5,8-

tetraazaphenanthrene or 1,4,5,8,9,12-hexaazatriphenylene, would yield a group of various related ruthenium(II) complexes. The cytotoxicity of all these compounds should be tested, as well as their ways of interaction with DNA and their DNA cleavage ability. Some structure-activity relationships could be extracted from the differences in their properties and anticancer activities.

Work in these compounds has not gone yet any further than the synthesis and testing of the chosen parent compound against some selected cancer cell lines. The activity displayed by  $[\text{Ru}(\text{abpt})(\text{bpy})_2](\text{PF}_6)_2$  was disappointing in most of the cell lines (see Tables 5.1 and 5.2). Considering that this compound is structurally very different from the other compounds described in this thesis, no conclusions can be extracted by comparison of the results listed in Tables 5.1 and 5.2 with the results described in chapter 4.

Table 5.1.  $IC_{50}$  values ( $\mu\text{M}$ ) of  $[\{\text{Ru}(\text{tpy})\text{Cl}\}_2(\mu\text{-paa})](\text{BF}_4)_2$  (**1h**),  $[\text{Ru}(\text{abpt})(\text{bpy})_2](\text{PF}_6)_2$  (**1i**) and the reference compound cisplatin in some selected cell lines

Tested compound	A2780	A2780R	L1210/0	L1210/2
$[\{\text{Ru}(\text{tpy})\text{Cl}\}_2(\mu\text{-paa})](\text{BF}_4)_2$ ( <b>1h</b> )	61	> 100	36	53
$[\text{Ru}(\text{abpt})(\text{bpy})_2](\text{PF}_6)_2$ ( <b>1i</b> )	> 200	> 200	> 200	75
Cisplatin	6	25	2	24

Table 5.2.  $IC_{50}$  values ( $\mu\text{M}$ ) of  $[\text{Ru}(\text{abpt})(\text{bpy})_2](\text{PF}_6)_2$  (**1i**) and the reference compound cisplatin in some selected cell lines

Tested compound	A498	EVSA-T	H226	IGROV	M19	MCF-7	WiDR
$[\text{Ru}(\text{abpt})(\text{bpy})_2](\text{PF}_6)_2$ ( <b>1i</b> )	43	43	14	>65	44	44	27
Cisplatin	7	1	11	1	2	2	3

## **5.2. Interactions between metallo drugs and other biological molecules**

### **5.2.1. Introduction on serum proteins**

#### **Albumin**

Serum albumin is the most abundant plasma protein. It plays a key role in a number of physiological functions, such as the control of osmotic blood pressure; transport, metabolism and distribution of various compounds; radical deactivation, and delivery of amino-acids after hydrolysis for the synthesis of other proteins.<sup>37</sup>

#### **Transferrin**

The transferrins are a class of iron-binding and transporting proteins, widely distributed in the extracellular fluids of vertebrates. Most of the transferrins consist of a single polypeptide chain with a molecular weight of around 80 kDa, constituted by two remarkably similar amino acid sequences, each accounting for half of the molecule and each carrying an iron-binding site.<sup>38</sup>

Binding of iron is dependent on concomitant binding of carbonate, hydrogencarbonate or some other synergistic anion, which serves as a bridging ligand between protein and metal. The role of the bridging anion may be to prevent water from binding in the coordination sphere of the metal, locking it tightly to the protein and avoiding hydrolysis. Iron binding is strong enough to resist hydrolysis in the extracellular fluids, but still allows iron to be released within specific intracellular compartments. The metal binding site with its associated anion-binding site is a characteristic of all transferrins.<sup>38</sup>

The iron-binding cleft in the C-lobe is closed, both in the presence and in the absence of the metal. However, the cleft in the N-lobe is wide open in apotransferrin, exposing three basic side chains, which are buried within it in the iron-loaded transferrin. These side chains are Arg 121, Arg 120 and Lys 301; they may serve to attract the carbonate anion as the first step in binding.<sup>38</sup>

Transferrin receptors are present in all dividing cells, in a number varying from several tens of thousands to almost a million. This number increases when a cell is in need of iron. Transferrin receptors are continuously traveling between the surface and the interior of the cell.<sup>38</sup>

At the slightly alkaline extracellular pH of 7.4, transferrin can bind 1 or 2 ferric ions, and 2 iron-bearing transferrin molecules can bind the dimeric transferrin receptor. Iron-free transferrin is not recognized by the receptor at this pH.<sup>38</sup>

Transferrin is thought to release its iron within the cell in an endosomal compartment which has a pH of 5.5. Then the apotransferrin-transferrin receptor complex travels back to the membrane, and the apotransferrin is released again in the extracellular medium.<sup>38</sup>

### **Cytochrome *c***

Cytochrome *c* is a mitochondrial peripheral membrane protein. Its function in the respiratory chain in the inner mitochondrial membrane consists on electron transfer from cytochrome *c* reductase to cytochrome *c* oxidase.<sup>39</sup> In 1996 it has been reported that, when released into the cytosol, cytochrome *c* activates a programmed cell death cascade (apoptosis).<sup>40</sup>

### **Other proteins**

Haemoglobin is a globular tetrameric protein consisting of four subunits (two  $\alpha$ - and two  $\beta$ -polypeptide chains) bound through non-covalent interaction. Each protein subunit carries a haeme group including a Fe(II) as the central atom.<sup>37</sup> Haemoglobin is in charge of O<sub>2</sub> and CO<sub>2</sub> transport in the blood.

Ubiquitin is a small cytoplasmic protein which has two potential binding sites for cisplatin. It was chosen as a model protein to study the formation of protein-cisplatin adducts.<sup>41, 42</sup>

Another family of essential metal-transporting serum proteins are the  $\gamma$ -globulins.<sup>37</sup>

### **5.2.2. Interactions between metallodrugs and serum proteins**

Protein interactions with platinum drugs, amongst which cisplatin and carboplatin, have been studied thoroughly, using various techniques. The influence of these interactions in the distribution and pharmacokinetics of the drugs has been recognised.<sup>37, 39</sup>

### **Albumin**

Cisplatin binds preferentially to haemoglobin, followed by albumin.<sup>37</sup> The efficient binding to the latter can be explained by the high affinity of platinum to sulfur. Hence, the most likely binding point of cisplatin to albumin is the cysteine-34 residue. Cisplatin

irreversible binding leads to cleavage of albumin disulfide bonds, inducing changes in the structure of the protein, thus affecting its activity. Other platinum compounds, such as oxaliplatin (see chapter 1, section 1.3), display the same behaviour with albumin; the interaction between albumin and transplatin is reported to be not very significant.<sup>37</sup>

### **Transferrin**

In an analogous way, cisplatin binds to sulfur-containing residues of transferrin, although the exact interaction position is a subject of debate.<sup>43, 44</sup> This interaction was proven to be determinant of properties such as cytotoxicity, *in vivo* distribution of the drug and tumour-specificity.<sup>45</sup>

Certain anticancer ruthenium(III) complexes, such as indazolium *trans*-[tetrachloridobis(indazole)ruthenate(III)], KP1019, were also proven to bind to both albumin and transferrin. Particularly the interaction of KP1019 with the latter suggested the theory that this ruthenium(III) complex could act as a virtually non-toxic prodrug that enters the cell when it is bound to transferrin. This prodrug would then be activated by intracellular reduction to a ruthenium(II) complex, which would be the actual cytotoxic drug.<sup>46</sup> This mechanism would also account for a selective entrance of the drug in the tumorous cells, which express an increased number of transferrin receptors in their membranes, due to their higher iron requirements.<sup>39</sup>

A study of the ability of ruthenium(III) cytotoxic compounds to bind to transferrins was carried out in 1996.<sup>47</sup> The presence of a large water-filled cavity in the interdomain cleft of each transferrin lobe, in which the metal- and anion-binding site is found, apparently allows some flexibility in the species that can be bound, while domain closure is still possible. Cell-culture experiments have given evidence that the antitumour capacity of some ruthenium(III) complexes is enhanced by binding to transferrin,<sup>47</sup> and so the role of serum transferrin in the accumulation of ruthenium(III) complexes in tumours is suspected to be important. The ruthenium complex binds via a coordinative interaction with a histidine residue in the N-lobe of transferrin. The heterocyclic ligands remain bound to ruthenium, and this is presumably essential for antitumour activity following the release of the complex.<sup>37, 47</sup>

### **Cytochrome *c***

The results obtained with various techniques indicate that the binding of the ruthenium(III) complex KP1019 to cytochrome *c* induces conformational changes in the protein. A loss of tertiary structure is experienced, together with changes in the haeme group and an increase in the  $\alpha$ -helical content of apocytochrome *c*.<sup>48</sup> These conformational changes are expected to have an influence in the biological activity of cytochrome *c*, and subsequently, in its ability to induce cell apoptosis.

### **Other proteins**

The binding of different platinum complexes to the serum proteins haemoglobin, ubiquitin and  $\gamma$ -globulins has been widely studied and a review of these interactions is available.<sup>37</sup> On the other hand, the studies involving ruthenium(III) complexes have been mainly focused on the interactions between these drugs and transferrin or cytochrome *c*.

#### ***5.2.3. Interactions between Ru(II) polypyridyl complexes and serum transport proteins***

Some ruthenium(III) complexes are hypothesised to act as inactive prodrugs, which may get activated by reduction to ruthenium(II) once they entered the cells, *vide supra*. Serum transport proteins, such as transferrin, might be involved in this cellular uptake process. Hence the interest in studying the interactions between these proteins and the anticancer active ruthenium(III) complexes. However, while a number of ruthenium(II) complexes are known that display a considerable activity in cell tests, to the best of my knowledge no studies have been reported of the interaction between these complexes and transferrin. Therefore, a preliminary experiment was carried out to explore whether or not such interactions could occur.

Two 5  $\mu$ M solutions of  $[\text{Ru}(\text{apy})(\text{tpy})(\text{H}_2\text{O})](\text{ClO}_4)_2 \cdot 2\text{H}_2\text{O}$  in phosphate buffered saline (PBS) were prepared. Human serum transferrin (Invitrogen) was added to one of them to give a 1  $\mu$ M concentration. Both solutions were incubated for 3 hours at 37 °C. Both samples were ultrafiltered (Millipore centricon 10,000 MWCO) and the filter was washed four times with PBS. The unbound ruthenium complex should have been recovered after going through the filter in both cases. The portion that did not go through the filter should contain no ruthenium in the control experiment, and the transferrin-bound ruthenium, in the sample containing the protein. The four portions were analysed for ruthenium by inductively coupled plasma (ICP).

70% of the initial ruthenium was recovered in the portion of the control experiment that went through the membrane filter. The detected ruthenium in the portion that did not pass through the filter was negligible. From the sample that contained transferrin, the portion that went through the filter contained 34% of the initial ruthenium (unbound ruthenium), while the portion that did not go through the filter contained 35% of the initial ruthenium. This implies that after just 3 hours in PBS at 37 °C, at least 35% of the initial ruthenium was bound to transferrin.

The results obtained clearly encourage further studies of the interactions between transferrin and other ruthenium(II) polypyridyl complexes, such as those described in this thesis. Important questions still remain unanswered, such as whether this interaction has an influence in the cytotoxicity and tumour-selectivity of the compounds, or to what extent the results obtained in the performed cell tests are valid, without the involvement of serum transferrin in them.

### **5.3. Ruthenium complexes and metastasis**

The existence of ruthenium drugs which, despite showing no significant activity against the primary tumour (and no *in vitro* cytotoxicity), do yield an important activity against metastases,<sup>49, 50</sup> illustrates the importance of testing ruthenium complexes not only against cancerous cell lines, but also for antimetastatic activity.

Well-known *in vitro* methods for antimetastatic ability determination are migration and invasion assays. However, since apoptotic cells do not migrate and not all cancerous cells are invasive, cytotoxic compounds are not susceptible to these studies, nor is every type of cell lines.

The ability of a drug to diminish migration of a malignant cell from the initial tumour to another tissue can be measured in experiments involving Boyden chambers.<sup>51</sup> On the other hand, the invasion of basement membranes by tumour cells, a property which is characteristic of metastatic cells, can be studied by using Matrigel, a reconstituted membrane.<sup>52-54</sup>

In conclusion, a new testing routine is necessary for potential anticancer/antimetastatic ruthenium complexes. Not only should the interactions of these compounds with proteins be studied, which could lead to both selective apoptosis and a decrease in resistance to the drug, but also the antimetastatic ability of these drugs should

be tested. A broader knowledge of all these factors is expected to lead to a better understanding of the mechanism of action of ruthenium anticancer agents.

#### 5.4. References

1. Ang, W. H.; Dyson, P. J., *Eur. J. Inorg. Chem.* **2006**, 4003-4018.
2. Clarke, M. J., *Coord. Chem. Rev.* **2003**, *236*, 209-233.
3. Komeda, S.; Moulaei, T.; Woods, K. K.; Chikuma, M.; Farrell, N. P.; Williams, L. D., *J. Am. Chem. Soc.* **2006**, *128*, 16092-16103.
4. Hannon, M. J., *Chem. Soc. Rev.* **2007**, *36*, 280-295.
5. Lerman, L. S., *J. Mol. Biol.* **1961**, *3*, 18-30.
6. Long, E. C.; Barton, J. K., *Accounts Chem. Res.* **1990**, *23*, 271-273.
7. Jennette, K. W.; Lippard, S. J.; Vassiliades, G. A.; Bauer, W. R., *Proc. Natl. Acad. Sci. U. S. A.* **1974**, *71*, 3839-3843.
8. Howe-Grant, M.; Wu, K. C.; Bauer, W. R.; Lippard, S. J., *Biochemistry* **1976**, *15*, 4339-4346.
9. Howe-Grant, M.; Lippard, S. J., *Biochemistry* **1979**, *18*, 5762-5769.
10. Erkkila, K. E.; Odom, D. T.; Barton, J. K., *Chem. Rev.* **1999**, *99*, 2777-2795.
11. Kielkopf, C. L.; Erkkila, K. E.; Hudson, B. P.; Barton, J. K.; Rees, D. C., *Nat. Struct. Biol.* **2000**, *7*, 117-121.
12. Friedman, A. E.; Chambron, J. C.; Sauvage, J. P.; Turro, N. J.; Barton, J. K., *J. Am. Chem. Soc.* **1990**, *112*, 4960-4962.
13. Morgan, R. J.; Chatterjee, S.; Baker, A. D.; Streckas, T. C., *Inorg. Chem.* **1991**, *30*, 2687-2692.
14. Friedman, A. E.; Kumar, C. V.; Turro, N. J.; Barton, J. K., *Nucleic Acids Res.* **1991**, *19*, 2595-2602.
15. Hartshorn, R. M.; Barton, J. K., *J. Am. Chem. Soc.* **1992**, *114*, 5919-5925.
16. Gao, F.; Chao, H.; Zhou, F.; Yuan, Y. X.; Peng, B.; Ji, L. N., *J. Inorg. Biochem.* **2006**, *100*, 1487-1494.
17. Gao, F.; Chao, H.; Zhou, F.; Xu, L. C.; Zheng, K. C.; Ji, L. N., *Helv. Chim. Acta* **2007**, *90*, 36-51.
18. Wilhelmsson, L. M.; Westerlund, F.; Lincoln, P.; Nordén, B., *J. Am. Chem. Soc.* **2002**, *124*, 12092-12093.
19. Rehmman, J. P.; Barton, J. K., *Biochemistry* **1990**, *29*, 1701-1709.
20. Satyanarayana, S.; Dabrowiak, J. C.; Chaires, J. B., *Biochemistry* **1992**, *31*, 9319-9324.
21. Eriksson, M.; Leijon, M.; Hiort, C.; Nordén, B.; Gräslund, A., *Biochemistry* **1994**, *33*, 5031-5040.
22. Kumar, C. V.; Barton, J. K.; Turro, N. J., *J. Am. Chem. Soc.* **1985**, *107*, 5518-5523.
23. Barton, J. K.; Goldberg, J. M.; Kumar, C. V.; Turro, N. J., *J. Am. Chem. Soc.* **1986**, *108*, 2081-2088.
24. Armitage, B., *Chem. Rev.* **1998**, *98*, 1171-1200.
25. Lentzen, O.; Moucheron, C.; Kirsch-De Mesmaeker, A., *Metallotherapeutic drugs & metal-based diagnostic agents*. West Sussex, **2005**; p 359-378.
26. Mongelli, M. T.; Heinecke, J.; Mayfield, S.; Okyere, B.; Winkel, B. S. J.; Brewer, K. J., *J. Inorg. Biochem.* **2006**, *100*, 1983-1987.
27. Elias, B.; Kirsch-De Mesmaeker, A., *Coord. Chem. Rev.* **2006**, *250*, 1627-1641.
28. Hage, R.; Dijkhuis, A. H. J.; Haasnoot, J. G.; Prins, R.; Reedijk, J.; Buchanan, B. E.; Vos, J. G., *Inorg. Chem.* **1988**, *27*, 2185-2189.

29. Barigelletti, F.; De Cola, L.; Balzani, V.; Hage, R.; Haasnoot, J. G.; Reedijk, J.; Vos, J. G., *Inorg. Chem.* **1989**, *28*, 4344-4350.
30. Hughes, H. P.; Martin, D.; Bell, S.; McGarvey, J. J.; Vos, J. G., *Inorg. Chem.* **1993**, *32*, 4402-4408.
31. D'Alessandro, D. M.; Dinolfo, P. H.; Hupp, J. T.; Junk, P. C.; Keene, F. R., *Eur. J. Inorg. Chem.* **2006**, 772-783.
32. Giuffrida, G.; Ricevuto, V.; Guglielmo, G.; Campagna, S.; Ciano, M., *Inorg. Chim. Acta* **1992**, *194*, 23-29.
33. Stratton, W. J.; Busch, D. H., *J. Am. Chem. Soc.* **1958**, *80*, 1286-1289.
34. Geldard, J. F.; Lions, F., *J. Org. Chem.* **1965**, *30*, 318-319.
35. Sullivan, B. P.; Salmon, D. J.; Meyer, T. J., *Inorg. Chem.* **1978**, *17*, 3334-3341.
36. Adcock, P. A.; Keene, F. R.; Smythe, R. S.; Snow, M. R., *Inorg. Chem.* **1984**, *23*, 2336-2343.
37. Timerbaev, A. R.; Hartinger, C. G.; Aleksenko, S. S.; Keppler, B. K., *Chem. Rev.* **2006**, *106*, 2224-2248.
38. Crichton, R. R., *Inorganic Biochemistry of Iron Metabolism*. Chichester, **1991**; p 90-130.
39. Kostova, I., *Curr. Med. Chem.* **2006**, *13*, 1085-1107.
40. Cai, J. Y.; Yang, J.; Jones, D. P., *Biochim. Biophys. Acta-Bioenerg.* **1998**, *1366*, 139-149.
41. Peleg-Shulman, T.; Gibson, D., *J. Am. Chem. Soc.* **2001**, *123*, 3171-3172.
42. Peleg-Shulman, T.; Najajreh, Y.; Gibson, D., *J. Inorg. Biochem.* **2002**, *91*, 306-311.
43. Cox, M. C.; Barnham, K. J.; Frenkiel, T. A.; Hoeschele, J. D.; Mason, A. B.; He, Q. Y.; Woodworth, R. C.; Sadler, P. J., *J. Biol. Inorg. Chem.* **1999**, *4*, 621-631.
44. Khalaila, I.; Allardyce, C. S.; Verma, C. S.; Dyson, P. J., *Chembiochem* **2005**, *6*, 1788-1795.
45. Hoshino, T.; Misaki, M.; Yamamoto, M.; Shimizu, H.; Ogawa, Y.; Toguchi, H., *J. Control. Release* **1995**, *37*, 75-81.
46. Clarke, M. J.; Zhu, F.; Frasca, D. R., *Chem. Rev.* **1999**, *99*, 2511-2533.
47. Smith, C. A.; Sutherland-Smith, A. J.; Keppler, B. K.; Kratz, F.; Baker, E. N., *J. Biol. Inorg. Chem.* **1996**, *1*, 424-431.
48. Trynda-Lemiesz, L., *Acta Biochim. Pol.* **2004**, *51*, 199-205.
49. Sava, G.; Pacor, S.; Bergamo, A.; Cocchietto, M.; Mestroni, G.; Alessio, E., *Chem.-Biol. Interact.* **1995**, *95*, 109-126.
50. Alessio, E.; Mestroni, G.; Bergamo, A.; Sava, G., *Curr. Top. Med. Chem.* **2004**, *4*, 1525-1535.
51. Karp, J. M.; Tanaka, T. S.; Zohar, R.; Sodek, J.; Shoichet, M. S.; Davies, J. E.; Stanford, W. L., *Bone* **2005**, *37*, 337-348.
52. Zorzet, S.; Bergamo, A.; Cocchietto, M.; Sorc, A.; Gava, B.; Alessio, E.; Iengo, E.; Sava, G., *J. Pharm. & Exp. Therapeutics* **2000**, *295*, 927-933.
53. Sherwood, D. R., *Trends Cell Biol.* **2006**, *16*, 250-256.
54. Sava, G.; Frausin, F.; Cocchietto, M.; Vita, F.; Podda, E.; Spessotto, P.; Furlani, A.; Scarcia, V.; Zabucchi, G., *Eur. J. Cancer* **2004**, *40*, 1383-1396.

## 6. Summary, general evaluation and future developments

The contents that can be found in each chapter of this thesis are briefly exposed. Some conclusions are extracted from the results obtained during the course of this research. Proposals are presented for further work in this line of investigation.

### 6.1. Introduction

Several ruthenium(II) polypyridyl complexes were synthesised, with two main purposes: finding new potential anticancer metallodrugs and getting some insight in their mechanism of action. The obtained results are presented in this thesis. This last chapter gives a brief overview of all the herein described work, and it provides a number of suggestions for further research.

### 6.2. Summary

It is not possible to understand the role of ruthenium in the field of anticancer metallodrugs without a previous reference to platinum chemistry. With this in mind, a brief historical introduction to cisplatin is given in [Chapter 1](#), followed by an explanation of its mechanism of action and the development of second and third generation platinum anticancer agents. Ruthenium chemistry is presented as a possible alternative to platinum therapy. A classification of ruthenium compounds with proven anticancer activity is provided, and their possible mechanisms of action are discussed, providing examples from relevant literature.

In [Chapter 2](#), the synthesis and characterisation of three carefully-chosen, closely-related ruthenium(II) polypyridyl complexes is described. The structural information deduced from NMR spectroscopy supports the results obtained from the elucidation of the crystal structures. The distinct 3D packing of each of the three complexes is interesting to mention, as well as the formation of a hydrogen-bond net in one of the cases.

The reasons for the choice of these three ruthenium complexes are further detailed in [Chapters 3 and 4](#), in which a kinetic study is described of the reactions between each of these complexes and the DNA model base 9-ethylguanine. A parallel study of the cytotoxicity of each complex sheds some light on the importance of the leaving group and the kinetics, *vide infra*. Moreover, NMR spectroscopy was proven to be a valuable tool in the study of some interesting temperature-dependant conformational changes in the formed ruthenium-DNA model-base adduct, while CD and LD were the techniques of choice for the study of conformational changes provoked by the tested ruthenium compounds in the DNA molecule.

A look beyond any possible coordinative interactions between the metal atom and the DNA nucleic bases has resulted in [Chapter 5](#), in which other alternative interaction modes are dealt with. The synthesis and characterisation of a possible intercalator and a possible

groove-binder are described, as well as some cell tests. Further work needs to be done in order to establish the mechanism of action of these novel compounds.

Also in Chapter 5, the study of the interaction between potential ruthenium(II) anticancer agents and some selected serum transport proteins, such as transferrin, is discussed. Finally, a reminder is made of the fact that some ruthenium complexes that were proven to be inactive against primary tumours, showed nevertheless an important antimetastatic activity.

The Appendix to this thesis deals with the formation of a planar hydrogen-bonded network of nucleic bases and formate residues in parallel sheets, which are of great theoretical importance and may have applications in nanotechnology.

### **6.3. Conclusions and future perspectives**

Two cytotoxic compounds were considered,  $\text{Ru}(\text{tpy})\text{Cl}_3$  and  $\alpha\text{-}[\text{Ru}(\text{azpy})_2\text{Cl}_2]$ , with an activity that seems to be due to the formation of intra- and/or interstrand cross-links,<sup>1</sup> in the same way cisplatin does. In this thesis, the design of a complex of formula  $[\text{Ru}(\text{apy})(\text{tpy})\text{L}]^{(2-n)+}$  (L = leaving group) is described, which was based on the first two, but with an improved water-solubility.<sup>2</sup> However, this new complex is monofunctional; therefore it can only bind to one nucleic base. The new complex was proven to display a moderate and, in some cases, even a high activity against a number of cell lines.<sup>3</sup> Studies were carried out to elucidate its mechanism of action. First, the kinetic factor was taken into account. For that purpose, three variants of the same complex were obtained: those in which the leaving group was a chloro, an aqua residue and an acetonitrile, respectively. All three complexes were capable of binding the DNA model base 9-EtGua in the experimental conditions, although following different kinetics in each case.<sup>4</sup> The differences in the kinetics could not be correlated to the small differences in cytotoxicity.<sup>3</sup> These results seem to suggest that it does not matter how fast these molecules can bind to DNA.

The cytotoxicity of an analogous dinuclear complex with no ability to coordinatively bind to DNA was tested.<sup>3</sup> From the positive results obtained it can be concluded that coordination to DNA is not essential for cytotoxic activity, and it might be that the mechanism of these complexes does not involve DNA at all.<sup>3</sup>

In order to test this last theory, experiments with calf-thymus DNA were carried out. The results from the circular and linear dichroism show an extensive interaction of the dinuclear complex with the DNA molecule, which is clearly different from the way the

mononuclear complex interacted with the nucleic acid.<sup>3</sup> Therefore from these results an interaction with DNA cannot be ruled out as a key step in anticancer activity of this kind of ruthenium compounds.

Finally, two other ruthenium(II) complexes with heterocyclic ligands were studied in search for structure-activity relationships. According to these studies, the azo function might be essential for activity.<sup>3</sup>

To summarize, neither all compounds capable of DNA-coordination are anticancer-active, nor all ruthenium cytotoxic compounds can coordinate to DNA. This observation underlines the importance of alternative ways of DNA recognition. Several strategies for further research in this direction are suggested in this thesis, including some examples of possible candidate compounds (Chapter 5, section 5.1.1).

A better understanding of the mechanisms of action is crucial for the development of new ruthenium drugs. The study of the interactions between a potential metallodrug and DNA is of utmost importance, as well as the interactions between ruthenium complexes and serum transport proteins.<sup>5</sup>

Simultaneously, an effort should be made to improve and standardize the tests used to screen a metallodrug for anticancer activity, including tests of drug uptake and of antimetastatic activity.

#### 6.4. References

1. Clarke, M. J., *Coord. Chem. Rev.* **2003**, *236*, 209-233.
2. Corral, E.; Hotze, A. C. G.; Tooke, D. M.; Spek, A. L.; Reedijk, J., *Inorg. Chim. Acta* **2006**, *359*, 830-838.
3. Corral, E.; Hotze, A. C. G.; den Dulk, H.; Hannon, M. J.; Reedijk, J., **2007**, *to be submitted for publication in J. Biol. Inorg. Chem.*
4. Corral, E.; Hotze, A. C. G.; Magistrato, A.; Reedijk, J., *Inorg. Chem.* **2007**, *46*, 6715-6722.
5. Kostova, I., *Curr. Med. Chem.* **2006**, *13*, 1085-1107.

## Appendix. Nucleic acids in two dimensions: layers of base pairs linked by carboxylate<sup>\*</sup>

The formation of a planar 2D hydrogen-bonded network between DNA bases and formate residues is reported, leading to unprecedented parallel sheets of DNA analogues.

---

<sup>\*</sup> This appendix is based on Corral, E.; Kooijman, H.; Spek, A.L.; Reedijk, J., *New J. Chem.*, **2007**, *31*, 21-24.

### **A.1. Introduction**

Nucleic acids, such as DNA, RNA and their fragments, occur naturally in three-dimensional chain-based structures derived from the double chain structure first described by Watson and Crick in 1953.<sup>1</sup> The principal forces holding this spatial organization together are the Watson-Crick base pairing and the stacking between the bases; the chains are built of sugar-phosphate links. Several deviations of these structures are known to occur naturally. These abnormalities are the subject of intense studies and in some cases they are provoked in search for therapeutic applications.<sup>2-5</sup> Bends and kinks usually arise as a consequence of the presence of special sequences or mismatching, for instance in some RNA's.<sup>6-8</sup> Triple-helix chains are also known,<sup>2, 4</sup> as well as some quadruplex structures,<sup>3, 9-12</sup> knots and features such as hammerhead and other junctions.<sup>5</sup> In all cases the 1D organisation is one of the factors that determine the structure.

Much work has been done to create new artificial base-association ways. Different approaches, such as metal-assisted hydrogen-bonding<sup>13, 14</sup> and incorporation of artificial bases into DNA,<sup>15, 16</sup> have been used to develop new DNA base pairs or duplexes, many of which can be enzymatically replicated in search for possible new biological applications.<sup>17</sup>

More recently research has been reported on the synthesis of ion channels that consist of self-assembled supramolecular rosettes. These rosettes contain nucleic acids and other DNA-based artificial nucleosides, which associate with each other in unusual ways. The rosettes pile up due to  $\pi$ -stacking.<sup>18-20</sup>

Following these lines of investigation also some supramolecular helical,<sup>21</sup> linear,<sup>22</sup> and macrocyclic structures<sup>23-25</sup> have been obtained.

So far, a complete 2D organized flat structure of nucleic acid bases has never been achieved by self-assembly of the nucleobases in solution, and it has been questioned whether such a flat structure, with only hydrogen bonding within the plane, would be possible. In fact, when having a close look at the common nucleic acid bases it is not difficult to imagine that such structures should be possible, either with neutral bases or with cationic or anionic bases in combination with small cations or flat anions, respectively.

### **A.2. Results and discussion**

To explore this possibility in detail a simple DNA model base that resembles a nucleotide and that has been used in many model systems, namely 9-ethylguanine,<sup>26-28</sup> was selected in combination with the smallest bifunctional flat anion, i.e. formate. Simple

modelling shows that in this case all strong H-bond donors and H-bond acceptors would match, originating a H-bond net. Indeed when the 9-ethylguanine (eg, previously abbreviated in this thesis as 9-EtGua) was crystallised from a formic acid solution at a proper concentration at RT, crystals of (H7eg)(HCOO) could be isolated, where the guanine moiety is protonated in position 7 (see Fig.A.1).

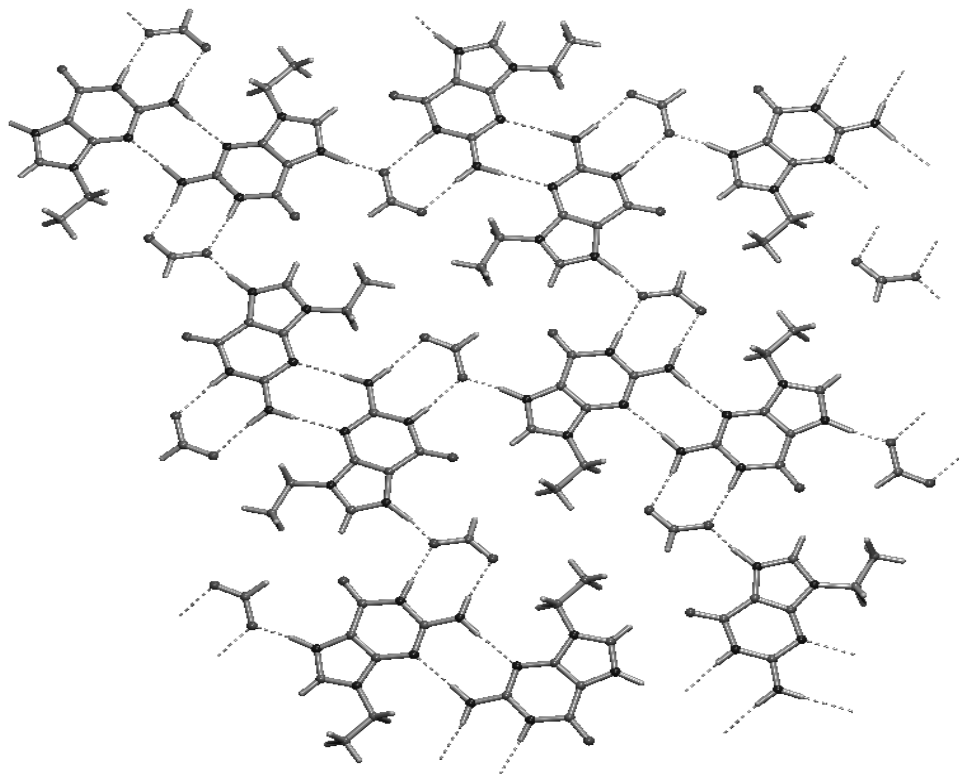


Fig.A.1. PLATON projection of (H7eg)(HCOO) showing the hydrogen bonding.

The asymmetric unit contains two (H7eg)(HCOO) ion pairs. The packing environment of these pairs is virtually identical. The formate anion plays an indispensable role in the formation of a hydrogen-bond net (see Table A.1 and Fig.A.2) in which the 9-Ethylguaninium residues are associated to each other by the unusual 12-Trans Sugar Edge/Sugar Edge interactions, as described in the Leontis/Westhof classification.<sup>29, 30</sup> These base pairs belong to the so-called class IV from the Saenger classification,<sup>31</sup> which a more recent designation classifies as GG N3-amino, symmetric.<sup>32</sup> To the best of our knowledge only one example is known of an organism containing this kind of base-pairing in a cellular organelle: the *Haloarcula marismortui* ribosome, in its pairs G315:G336 and G2428:G2466.<sup>33</sup> This base-pair association has never before been achieved artificially

without a simultaneous inclusion of metal atoms in the structure, such as gold or cadmium,<sup>34</sup> or the blockage of the N7 of the purine ring with a metal atom or a methyl group.<sup>13, 35</sup>

Table A.1. Selected distances (Å) and angles (°) in the crystal structure of (H7eg)(HCOO). Only data for one of the independent ion pairs is given. The atom numbering is indicated in Fig.A.2.

Interatomic distances		Angles (°)	
Donor-H...Acceptor	D..A (Å)		
N(24)-H(24)...O(31 <sub>II</sub> )	2.545(3)	N(21)-C(21)-N(22)	117.0(2)
N(21)-H(21)...O(41 <sub>I</sub> )	2.776(3)	N(22)-C(21)-N(23)	119.4(2)
N(22)-H(22A)...O(42 <sub>I</sub> )	2.883(3)	O(41 <sub>I</sub> )-N(21)-C(21)	116.09(16)
N(22)-H(22B)...N(23 <sub>III</sub> )	3.026(3)	N(22)-O(42 <sub>I</sub> )-C(41 <sub>I</sub> )	112.04(17)
		O(42 <sub>I</sub> )-N(22)-H(22B)	115.5 (2)

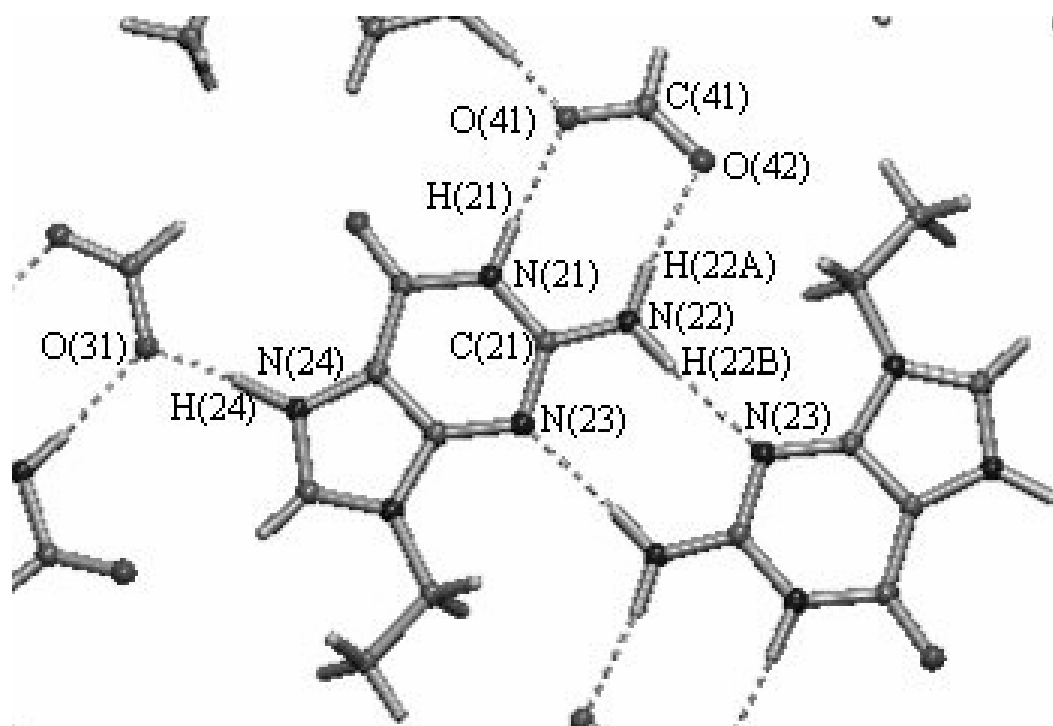
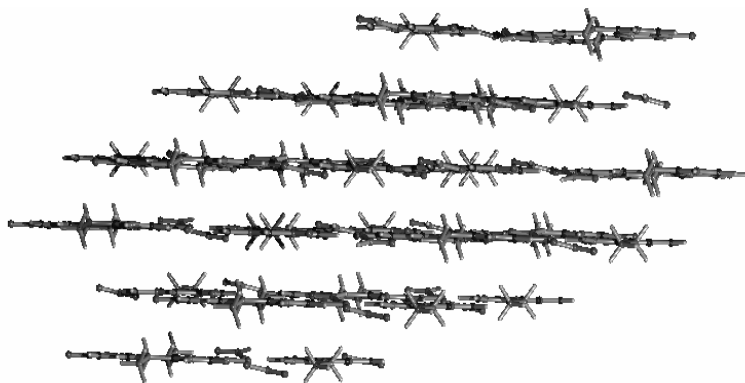


Fig.A.2. Detail of Fig.A.1, with numbering of major atoms. The Roman subscripts are the same as in Table A.1.

The nucleoside-formate sheets herein described were found to allow a very close base-pair stacking, with a distance between parallel layers of only 3.288(1) Å (see Fig.A.3) (the distance between base-pair planes in B-DNA is 3.46 Å).



*Fig.A.3. Packing of (H7eg)(HCOO), forming parallel layers.*

The structure described in this appendix is not the only possible example of 2D nucleoside packing that can be thought of. Current work is focusing on such systems, by changing both the nucleic acid bases and the counter ions. Formate has proven to be a valid example of a counter ion that, due to its simplicity as much as to its planar geometry, could help to build these systems. Although in principle nitrate could also be thought suitable to yield a planar crystal structure, it does not have a hydrophobic part in the proximity of the ethyl group, and cannot form such a lattice. The formate hydrogen, however, fits perfectly in the “gap” existing between the 2 ethyl groups of the neighbouring guanine moieties, while the corresponding nitrate oxygen atom would provoke repulsion forces that would distort the 2D structure.

The self-organisation of organic molecules into non-covalently bonded nanostructures, such as flat solid surfaces, gives structures with a high degree of order, thereby opening a wide range of applications, for example, in electronic and optical devices,<sup>36</sup> in corrosion inhibition<sup>37</sup> and in supramolecular chemistry.<sup>38</sup> In molecular electronics, gold nanoparticles are embedded in ultrathin organic films, which could be used to interconnect gold nanoelectrodes in a molecular-scale electronic device, as suggested by Samorí and co-workers.<sup>39</sup>

The possible uses of these nucleoside layers in nanotechnology are barely starting to emerge,<sup>40</sup> and much research is currently being done in fields such as DNA computation. DNA biosensors could be made by taking advantage of the specificity in the binding of the base pairs.<sup>41, 42</sup>

Ribbon-like architectures have been described, which were formed by self-assembly of guanosines in solution and in the solid state.<sup>43-45</sup> Different applications of these ribbon structures in fields such as surface chemistry and photochemistry are being studied.<sup>46-49</sup> The exploitation of DNA fragments and their mutual hydrogen bonding interactions for material purposes was extensively reviewed by Seeman.<sup>50</sup>

From a theoretical point of view, this kind of structures is of interest in the study of the emergence of life.<sup>51</sup> It has been suggested that purine and pyrimidine monolayers could be candidates for a stationary phase in organic molecule separation systems and as templates for the assembly of higher ordered polymers at the prebiotic solid-liquid interface.<sup>52, 53</sup>

In conclusion, a new type of arrangement of DNA-base hydrogen bonding in layers is reported, which provides insights in novel templates for nanotechnology based in 2D structures of nucleosides linked by a very simple carboxylate-containing molecule.

### ***A.3. Experimental***

#### **Materials and reagents**

9-ethylguanine was purchased from Sigma and used as supplied. All other chemicals and solvents were reagent grade commercial materials and used as received, without further purification.

#### **Physical measurements**

C, H and N determinations were performed on a Perkin Elmer 2400 Series II analyzer. NMR spectra were recorded on a Bruker DPX-300 spectrometer operating at a frequency of 300 MHz. Chemical shifts were calibrated against tetramethylsilane (TMS).

#### **Experimental procedure**

A 0.014 M solution of 9-ethylguanine in formic acid-benzyl alcohol (1:1) was prepared. A white crystalline solid appeared. The crystals obtained were found to be suitable for X-ray diffraction measurements. The product was collected by filtration,

washed with little ice-cold water and dried in vacuo over silica. *Anal. Calc.* for  $C_7H_{10}N_5O \cdot CHO_2$ : C, 42.7; H, 4.9; N, 31.1%. Found: C, 42.4; H, 5.0; N, 30.8%.  $^1H$  NMR (DMSO- $d_6$ ):  $\delta$  (ppm): 10.46 (1H, s, NH), 8.12 (1H, s, HCOO), 7.67 (1H, s, C(8)H), 6.37 (2H, s,  $NH_2$ ), 3.94 (2H, dd, 7.3 Hz, 14.5 Hz,  $CH_2$ ), 1.31 (3H, t, 7.3 Hz,  $CH_3$ ).

### X-ray structural determination

*Crystal data:*  $C_7H_{10}N_5O \cdot CHO_2$ ,  $M = 225.22$ , triclinic, space group P-1 (No. 2) with  $a = 7.4575(12)$ ,  $b = 11.6882(12)$ ,  $c = 12.8664(15)$  Å,  $\alpha = 114.651(10)$ ,  $\beta = 94.767(11)$ ,  $\gamma = 101.729(10)^\circ$ ,  $V = 980.1(2)$  Å<sup>3</sup>,  $Z = 4$ ,  $D_c = 1.5263(3)$  g cm<sup>-3</sup>,  $\mu(\text{Mo K}\alpha) = 0.120$  mm<sup>-1</sup>,  $T = 150$  K, 23598 reflections measured, 3550 independent,  $R_{\text{int}} = 0.1231$  (before detwinning),  $R_\sigma = 0.0559$ . The measured crystal was a twin, with a two-fold rotation around the  $b + c$  direction as twin operation. Data were detwinned using PLATON.<sup>54</sup> Refinement of 356 parameters converged at a final  $wR2$  value of 0.1540 (all data),  $R1 = 0.0515$  (for 2847 reflections with  $I > 2\sigma(I)$ ),  $S = 1.085$ ,  $-0.29 < \Delta\rho < 0.27$  e Å<sup>-3</sup>. Crystallographic data (excluding structure factors) for the structure reported in this appendix have been deposited at the Cambridge Crystallographic Data Centre as number CCDC 612070.

### A.4. References

1. Watson, J. D.; Crick, F. H. C., *Nature* **1953**, *171*, 737-738.
2. Sun, J. S.; Carestier, T.; Hélène, C., *Curr. Opin. Struct. Biol.* **1996**, *6*, 327-333.
3. Keniry, M. A., *Biopolymers* **2001**, *56*, 123-146.
4. Guntaka, R. V.; Varma, B. R.; Weber, K. T., *Int. J. Biochem. Cell Biol.* **2003**, *35*, 22-31.
5. Citti, L.; Rainaldi, G., *Curr. Gene Ther.* **2005**, *5*, 11-24.
6. Klein, D. J.; Schmeing, T. M.; Moore, P. B.; Steitz, T. A., *Embo J.* **2001**, *20*, 4214-4221.
7. Duarte, C. M.; Wadley, L. M.; Pyle, A. M., *Nucleic Acids Res.* **2003**, *31*, 4755-4761.
8. Wadley, L. M.; Pyle, A. M., *Nucleic Acids Res.* **2004**, *32*, 6650-6659.
9. Sen, D.; Gilbert, W., *Nature* **1988**, *334*, 364-366.
10. Sundquist, W. I.; Klug, A., *Nature* **1989**, *342*, 825-829.
11. Blackburn, E. H., *Cell* **1994**, *77*, 621-623.
12. Rhodes, D.; Giraldo, R., *Curr. Opin. Struct. Biol.* **1995**, *5*, 311-322.
13. Sigel, R. K. O.; Freisinger, E.; Metzger, S.; Lippert, B., *J. Am. Chem. Soc.* **1998**, *120*, 12000-12007.
14. Schimanski, A.; Freisinger, E.; Erxleben, A.; Lippert, B., *Inorg. Chim. Acta* **1998**, *283*, 223-232.
15. Piccirilli, J. A.; Krauch, T.; Moroney, S. E.; Benner, S. A., *Nature* **1990**, *343*, 33-37.
16. Kool, E. T., *Accounts Chem. Res.* **2002**, *35*, 936-943.
17. Switzer, C. Y.; Moroney, S. E.; Benner, S. A., *Biochemistry* **1993**, *32*, 10489-10496.

18. Rakotondradany, F.; Palmer, A.; Toader, V.; Chen, B. Z.; Whitehead, M. A.; Sleiman, H. F., *Chem. Commun.* **2005**, 5441-5443.
19. Sakai, N.; Kamikawa, Y.; Nishii, M.; Matsuoka, T.; Kato, T.; Matile, S., *J. Am. Chem. Soc.* **2006**, *128*, 2218-2219.
20. Kaucher, M. S.; Harrell, W. A.; Davis, J. T., *J. Am. Chem. Soc.* **2006**, *128*, 38-39.
21. Giorgi, T.; Lena, S.; Mariani, P.; Cremonini, M. A.; Masiero, S.; Pieraccini, S.; Rabe, J. P.; Samori, P.; Spada, G. P.; Gottarelli, G., *J. Am. Chem. Soc.* **2003**, *125*, 14741-14749.
22. Mezzina, E.; Mariani, P.; Itri, R.; Masiero, S.; Pieraccini, S.; Spada, G. P.; Spinozzi, F.; Davis, J. T.; Gottarelli, G., *Chem.-Eur. J.* **2001**, *7*, 388-395.
23. Sessler, J. L.; Sathiosatham, M.; Doerr, K.; Lynch, V.; Abboud, K. A., *Angew. Chem.-Int. Edit.* **2000**, *39*, 1300-1303.
24. Sessler, J. L.; Jayawickramarajah, J.; Sathiosatham, M.; Sherman, C. L.; Brodbelt, J. S., *Org. Lett.* **2003**, *5*, 2627-2630.
25. Davis, J. T., *Angew. Chem.-Int. Edit.* **2004**, *43*, 668-698.
26. Grover, N.; Welch, T. W.; Fairley, T. A.; Cory, M.; Thorp, H. H., *Inorg. Chem.* **1994**, *33*, 3544-3548.
27. van Vliet, P. M.; Haasnoot, J. G.; Reedijk, J., *Inorg. Chem.* **1994**, *33*, 1934-1939.
28. van der Schilden, K.; García, F.; Kooijman, H.; Spek, A. L.; Haasnoot, J. G.; Reedijk, J., *Angew. Chem.-Int. Edit.* **2004**, *43*, 5668-5670.
29. Leontis, N. B.; Westhof, E., *RNA-Publ. RNA Soc.* **2001**, *7*, 499-512.
30. Leontis, N. B.; Stombaugh, J.; Westhof, E., *Nucleic Acids Res.* **2002**, *30*, 3497-3531.
31. Saenger, W., Principles of Nucleic Acid Structure. ed. Springer-Verlag New York Inc., New York, **1984**; p 120.
32. Nagaswamy, U.; Voss, N.; Zhang, Z. D.; Fox, G. E., *Nucleic Acids Res.* **2000**, *28*, 375-376.
33. Ban, N.; Nissen, P.; Hansen, J.; Moore, P. B.; Steitz, T. A., *Science* **2000**, *289*, 905-920.
34. Amo-Ochoa, P.; Rodríguez-Tapiador, M. I.; Alexandre, S. S.; Pastor, C.; Zamora, F., *J. Inorg. Biochem.* **2005**, *99*, 1540-1547.
35. Sigel, R. K. O.; Freisinger, E.; Abbate, M.; Lippert, B., *Inorg. Chim. Acta* **2002**, *339*, 355-365.
36. Swalen, J. D.; Allara, D. L.; Andrade, J. D.; Chandross, E. A.; Garoff, S.; Israelachvili, J.; McCarthy, T. J.; Murray, R.; Pease, R. F.; Rabolt, J. F.; Wynne, K. J.; Yu, H., *Langmuir* **1987**, *3*, 932-950.
37. Kowalik, T.; Adler, H. J. P.; Plagge, A.; Stratmann, M., *Macromol. Chem. Phys.* **2000**, *201*, 2064-2069.
38. Russell, V. A.; Ward, M. D., *Chem. Mat.* **1996**, *8*, 1654-1666.
39. Samorí, P.; Francke, V.; Müllen, K.; Rabe, J. P., *Chem.-Eur. J.* **1999**, *5*, 2312-2317.
40. Yan, H., *Science* **2004**, *306*, 2048-2049.
41. Wang, S. G.; Wang, R.; Sellin, P. J.; Zhang, Q., *Biochem. Biophys. Res. Commun.* **2004**, *325*, 1433-1437.
42. Ferancová, A.; Ovádeková, R.; Vanícková, M.; Satka, A.; Víglašký, R.; Zima, J.; Barek, J.; Labuda, J., *Electroanalysis* **2006**, *18*, 163-168.
43. Gottarelli, G.; Masiero, S.; Mezzina, E.; Pieraccini, S.; Rabe, J. P.; Samorí, P.; Spada, G. P., *Chem.-Eur. J.* **2000**, *6*, 3242-3248.
44. Araki, K.; Takasawa, R.; Yoshikawa, I., *Chem. Commun.* **2001**, 1826-1827.
45. Giorgi, T.; Grepioni, F.; Manet, I.; Mariani, P.; Masiero, S.; Mezzina, E.; Pieraccini, S.; Saturni, L.; Spada, G. P.; Gottarelli, G., *Chem.-Eur. J.* **2002**, *8*, 2143-2152.

46. Gottarelli, G.; Masiero, S.; Mezzina, E.; Pieraccini, S.; Spada, G. P.; Mariani, P., *Liq. Cryst.* **1999**, *26*, 965-971.
47. Rinaldi, R.; Branca, E.; Cingolani, R.; Masiero, S.; Spada, G. P.; Gottarelli, G., *Appl. Phys. Lett.* **2001**, *78*, 3541-3543.
48. Kato, T., *Science* **2002**, *295*, 2414-2418.
49. Maruccio, G.; Visconti, P.; Arima, V.; D'Amico, S.; Biasco, A.; D'Amone, E.; Cingolani, R.; Rinaldi, R.; Masiero, S.; Giorgi, T.; Gottarelli, G., *Nano Letters* **2003**, *3*, 479-483.
50. Seeman, N. C., *Nature* **2003**, *421*, 427-431.
51. Sowerby, S. J.; Edelwirth, M.; Heckl, W. M., *J. Phys. Chem. B* **1998**, *102*, 5914-5922.
52. Sowerby, S. J.; Heckl, W. M.; Petersen, G. B., *J. Mol. Evol.* **1996**, *43*, 419-424.
53. Sowerby, S. J.; Heckl, W. M., *Orig. Life Evol. Biosph.* **1998**, *28*, 283-310.
54. Spek, A. L., *J. Appl. Crystallogr.* **2003**, *36*, 7-13.



# Samenvatting

“Ruthenium-polypyridylcomplexen met activiteit tegen kanker. Synthese, karakterisatie en mechanisme studies op zoek naar structuur-activiteitsrelaties”.

Het perfecte medicijn tegen kanker bestaat uit een verbinding die kankercellen doodt zonder schade aan de gezonde weefsels te veroorzaken. In dit onderzoek wordt de zoektocht naar dat ideale geneesmiddel, op rutheniumverbindingen gebaseerd, voortgezet.

Hoofdstuk 1 is een inleiding over de rol van metalen in geneeskunde. Het initiële succes van cisplatina in het bestrijden van kanker werd het beginpunt van een aantal studies. Het mechanisme van deze verbinding werd onderzocht. Cisplatina bindt aan DNA en veroorzaakt een structuurverstoring van dat molecuul (Fig.1.3). De tumorcel kan niet meer delen en sterft. Gezonde cellen kunnen deze schade beter repareren en dus meestal overleven zij.

Cisplatina-chemotherapie is niet volmaakt. Ten eerste is niet iedere type kanker gevoelig voor cisplatina. Sommige gevoelige types kunnen zelf na verloop van tijd een resistentie ontwikkelen. Bovendien heeft cisplatina een aantal bijverschijnselen, onder andere nierschade en schade aan het zenuwstelsel.

Verbeterde verbindingen zijn dus nodig. De meest succesvolle gevallen zijn in Hoofdstuk 1 beschreven. Ten eerste wordt een lijst platinaverbindingen besproken. Daarna is ruthenium ook in overweging genomen. Ruthenium is een metaal dat in dezelfde familie hoort als platina. Zijn octaëdrische structuur, in tegenstelling tot de vlakvierkante geometrie van de meeste platinaverbindingen, kan een voordeel zijn in de ontwikkeling van kankermedicijnen.

Mijn werk is gebaseerd op succesvolle structuren zoals die van Fig.1.14 en Fig.1.15. In Hoofdstuk 2 wordt besproken hoe een ruthenium-polypyridylverbinding werd ontworpen, die geïnspireerd werd door de structuren van Fig.1.14 en Fig.1.15. Drie variaties van de verbinding werden ontwikkeld, die worden **1a**, **1b** en **1c** genoemd. De synthese en karakterisatie door middel van NMR en röntgendiffractie van **1a-c** worden in Hoofdstuk 2 beschreven.

Hoofdstuk 3 gaat over een theoretische studie. Het is zeer belangrijk om het mechanisme van deze verbindingen uit te vinden. Cisplatina vormt een coördinatiebinding met DNA. Dat is een vrij sterke interactie. De vraag was dus of de rutheniumverbindingen die ik gesynthetiseerd heb ook DNA kunnen binden; in welke positie en op welke manier. De experimenten die gericht zijn om die vragen te beantwoorden worden in Hoofdstuk 3 beschreven. De ruthenium-guanineverbinding **1d** (Fig.3.1) werd gesynthetiseerd en gekarakteriseerd. De reactie tussen **1b** en guanine werd per NMR gestudeerd (Fig.3.2). Hetzelfde experiment werd met **1c** gedaan (Fig.3.3). De belangrijkste conclusie hiervan is dat de rutheniumverbindingen **1a-c** aan guanine kunnen coördineren. De oriëntatie van guanine in **1d** werd met behulp van DFT (Fig.3.5) en NMR bij variabele temperatuur (Fig.3.6) bestudeerd.

In Hoofdstuk 4 worden de verschillende interacties tussen rutheniumverbindingen en DNA behandeld. Een antwoord is gezocht op de vraag: is er een relatie tussen de ruthenium-DNA-interacties en de cytotoxiciteit van de rutheniumcomplexen? Voor deze studie worden de complexen **1a-c** gebruikt, de structuur-gerelateerde complexen **1e** en **1f** (Fig.4.1), en het dinucleaire complex **1g** (Fig.4.2). Iedere coördinatiepositie van **1g** is bezet dus coördinatie van deze rutheniumverbinding aan DNA is niet mogelijk.

Ten eerste wordt er aangetoond dat zowel **1e** als **1f** met guanine kunnen coördineren. NMR en MS zijn daarvoor gebruikt. Daarnaast zijn CD en LD gebruikt om de interacties tussen ieder rutheniumcomplex en DNA te bestuderen. De verschillen zijn duidelijk (Fig.4.4 en Fig.4.5). Het complex **1g** (Fig.4.2) vormt een sterk interactie met DNA, zelfs als er geen coördinatie-interactie tussen die twee moleculen kan ontstaan.

Er zijn verschillende mogelijke interacties tussen metaalverbindingen en DNA. Sommige van deze interacties worden in Hoofdstuk 5 beschreven, hoewel zij ook van belang zijn om de conclusies van Hoofdstuk 4 te begrijpen. Een interactie-type is **coördinatie**; die werd al eerder beschreven. Een andere mogelijkheid is de **invoeging** van de aromatische gedeelte van de verbinding tussen de DNA-basen. Metaalverbindingen kunnen ook in de **groeven** van DNA passen. Het rutheniumcomplex **1g** kan niet coördineren, maar het kan wel op een ander manier aan DNA binden, waarschijnlijk via de DNA-groeven.

Een relatie wordt in Hoofdstuk 4 gezocht tussen DNA-binding en cytotoxiciteit. De activiteiten van de verbindingen **1a-c**, **1e-g** in verschillende kankercellen worden in de Tabellen 4.3 en 4.4 aangetoond. Ook de activiteit van de referentieverbindingen cisplatina

en  $\alpha$ -[Ru(azpy)<sub>2</sub>Cl<sub>2</sub>] (Fig.1.15) worden ter vergelijking aangegeven. De resultaten van de guanine-experimenten, van de CD/LD-metingen en van de celtesten leiden tot de volgende conclusies:

De bestudeerde verbindingen kunnen als actief of matig-actief beschouwd worden, met uitzondering van het complex **1f**, dat niet actief is. Volgens de NMR-studies kan **1f** wél met guanine binden. Volgens de CD/LD-studies kan deze verbinding door invoeging tussen de basen of door de DNA-groeven aan DNA binden. **1f** is de enige van de bestudeerde verbindingen die geen azo-groep bevat. Deze groep lijkt dus essentieel voor de cytotoxiciteit.

Van de studies met complexen **1a-c** blijkt dat de uitgaande groep (Cl, H<sub>2</sub>O, CH<sub>3</sub>CN) geen invloed heeft op de cytotoxiciteit van de verbinding.

Met guanine reageert **1e** als snelste en **1c** als langzaamste. Er is ook geen relatie gevonden tussen deze data en de cytotoxiciteit.

Tenslotte, geen van de verbindingen **1b**, **1e** en **1g** lijkt door invoeging aan DNA te binden. **1b** en **1e** worden verwacht om met DNA te coördineren. **1g** bindt waarschijnlijk via de DNA-groeven. Alle drie vertonen enige activiteit in verschillende kankercellen.

Hoofdstuk 5 begint met een beschrijving van de verschillende types van interactie tussen metaalverbindingen en DNA. Een paar voorbeelden worden gegeven van rutheniumverbindingen die op die manieren aan DNA zouden kunnen binden. De synthese van de complexen in Fig.5.2 is in detail beschreven. Data van cytotoxiciteit zijn in de Tabellen 5.1 en 5.2 te vinden.

De interacties tussen metaalverbindingen en andere biologische moleculen worden ook in Hoofdstuk 5 vermeld. Een experiment is beschreven waarin wordt aangetoond dat het complex **1b** aan het transporteiwit transferrin kan binden. Het zou belangrijk zijn om te ontdekken of er een relatie is tussen deze binding en de cytotoxiciteit van **1b**.

Tenslotte het belang van testen voor antimetastatische activiteit wordt benadrukt.

Hoofdstuk 6 geeft een samenvatting in het Engels van de resultaten in dit proefschrift beschreven en de conclusies die daaruit volgen, alsmede suggesties voor verder werk.

Tijdens de experimenten met guanine is een interessant project ontstaan dat niet direct te maken heeft met ruthenium of met kanker. Dit werk wordt als Appendix van dit proefschrift gepresenteerd. De kristalstructuur van bidimensionale, parallelle vlakken van guanine is aangetoond (Fig.A.1 en Fig.A.3). Deze structuur zou praktische aanpassingen in nanotechnologie kunnen hebben.

# Resumen de la tesis doctoral:

“Complejos polipiridilo de rutenio con propiedades anticáncer. Síntesis, caracterización y estudios mecanísticos en busca de relaciones estructura-actividad”.

El siguiente resumen está escrito de modo que pueda ser comprendido por la mayor parte de los lectores. Por ello puede contener algunas simplificaciones e inexactitudes. Un resumen más científico de la tesis se puede encontrar en inglés, en el Capítulo 6 de la misma.

En esta tesis se habla constantemente de “complejos de rutenio”, así que no sería mala idea empezar por ahí. El **rutenio** es un metal de la familia del platino. Un **complejo** es una unidad formada por un átomo de rutenio y una serie de “ligandos”, que son moléculas orgánicas. Podemos imaginarnos un esqueleto octaédrico con el átomo de rutenio en el centro, y los ligandos distribuidos a su alrededor. Un ligando **polipiridilo** es una serie de anillos aromáticos unidos entre sí de diversas formas. Estos anillos tienen átomos de nitrógeno, que son muy importantes porque son los puntos en los que se anclan al átomo de rutenio.

El objetivo a largo plazo de esta investigación es diseñar compuestos, en mi caso **complejos polipiridilo de rutenio**, tal que sean capaz de matar tumores sin dañar los tejidos sanos. Hay dos estrategias principales para buscar esos compuestos. La primera consiste en hacer muchos compuestos, y ver si funcionan. A la vez, mediante la segunda estrategia se intenta entender cómo funcionan estos compuestos, para así poderlos diseñar de una manera más racional.

En la introducción de la tesis se explica por qué partimos de estos compuestos en particular: por qué usamos rutenio y por qué los ligandos polipiridilo, entre otras cosas. Primero se introduce el papel que los metales han desempeñado en la historia de la medicina, y más adelante se explica el ejemplo concreto del platino y el cáncer. Tras el descubrimiento casual de la actividad antitumoral del cisplatino, que es un complejo muy sencillo de platino, se empezó a indagar sobre qué hacía el cisplatino, que desembocaba en la muerte de la célula tumoral. Es decir, el mecanismo de acción del cisplatino. Enseguida se comprobó que el cisplatino interacciona con el ADN, doblándolo (ver la Fig.1.3 en el

Capítulo 1) y haciéndolo inservible, de modo que la célula muere. Es cierto que el cisplatino mata también células sanas, aunque ataca preferentemente a las células enfermas.

La quimioterapia con cisplatino no es la Panacea. Primero, cada cáncer se comporta de una manera distinta y, mientras algunos son extremadamente sensibles al cisplatino, otros apenas resultan afectados. Además, incluso esos cánceres sensibles acaban desarrollando una resistencia al cisplatino, de modo análogo a como las bacterias pueden desarrollar una resistencia a los antibióticos. Por otro lado, el cisplatino es bastante agresivo, y provoca algunos problemas “menores”, como los conocidos vómitos y la pérdida capilar, y otros mucho más graves, como fallos renales y problemas nerviosos, que pueden llegar a ser tan serios que hacen necesario interrumpir la terapia.

Hace falta encontrar compuestos que funcionen mejor, y una parte importante de la comunidad científica dedica actualmente todos sus esfuerzos a este fin. En el Capítulo 1 de esta tesis se da una clasificación de los compuestos más exitosos publicados hasta el momento, sus ventajas respecto del cisplatino y también sus inconvenientes. Los primeros compuestos descritos son todos de platino, y después se pasa a los complejos de rutenio. El rutenio es un metal de la familia del platino que presenta ciertas propiedades químicas que lo convierten en un buen candidato a complementar o sustituir al platino en el campo de las medicinas contra el cáncer.

El punto de partida de mi trabajo son estructuras como las que aparecen en las Figs.1.14 y 1.15. El compuesto de la derecha en la Fig.1.14, así como el compuesto de la Fig.1.15, resultaron eficientes en matar células tumorales en ensayos realizados *in vitro*, esto es, en placas de células. Sin embargo, estos compuestos no se pueden disolver en agua, lo cual hace complicada su inyección en pacientes. En el Capítulo 2 se explica cómo, inspirándome en estos dos compuestos, diseñé un compuesto que es una combinación de los dos. Lo sintetiqué en tres variantes: con un átomo de cloro en uno de los vértices del octaedro, con una molécula de agua en lugar del cloro, o sustituyéndolo por una molécula de acetonitrilo (ver las Figs.2.2 y 2.6). A estos compuestos los llamo **1a**, **1b** y **1c**.

En el Capítulo 2 se describen la síntesis y la caracterización de los compuestos **1a-c**, es decir, cómo los hice en el laboratorio y por qué sé que tienen las estructuras que describo. Para ello uso fundamentalmente dos herramientas: resonancia magnética nuclear (RMN) y difracción de rayos X.

El Capítulo 3 describe un estudio teórico. Me centré en la segunda propuesta que acabo de explicar: entender cómo funcionan estos compuestos. Se sabe que el cisplatino se

relaciona con el ADN por medio de una interacción muy fuerte, que llamamos enlace de coordinación. El platino se “ancla” al ADN, y su punto de anclaje preferido es también conocido: un átomo de nitrógeno determinado de la guanina, que es a su vez uno de los ladrillos del ADN. Aplicando estos conocimientos a los compuestos **1a-c**, intenté comprobar si el rutenio también era capaz de anclarse a la guanina, y si para ello elegía el mismo punto de anclaje que el cisplatino. Es necesario aclarar que el rutenio sólo puede “coordinarse” a 6 átomos. Pero, en los compuestos **1a-c**, el rutenio ya está coordinado a 6 átomos, ¿cómo puede coordinarse con el ADN? El rutenio no le tiene demasiado apego al cloro, el agua o el acetonitrilo, así que en cuanto se pone en contacto con el ADN, pierde esta molécula y se queda con una posición libre para reaccionar con el ADN.

Conseguí sintetizar el compuesto **1d** en el laboratorio (ver la Fig. 3.1). Así, pude caracterizarlo y tomar su “huella digital” por RMN. A continuación disolví algo del compuesto **1b** en agua, añadí un modelo de guanina, y gracias al RMN pude seguir la reacción en condiciones “fisiológicas” (agua y 37 °C) en el tiempo. Conociendo el aspecto del RMN de **1b** y el aspecto del RMN de **1d**, pude conocer si **1b** en efecto reacciona con la guanina para dar **1d**, y a qué velocidad lo hace. Así, en la Fig.3.2 vemos el aspecto del RMN de **1b**, abajo, y según va ocurriendo la reacción, vemos cómo se va formando **1d**, y cómo después de 5 horas la reacción ya no va más allá.

En la Fig.3.3 se muestra el mismo experimento partiendo de **1c**. Es algo más complicado, porque **1c** en agua da **1b** (recordemos que **1b** es igual que **1c**, pero sustituyendo el acetonitrilo por agua). Pero también se puede ver que **1c** reacciona con la guanina para dar **1d**. El compuesto **1a** apenas se disuelve en agua, así que no lo pude utilizar para hacer este estudio.

La conclusión que se puede obtener hasta el momento es que los compuestos **1a-c** son en principio capaces de interaccionar con el ADN de la misma forma que el cisplatino, esto es, mediante un enlace muy fuerte llamado de coordinación.

El resto del Capítulo 3 describe un estudio teórico desarrollado para investigar la orientación de la guanina unida al compuesto de rutenio. Las técnicas utilizadas son una simulación por ordenador (DFT), que predice las orientaciones que vemos en la Fig.3.5, y RMN a distintas temperaturas (Fig.3.6).

Tal vez la parte más importante de la tesis está expuesta en el Capítulo 4. En él nos preguntamos cómo interaccionan los compuestos propuestos en esta tesis con el ADN, y si hay alguna correlación entre estas interacciones y la capacidad de estos compuestos de

matar células tumorales. Además de los complejos **1a-c**, utilizamos otros dos de estructuras muy similares, **1e** y **1f** (Fig.4.1), y un compuesto que es como dos unidades de los compuestos **1a-c**, unidos por una cadena (**1g**, Fig.4.2). Lo interesante es que para que esta cadena se pueda unir a los átomos de rutenio, el compuesto inicial pierde el cloro, el agua o el acetonitrilo, y, puesto que la cadena se une fuertemente al rutenio, éste ya no puede anclarse al ADN, al contrario que el resto de compuestos **1a-c**, **1e** y **1f**, que sí pueden.

Lo primero es demostrar que **1e** y **1f** sí pueden coordinarse a la guanina. Para ello hice uso de dos técnicas: RMN y espectrometría de masas, en las siglas inglesas, MS. A continuación tomé la cadena entera de ADN y estudié la interacción entre cada compuesto y el ADN, utilizando otras dos técnicas: dicroísmo circular y lineal (CD y LD, en las siglas inglesas). Las diferencias entre las formas de interactuar de estos compuestos con el ADN son evidentes (ver los CDs de la Fig.4.4 y los LDs de la Fig.4.5). Tal vez lo más interesante sea que el compuesto **1g** (Fig.4.2) que, como ya he explicado, no tiene ninguna posición de anclaje al ADN, es, de todos los compuestos estudiados, el que mayor cambio provoca en el CD y el LD. Esto quiere decir que interacciona con el ADN de un modo nada desdeñable. Pero, si no puede anclarse, ¿cómo interacciona con el ADN?

Aunque los diferentes modos de interacción de los compuestos metálicos con el ADN están explicados en el [Capítulo 5](#), es necesario mencionarlos ahora para poder entender las conclusiones del [Capítulo 4](#). Uno de estos modos de interacción es el que se ha discutido ya: la **coordinación**, una interacción muy fuerte entre el rutenio y un punto de anclaje del ADN: un átomo de nitrógeno de la guanina. Otra posibilidad es la **intercalación** de los anillos aromáticos del compuesto (la parte “polipiridilo”) entre los pares de bases nucleicas del ADN. Podemos pensar en la molécula de ADN como una escalera de mano retorcida verticalmente, en cuyo caso los pares de bases serían los peldaños. Y los ligandos polipiridilo encajarían perfectamente entre esos peldaños. Aunque se conocen varios modos de interacción con el ADN, sólo mencionaré uno más: la **unión a los surcos** del ADN. Al retorcerse la escalera, se forman unos surcos externos. Algunas moléculas encajan perfectamente en esos surcos. El compuesto **1g** no puede coordinarse, pero sí puede interaccionar de uno de los otros modos. Observando la forma del compuesto, considero que probablemente se una a los surcos del ADN.

Volviendo a la otra gran pregunta de este capítulo: ¿hay alguna correlación entre las interacciones de los compuestos con el ADN y su capacidad de matar células tumorales?

Para responder a esa pregunta, medimos la toxicidad de los compuestos **1a-c**, **1e-g** en varios tipos de cáncer: cáncer de ovario, de mama, leucemia de ratón, etc. Vayamos a las Tablas 4.3 y 4.4. Cada fila se corresponde con un compuesto; cada columna, con un tipo de cáncer. Cuanto menor sea el número, más activo es el compuesto. Estos valores siempre se estudian de modo relativo, es decir, comparamos los números obtenidos en cada compuesto con aquellos obtenidos con compuestos que sabemos que son activos. Las referencias tomadas son el cisplatino y el compuesto  $\alpha$ -[Ru(azpy)<sub>2</sub>Cl<sub>2</sub>], que es el compuesto de la Fig.1.15, en el que me inspiré para comenzar la síntesis de los compuestos descritos en esta tesis doctoral.

Combinando los resultados de los experimentos llevados a cabo con la guanina con aquellos obtenidos en las mediciones con ADN y con los números de las Tablas 4.3 y 4.4, llegamos a las siguientes conclusiones:

Se puede decir que los compuestos estudiados son activos o moderadamente activos contra varios tipos de tumores, a excepción del compuesto **1f**. Éste sí parece capaz de coordinarse con la guanina, de hecho es el compuesto que mayor conversión alcanza de todos los estudiados. Del CD y del LD se puede deducir que este compuesto puede intercalarse o interaccionar con el surco del ADN, y esta relación no altera la longitud de la cadena de ADN. De todos los compuestos estudiados, éste es el único que carece de dos nitrógenos unidos por un doble enlace (grupo azo). De ello se deduce que el grupo azo es fundamental para que el compuesto sea activo.

Estudiando los compuestos **1a-c** se concluye que el grupo saliente (esto es, el cloro, el agua, el acetonitrilo) no parece tener ninguna influencia en la toxicidad. De modo que podemos basarnos puramente en la solubilidad en agua para juzgar qué compuesto es “mejor” (en este caso, **1a** es menos útil, porque no se disuelve bien en agua).

En cuanto a la cinética de la reacción con guanina, **1e** es el compuesto que se coordina más rápidamente, y **1c** es el más lento. Sin embargo, esta diferencia tampoco se refleja en los datos de citotoxicidad.

Por último, de los compuestos **1b**, **1e** y **1g** no cabe esperar una interacción intercalativa. Se puede deducir que tanto **1b** como **1e** se coordinarán al ADN, mientras que **1g** encajará en su surco. Como ya he mencionado, los tres son activos o moderadamente activos contra ciertos tipos de tumores.

El Capítulo 5 comienza con una descripción de los diferentes modos de interacción de los compuestos metálicos con el ADN, incluyendo las ya mencionadas unión con el surco e

intercalación. Se proponen varios ejemplos de compuestos que podrían interaccionar con el ADN de cada uno de estos dos últimos modos. Los complejos de la Fig. 5.2 fueron sintetizados y algunas pruebas ya se han llevado a cabo con ellos, como demuestran las Tablas 5.1 y 5.2, aunque aun queda mucho trabajo por hacer.

A continuación se trata el tema de las interacciones entre los compuestos metálicos y otras moléculas biológicas, en particular las proteínas encargadas del transporte y almacenamiento de elementos esenciales como el hierro, de oxígeno, etc. Aunque el estudio de las interacciones de los compuestos sintetizados con el ADN es fundamental, no podemos olvidarnos de que tanto en la sangre como en las células hay muchos otros componentes, con los que los compuestos de rutenio también pueden relacionarse. En este apartado se describe un experimento con el que se demuestra que, en efecto, el compuesto **1b** reacciona con la transferrina, una proteína que transporta el hierro desde la sangre hacia el interior de las células. Es importante preguntarse si puede haber alguna influencia entre esta interacción y la toxicidad del compuesto.

Por último se plantea la necesidad de comprobar si los compuestos sintetizados tienen actividad antimetastática. Hoy en día las intervenciones quirúrgicas para eliminar tumores primarios son muy eficientes. Sin embargo, a menudo el tumor reaparece en otra parte del cuerpo, es lo que se conoce como metástasis. En la actualidad se está empezando a comprender cómo se lleva a cabo este proceso, y en consecuencia se están proponiendo formas de medir si un compuesto tiene propiedades antimetastáticas.

En el Capítulo 6 se ofrece un resumen en inglés de los contenidos de la tesis, así como de las conclusiones que de ella se derivan.

Al trabajar con guanina surgió un interesante trabajo que nada tiene que ver con el rutenio o con el cáncer. Por esto, se presenta en la forma de Apéndice a la tesis. En él se describe la obtención de una estructura cristalina de guanina en capas bidimensionales y paralelas entre sí (ver Figs.A.1 y A.3), con posibles aplicaciones teóricas, así como en el campo de la nanotecnología.

Para finalizar se ofrecen un breve currículum de la autora de la tesis, una lista de los artículos publicados en los que se presentan partes de los resultados de dicha tesis y, en último lugar, los agradecimientos.

# Curriculum Vitae

The author of this thesis was born in Miranda de Ebro (Spain) on the 24<sup>th</sup> August 1979. After attending secondary school in Colegio Sagrados Corazones (Miranda de Ebro, Spain), where she graduated cum laude (Matrícula de Honor) in 1997, she started her chemistry degree at the Universidad de Salamanca (Spain). During her studies she received a Socrates study grant, which allowed her to spend her fourth year at the University of Bristol (UK). She went back to Salamanca to finish her studies, obtaining her Master of Science degree (Título de Licenciada) in January 2003.

In April 2003 she left her friends and family behind, including her newly-born niece, and went on a four-year adventure to the tulips country. She became a PhD student (AiO) in Prof. Dr. Jan Reedijk's group at the Universiteit Leiden, where she carried out the research presented in this thesis. She was appointed as the PhD representative during the year 2005. A part of the results presented in Chapter 4 of this thesis was obtained during a short-term scientific mission in the laboratories of Prof. Dr. Mike Hannon, at the University of Birmingham (UK). This collaboration was carried out in November and December 2006 with funding from the COST action D39.

The author had the opportunity to discuss part of her results with the academic community, both through oral presentations and posters, during national and international meetings, including the Pt-KWF meetings in Amsterdam (The Netherlands, 2003), the CW-NWO meeting in Lunteren (The Netherlands, 2004), the ICBIC-12 in Michigan (USA, 2005), the HRSMC Symposium in Amsterdam (The Netherlands, 2005), the COST D20 meeting in Brno (Czech Republic, 2006), the EUROBIC8 in Aveiro (Portugal, 2006) and the ESF-COST High-Level Research Conference in Metal-Nucleic Acid interactions in Athens (Greece, 2006).

# Curriculum Vitae

La autora de esta tesis doctoral nació en Miranda de Ebro (Burgos, España) el 24 de agosto de 1979. Fue alumna de BUP y COU en el Colegio Sagrados Corazones de Miranda de Ebro, finalizando sus estudios con Matrícula de Honor en 1997. En el mismo año comenzó su carrera de Química en la Universidad de Salamanca (España). El cuarto curso lo llevó a cabo en la Universidad de Bristol (Reino Unido), dentro del programa de becas Sócrates. A continuación regresó a Salamanca, donde terminó sus estudios de Química, obteniendo el Título de Licenciada en enero de 2003.

En abril del mismo año dejó atrás a su familia, incluyendo a su sobrinita recién nacida, y a sus amigos para embarcarse en una aventura de cuatro años en el país de los tulipanes. Se incorporó como estudiante de doctorado al grupo del profesor Reedijk en la Universidad de Leiden (Países Bajos), en el que desarrolló la investigación que se presenta en esta tesis doctoral. En este periodo dio prácticas a alumnos de primer y segundo curso de Química y de Molecular Science and Technology, supervisó pequeños proyectos de estudiantes de Química y fue elegida representante de los doctorandos durante el año 2005. Una parte de los resultados presentados en el Capítulo 4 de esta tesis doctoral se obtuvo mediante una colaboración con el profesor Hannon, de la Universidad de Birmingham (Reino Unido), durante una estancia en sus laboratorios que se llevó a cabo en noviembre y diciembre de 2006, con el apoyo económico de la acción COST D39.

La autora tuvo la oportunidad de compartir parte de sus resultados con la comunidad científica en forma de presentaciones orales y pósteres, tanto en reuniones a nivel nacional (Países Bajos) como en conferencias internacionales. Entre los citados eventos cabe destacar las reuniones Pt-KWF en Ámsterdam (Países Bajos, 2003), la reunión CW-NWO en Lunteren (Países Bajos, 2004), la ICBIC-12 en Michigan (EEUU, 2005), el simposio HRSMC en Ámsterdam (Países Bajos, 2005), la reunión COST D20 en Brno (República Checa, 2006), la EUROBIC8 en Aveiro (Portugal, 2006) y la conferencia ESF-COST de interacciones entre metales y ácidos nucleicos en Atenas (Grecia, 2006).

# List of publications

Corral, E.; Hotze, A.C.G.; Tooke, D.M.; Spek, A.L.; Reedijk, J., **“Ruthenium polypyridyl complexes containing the bischelating ligand 2,2'-azobispyridine. Synthesis, characterization and crystal structures”**, *Inorg. Chim. Acta*, **2006**, 359, 830-838.

Corral, E.; Kooijman, H.; Spek, A.L.; Reedijk, J., **“Nucleic acids in two dimensions: layers of base pairs linked by carboxylate”**, *New J. Chem.*, **2007**, 31, 21-24.

Corral, E.; Hotze, A.C.G.; Magistrato, A.; Reedijk, J., **“Interaction between the DNA model base 9-ethylguanine and a group of ruthenium polypyridyl complexes: kinetics and conformational temperature dependence”**, *Inorg. Chem.*, **2007**, 46, 6715-6722.

Corral, E.; Hotze, A.C.G.; den Dulk, H.; Hannon, M.J.; Reedijk, J., **“Ruthenium polypyridyl complexes and their modes of interaction with DNA: is there a correlation between these interactions and the antitumour activity of the compounds?”**, *J. Biol. Inorg. Chem.*, **2007**, submitted for publication.

# Nawoord



